

# Politecnico di Torino

Corso di laurea in Ingegneria per l'Ambiente e il Territorio
A.A. 2024/2025
Sessione di Laurea ottobre 2025

# Tesi Magistrale

# Assessing the retreat of Adamello Glacier and its climatic impacts on Valcamonica: a GIS and remote sensing analysis

Relatore:

Prof. Paolo Dabove

Candidato:

Roberto Poiatti 331565

# Contents

1	. Intro	duction	4
	1.1	Driving factors behind the study	4
	1.2	Regional and climatic context	6
	1.3	Research goals and potential future applications	10
2	. State	of the Art	11
	2.1	Existing literature and previous studies	11
	2.2	Current applications	14
	2.2.1	ADA 270	14
	2.2.2	ClimaADA	15
	2.2.3	USIE	16
	2.3	Gap analysis	17
3	. Instru	ments and tools	19
	3.1	Satellite data overview	19
	3.2	MODIS	21
	3.3	Sentinel-2	22
	3.3.1	Level-2A Products	25
	3.3.2	Level-1C Products	26
	3.4	ARPA	27
	3.5	Data processing software	28
	3.5.1	QGIS	28
	3.5.2	MATLAB	29
4	. Meth	odology	30
	4.1	Data acquisition workflow for MODIS	30
	4.2	Data acquisition workflow for Sentinel-2	32
	4.3	Comparison between MODIS and Sentinel-2	33
	4.4	Delineation of contour	34
	4.5	Glacier area calculation	37
	4.6	Data acquisition workflow for ARPA Lombardia	38
	4.7	Temperature and Precipitation correlations with Glacier area	39
5	. Resul	Its and discussion	42
	5.1	Initial analysis of Glacier area variation	42
	5.2	Enhanced biennial analysis of Glacier area variation	56

	5.3	Climate Effects on Glacier Area in the Adamello-Valcamonica Region	61
	5.3.1	Temperature trends	61
	5.3.2	Precipitation trends	63
	5.3.3	Biennial Glacier-Climate relationships (Automatic method)	67
	5.3.4	Biennial Glacier-Climate relationships (Visual method)	72
	5.3.5	Annual Glacier-Climate relationships	77
6.	Conc	lusions and future trends	85
Re	eference	S	90

## Abstract

Climate change is accelerating the retreat of Alpine glaciers, significantly impacting water resources in mountain valleys. This thesis analyses the retreat of the Adamello Glacier over recent decades using satellite imagery and GIS techniques to map glacier perimeter variations and correlate these changes to climate variables, focusing on Valcamonica, the valley located beneath the glacier. The objective is to understand how the glacier surface area has been changing during the years and how its reduction is influenced by precipitation and temperature trends. The study is based on satellite data from MODIS and Sentinel-2 to provide a detailed assessment of glacier variations from 2000s to the present. Moreover, historical data of temperature and precipitation from ARPA Lombardia are analysed to study their fluctuations in the last period and examinate their correlation with glacier changes. The study aims to investigate the relationship between glacier retreat and environmental impacts on the surrounding territory, assessing potential implications for local biodiversity, agriculture, hydroelectric production and tourism. The findings will contribute to a better understanding of climate and water resource dynamics in mountain regions like Valcamonica, providing insights to support future strategies for climate change adaptation and mitigation.

## 1. Introduction

## 1.1 Driving factors behind the study

Glaciers represent a key component of Alpine environments, not only as iconic landscape elements but also due to their crucial role as regulators for local microclimates and freshwater resources. They are considered an essential resource for environmental monitoring due to their importance for tourism, their role in reflecting broader climatic trends and sustaining natural ecosystems. Moreover, hydropower plants located in Alpine regions largely depend on meltwater generated from snow and ice produced during the ablation season. Consequently, the hydrological cycle providing the natural inflow to the reservoirs is strongly dependent on the presence of glaciers and their evolution. For these reasons, variations that can occur in their physical and geomorphological characteristics are widely considered as reliable indicators of climate change [1].

Over the past 40 years, temperatures across the entire Alpine region have doubled, leading to significant ecosystem changes, with glacier retreat being one of the most evident. These transformations, which are accelerating over time, directly and indirectly impact the ecosystems located at high altitudes and those located in valley bottoms. One clear example is the role of glaciers in ensuring water availability, which has been increasingly compromised, with serious consequences for energy production, agriculture and biodiversity in the surrounding areas [2].

Since the end of the Little Ice Age, around the mid-19th century, Alpine glaciers have undergone a continuous phase of retreat and surface loss, with an acceleration in recent decades. In the Italian Alps, this process has been evident since 1957 when the first inventory of Italian glaciers was compiled. The last phase of limited expansion occurred during the late 1970s and early 1980s, after which glacier reduction has resumed more aggressively. The consequences over time were a significant loss of area and volume, as well as the fragmentation of larger glaciers into smaller bodies, leading to an increase in the total number of glacial entities. This phenomenon has, in turn, contributed to even faster melting processes. Notably, not only marginal glaciers but also the largest ice masses in the region are being affected by this trend, with a consequent negative mass balance and rapid retreat [3].

Shifting the focus to the Adamello Glacier, this study wants to explore the primary environmental and climatic drivers behind its recent evolution, concentrating particularly on its accelerated retreat in recent decades. The Adamello Glacier surface is changing at a faster rate than previously projected and is expected to disappear within a few decades due to global warming. Its surface area, which measured 15.7 km<sup>2</sup> in August 2007, had decreased to 13.1 km<sup>2</sup> by August 2022, reflecting a reduction of approximately 11% per decade. More than half of the original 870 million cubic metres of ice volume, recorded at the end of the 20th century, has already melted. The main cause of this rapid loss is attributed to reduced winter snowfall combined with rising temperatures. From systematic snow accumulation measurements conducted since the mid-1960s in the Sarca-Chiese-Oglio hydrological system, it was demonstrated that the decline was approximately 5-6% less per decade compared to the initial average of 800 millimetres of water equivalent recorded in April above 2500 metres. Moreover, air temperatures recorded at the Pantano d'Avio dam, located at the foot of Mount Adamello on the Lombardy side, have increased by approximately 0.4°C per decade. This warming trend involves serious consequences for the permafrost, whose thawing destabilises rock faces and increases the risk for mountaineers [4].

According to the Intergovernmental Panel on Climate Change (IPCC), temperatures in this part of the Alps have already risen by two degrees Celsius compared to pre-industrial levels. Furthermore, they will probably reach three degrees by 2050, and they could increase even more, between three and six degrees, by the end of the century, leading to the disappearance of the Adamello Glacier. Without drastic decarbonisation measures, mass loss could accelerate further due to the ongoing darkening of the glacier surface, caused by wind-borne dust deposits and the growth of organic substances. These factors enhance the glacier's ability to absorb solar radiation, thereby intensifying melting [4].

Therefore, all the aspects outlined above highlight the need to further explore a topic that is both timely and highly relevant. The different causes and contributing factors should be regarded as critical points of reflection within the broader framework of global warming and climate change.

## 1.2 Regional and climatic context

The Adamello Glacier is the largest glacier in both the southern Alps and Italy, extending over an area of 12.87 km<sup>2</sup> as of September 2023. It is also the thickest glacier in Italy, with ice thickness exceeding 250 metres in its upper sections, particularly in the Pian di Neve area [3].

The Adamello Glacier (Figure 1) is situated within the Adamello-Presanella mountain group, part of the Rhaetian Alps in the central-southern Alpine sector, and it lies on a plateau at an average altitude of 3000 m a.s.l. From an administrative perspective, around 90% of the glacier belongs to Lombardy region, while the remaining portion extends into Trentino-Alto Adige/Südtirol. Meltwater from the glacier feeds both the Oglio and Sarca rivers, that flow respectively in Valcamonica and Val di Genova. It is composed of six distinct glacial branches and presents some similar geomorphological characteristics with other glaciers that are located within the southwestern climatic subregion of the Alps. Regarding the size of the six hydrographic units, the Mandrone Glacier is the most extensive [1].

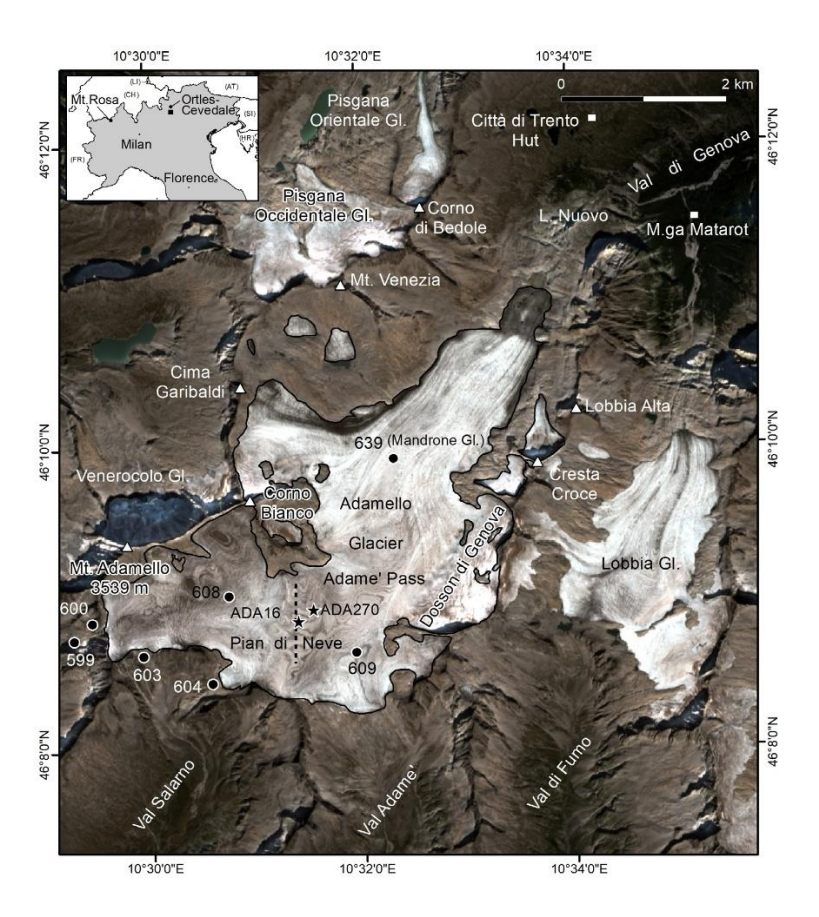


Figure 1: Location map of Adamello Glacier [5]

The unusual aspect of Adamello Glacier is its distinct shape compared to most other glaciers in the Alps. Instead of being surrounded by high mountain peaks, it spreads out over a broad and gently sloping surface, looking more like a Scandinavian ice plateau (*Figure 2*). The glacier's upper surface lies between 3100 and 3300 meters above sea level, while the surrounding peaks rise only about 150 meters above it [6].



Figure 2: quite flat surface of Adamello Glacier [6]

Beneath the ice there is a sort of hidden valley, currently buried under up to 260 meters of glacial ice. Because of the low elevation of its accumulation zone, even the highest parts of Adamello Glacier are experiencing significant ice loss. As the glacier melts and surface layers disappear, older ice layers gradually emerge. The ice currently present at the surface is from the 1990s; however, deeper layers are much older, probably around a thousand years. In fact, in 2021, a research team of scientists drilled into 224 meters thick ice, and modelling dated the basal ice to be 2000 years.

During the First World War (1914-1918), Adamello Glacier was the scene of the "White War", where Austrian and Italian troops fought their war at an altitude of around 3000 meters. The front line ran directly through the high alpine region and soldiers had to deal with extreme climatic conditions at those altitudes, with many who died due to the severe cold and heavy snowfall. Today, the main tongue of the glacier, the Vedretta Mandrone, occasionally reveals personal items and belongings of soldiers who crossed the glacier during that period [6].

When the ice field was much bigger, the Mandrone Glacier extended as a steep icefall down into the valley and connected with the Lobbia Glacier in the east. Now a shallow lake (Figure 3) is being originated in front of Mandrone snout due to its progressively retreat onto flatter terrain. Further retreat with the creation on new lakes is expected to occur in the next years, as documented by the thinning of 24 meters of the Mandrone tongue in the years 2020-2023. Besides significant thinning, the snout of the Adamello Glacier is also experiencing collapse as demonstrated by tension cracks that began to appear in summer 2022 (Figure 3). These cracks typically develop above cavities within or beneath the ice and are indicative of augmented melting processes. As the ice above these voids subsides, depressions with circular crevasses form on the glacier surface. Ultimately, the overlying ice collapses, creating rounded holes in the glacier body, as happened in 2023 for three such cavities [6].



Figure 3: Shallow lake in front of Mandrone Glacier (above), circular tension cracks (below) [6]

The Adamello Glacier is located within two major protected areas: *Parco Regionale dell'Adamello* on the Lombardy side and *Parco Naturale Adamello Brenta* on the Trentino Alto Adige side. Together with Parco Nazionale dello Stelvio and Parco Nazionale Svizzero in the Engadin region, they constitute the largest conservation zone in the Alpine region, with a protected area of over 400,000 hectares in the heart of Europe.

In particular, *Parco Regionale dell'Adamello* is located in the heart of the Rhaetian Alps and encompasses the entire Lombard side of the Adamello massif, situated in the northeastern portion of the province of Brescia. The park covers an area of 51,000 hectares (510 km²), stretching from the Tonale Pass to the Crocedomini Pass. Its eastern boundary follows the regional border between Lombardy and Trentino, while to the west it aligns just above the left bank of the Oglio River, Italy's fifth longest river. The park occupies the orographic left side of the Valcamonica valley [7].

On the other hand, *Parco Naturale Adamello Brenta* is the largest protected area in the Trentino region, covering a surface of 625.83 km<sup>2</sup>. Established in 1967, it is located in western Trentino and includes the Adamello and Brenta mountain ranges. The park is traversed by the Val Rendena and bordered by Val di Non, Val di Sole, and Val Giudicarie. Its elevation ranges from 477 to 3,558 meters above sea level [8].

These protected areas and nature parks are of great importance as they serve as key research sites, thanks to the presence of significant natural, climatic, and biological archives. These resources are essential for the study of the territory, particularly the mountainous glacier areas. They can also be considered as major biodiversity hotspots, hosting a wide range of flora and fauna species. For these reasons, they represent an important field of study for both scientific and environmental research, providing a strategic context for conservation and monitoring.

## 1.3 Research goals and potential future applications

This thesis aims to contribute to the ongoing research on climate change by focusing on an extremely sensitive indicator of global warming: glaciers. The Adamello glacier and the Valle Camonica region were selected as study areas due to the opportunity to personally observe the tangible effects of climate change over recent years.

The primary goal of this work is to investigate the surface reduction of the Adamello Glacier by analysing publicly available satellite imagery from open-source datasets. Specifically, remote sensing data from MODIS and Sentinel-2 are used to assess changes in glacier area over past years, up to the present day. The focus of this first part is therefore to detect spatial and temporal trends in glacier retreat to explore and predict potential future projections based on climatic scenarios.

The secondary goal of this project regards a broader analysis of the climatic impacts resulting from the glacier's retreat on Valle Camonica, an alpine region situated directly downstream of the glacier and therefore highly sensitive to its changes. In this case, historical data of temperature and precipitation will be retrieved from ARPA Lombardia, freely accessible by internet. This analysis will be carried out to identify these datasets trends and evaluate their correlation with observed glacier surface changes.

The ultimate purpose of the project is to illustrate the tangible effects of climate change on Italy's largest glacier, providing a real-world case study on the environmental consequences on a mountain region. Therefore, implications on Valcamonica hydrological system, agriculture, local tourism and communities are all aspects that are expected to be dependent on glacier dynamics and so interesting objects of study.

The data, analyses, results, and scenarios presented in this work could be useful references in the future for local authorities, mountain communities and regional stakeholders who might require a clear and updated understanding of the current glaciological situation. The goal is to provide a resource of datasets and information that may prevent the repetition of preliminary assessments and instead support informed decision-making and accelerate the future evaluation process at the site.

## 2. State of the Art

## 2.1 Existing literature and previous studies

The retreat of Alpine glaciers has been documented for nearly two centuries. According to the most recent report of the European Environment Agency on climate change impacts in Europe, these glaciers have lost approximately two-thirds of their total volume since 1850. This trend has been intensifying since the 1980s and is expected to continue even more in the coming decades. Although a lot of information has been collected worldwide to maintain global glacier inventories, there are still many actions that must be taken to afford climate change consequences and take initiatives for effective mitigation strategies. Specifically, more information related to national, regional and local studies should be provided, by focusing on real studies to better understand the phenomena underlying these environmental changes [1].

In recent years, different studies on the Adamello glacier were carried out, focusing on different aspects related to that vulnerable area. In one of them, for example, a physically based modelling approach was used to estimate the mass balance of the Mandrone Glacier, the largest glacier in the Adamello-Presanella group of the Italian Alps. Under current conditions, its specific mass balance (-1439 mm w.e./year) is expected to undergo a significant reduction in the future due to rising temperatures. The results were reasonably validated, although some uncertainties, using field ablation measurements and satellite-derived snow cover data. Different future scenarios indicate a worsening trend, with specific mass balances projected at approximately -2000 mm w.e and -3000 mm w.e by 2050 and reaching up to -5500 mm w.e. by the end of the century. The simulations suggest a real reduction of the glacier between 45-65% by 2050, with most of the ice potentially disappearing by 2100. Despite model uncertainties, the study's findings strongly confirm the ongoing and accelerating retreat of Alpine glaciers, with no signs of trend inversion or stabilization in the foreseeable future [1].

Another recent research analysed the stress and strain evolution of the slopes in the Adamè Valley, situated just at the bottom of the Glacier. The aim of the project was to apply a thermomechanical model by incorporating the typical creep behaviour of jointed rock masses. Glacial geological and geomorphological surveys based on

numerical stress-strain simulations carried out during the study highlighted the main factors contributing to slope displacements in the Adamè Valley during the post-LGM (Last Glacial Maximum) deglaciation. Factors such as glacial dynamics, viscoplastic creep, seasonal loading and strain effects were further investigated and combined with numerical models to assess both large and small-scale effects. The thermomechanical simulations demonstrated that the current temperature and stress—strain conditions observed across the valley slopes are mainly the result of the second complete glacial retreat. Moreover, the overall trend in thermomechanical effects, unless influenced by pronounced temperature variations, is expected to remain stable over the next thousand years [9].

There is a study [10], very similar to the one carried out in this thesis, that investigated the evolution of the Adamello glacier system over time, focusing particularly on glacial surface changes of small glaciers (< 1 km<sup>2</sup>) of Adamello group. The analysis relied on a series of glacier outlines from four different years: 1983, 1991, 1999, and 2003, analysed within a GIS (Geographic Information System) environment to track variations in glacier extent. The 1983, 1999, and 2003 data were obtained from colour aerial photographs and orthophotos, while the 1991 dataset was derived from previous studies. In particular, the 1983 images were stereoscopically derived from photos at a 1:20,000 scale and digitized over a Technical Regional Map (CTR) of Lombardy Region used as a raster base. For 1999 and 2003, high-resolution orthophotos (1 m and 0.5 m per pixel, respectively) were used, and in some cases supplemented by Differential Global Positioning System (DGPS) measurement campaigns to ensure accuracy. This multi-temporal geospatial approach allowed for consistent mapping and classification of glacier surfaces, providing a reliable framework for assessing long-term glacier changes in the region. The results highlighted an approximate surface area reduction of 19% of the Adamello glaciers between 1983 and 2003. This retreat accelerated mostly in the last recorded interval (1999-2003), with an average annual loss of about 0.34 km<sup>2</sup>, compared to 0.23 km<sup>2</sup>/year between 1991 and 1999. In addition, morphological changes such as glacier tongue separation, proglacial lake formation and increased supraglacial debris were observed as well. The trend observed coincides with strong local warming of around +0.85°C, demonstrating a regional climate response significantly stronger than the global average. Furthermore, a sharp decline in winter snow depth, particularly evident between 1999 and 2006 and probably linked to North Atlantic Oscillation (NAO) variability, may also have contributed to the noticeable effects. Overall, the findings underline the concerns over the sensitivity of these vulnerable glacial environments to global warming and ongoing climate change [10].

Another research regarding the evolution of the Adamello Glacier using satellite imagery, with a particular focus on the period from the Late Holocene onward, was carried out in the study [3]. In line with similar works, the main goal was to reconstruct the glacier's historical development, starting from the Late Holocene, by using data from various sources such as historical maps, aerial photographs, and satellite images. To recover glacier outlines from the 20th and early 21st centuries, multitemporal orthophotos, topographic maps and aerial surveys were manually acquired via national and regional geoportals. Orthophotos of 1988, 1994 and 2006 were specifically taken as Web Map Service (WMS) from the National Cartographic Portal (PCN), while the 2003 and 2015 ones were downloaded from the Geoportale Regione Lombardia. Finally, the most recent data were obtained from Sentinel-2, in the same way of what will be done for this work, by accessing the free Copernicus Data Space Environment. The reconstructions highlighted the glacier surface variation and progressive shrinkage, starting from an area of around 18 km<sup>2</sup> in the 1950s, followed by a slight expansion during the 1970s and 1980s, and then continuing with a progressive retreat up to nowadays. By 2023, the main glacial body had decreased to about 12.87 km<sup>2</sup>, or 13.54 km<sup>2</sup> considering also smaller fractioned detached ice bodies, equivalent to an overall areal loss of about 49% of the initial glaciated area. This areal reduction has also been accompanied by significant frontal retreat, particularly in the Mandrone Glacier sector, with over 2800 meters of retreat recorded since the Little Ice Age. This trend sharply increased in the last century, with a retreat of about 500 m in the last 25 years and 295 m in only 8 years, with a rate of more than 37 m a<sup>-1</sup>. Moreover, the glacier has not only lost surface area but has also thinned considerably, even at its highest elevations, as documented by the near-total absence of summer snow cover, indicating that the entire glacier now lies below the equilibrium line [3].

## 2.2 Current applications

#### 2.2.1 ADA 270

In recent years, two important and interconnected projects were carried out on Adamello Glacier, particularly in the area of Mandrone Glacier, that, with a thickness of 270 metres, is considered one of the most significant natural archives of climatic and environmental history in the Italian Alps. Therefore, with the aim to access and study the information preserved within this glacier, the first project called "ADA 270" was launched in April 2021, financed by various public and private institutions. The initiative led to the extraction of an ice core measuring 225 metres in total length, and at the same time to the installation of four fibre optic cables vertically along the borehole. The drilling took place over eleven days at a base camp located at an altitude of 3,200 metres, using a 10 cm borehole that allowed the extraction of one-meter-long cylindrical samples of ice. Figure 4 illustrates the last ice core extracted during the project, which measured about 30 cm and with inside some fragments of rock indicating the proximity to the underlying soil layer [11]. The drilling process was running 24 hours a day, supervised by three teams of scientists in eight-hour shifts. These ice cores will be very useful for reconstructing the climate and environmental history of the area over the past centuries and for monitoring the evolution of the glacier in the future. Moreover, the fibre optics installed in the glacier will allow researchers to track the glacier's vertical temperature profile and detect any kind of stretching or deformation occurring along the borehole over time [12].

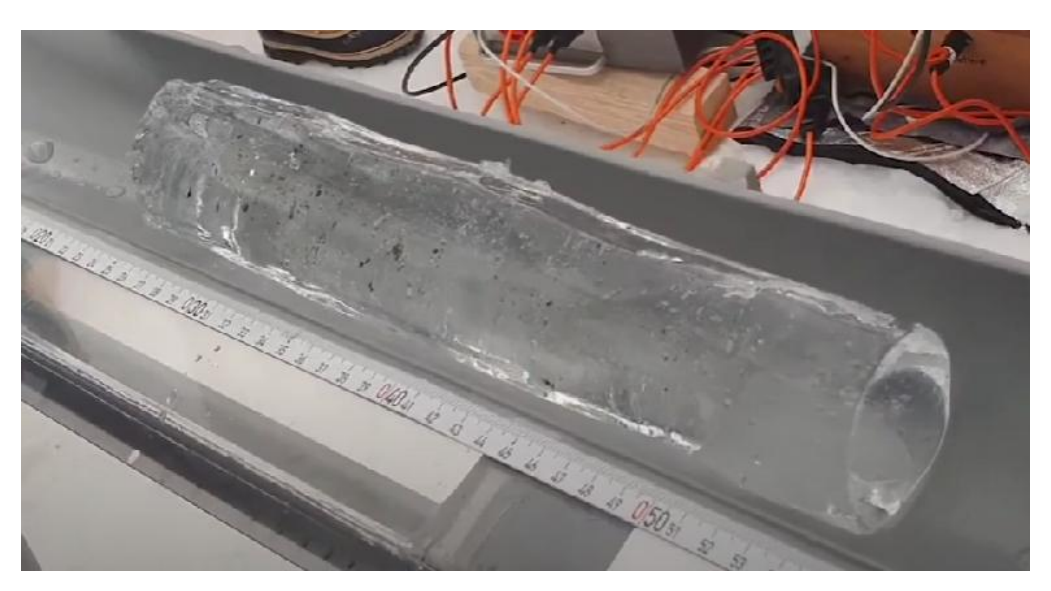


Figure 4: Last ice core extracted in the project ADA 270 [11].

#### 2.2.2 ClimaADA

Building on the legacy of the ADA270 project, the "ClimADA" project aims to reconstruct the climatic evolution of the past centuries, the anthropogenic impact and human influences on the mountain regions as well as the history of major wildfires and the plant species dynamics. The project, coordinated by *Fondazione Lombardia per l'Ambiente*, is carried out in collaboration with several academic and territorial institutions. Thanks to fibre-optic probe already installed during the ADA270 drilling, it is now possible to use sensor data to study the internal behaviour of the ice mass in detail, monitoring glacier evolution through factors like thermal profiles and ice deformation. These insights are essential for modelling its future development in response to external environmental changes and considering global warming scenarios.

Furthermore, another important goal of ClimADA project is to broaden the study of glaciers by combining both climatic and environmental perspectives and distributing data and research results not only to the scientific community but also to the public and local stakeholders. This initiative includes conferences, activities in schools, thematic workshops, summer camps and exhibitions that will involve policymakers, educators, local organizations as well as students and the younger generation. Therefore, the ultimate goal is to communicate effectively and clearly the impacts of climate change on the territory and also the current and future water availability, encouraging deeper awareness and respect for the preservation of natural ecosystems [13].

The project, specifically, focuses on different actions and initiatives that involve a reconstruction of climatic conditions of Mandrone glacier, by studying the ADA 270 ice core now conserved in the Euro Cold Lab of the University of Milano-Bicocca. These analyses allow to understand past climatic patterns and land use evolution by studying respectively the full stratigraphy of the ice core and the presence of pollen samples or other preserved plant species inside the ice. In addition, black carbon deposits are being analysed as well to reconstruct wildfire activity and vegetation dynamics over the centuries. As mentioned above, the fibre optic is being used by Polytechnic of Milan and University of Brescia to assess deformation, elongation and

temperature of the glacier, working on a thermo-fluid-dynamic model of glacier internal condition. This mathematical model that is being developed will be useful to better understand glacier's behaviour under different climate conditions and to run simulations for possible future scenarios [13].

#### 2.2.3 USIE

In recent years, the scientific communities have increasingly explored innovative approaches to glacier monitoring, particularly in the context of climate change. An example is the experimental research project denominated "Un Suono In Estinzione" (USIE). It consists in an artistic-scientific project which offers a multidisciplinary perspective on the effects of global warming on Alpine glaciers using sound analysis and comparing acoustic measurements and mathematical models on glacier melting. Launched in 2020 by researcher and sound artist Sergio Maggioni (known as *NEUNAU*) and expected to last for five years, the project brings together professionals from diverse fields with the aim of investigating glacier transformations using both scientific methods and artistic interpretation. Basically, the project is based on capturing sounds generated by the movement and melting of the glacial mass within its core and surrounding environment, with the aim of calibrating the parameters of mathematical models that predict the future evolution of the Adamello Glacier.

The project is structured into three phases:

Phase 1: Data acquisition on glaciers

Phase 2: Scientific analysis of the collected data

Phase 3: Public dissemination through artistic works and scientific publications

Over the course of three data collection campaigns carried out during the summers of 2021, 2022, and 2023, the team conducted 10 expeditions, covering 140 kilometres on foot and accumulating 12,000 metres of elevation gain., They collected more than 14,000 hours of sound recordings and temperature data using five bioacoustics recorders (*Figure 5*). These recorders were able to operate autonomously, capturing 24-hour audio logs for extended weeks and documenting almost imperceptible sonic phenomena occurring within the glacier environment.





Figure 5: bioacoustics recorders used to collect glacier sound [14].

This unique and growing sound archive not only preserves valuable evidence of ongoing cryosphere changes but also provides a basis for a wide range of future potential applications. The collected material is being used in support of scientific research, editorial publications, educational initiatives, public events, documentaries, and immersive multimedia installations. Therefore, the work raises the awareness and supports the urgency of glacier retreat in the face of global climate change [14].

# 2.3 Gap analysis

Although glaciers are widely recognized as valuable indicators of climate change due to their sensitivity to temperature and precipitation, consistent records of their mass balance and morphological changes in length and terminus position are relatively recent. In fact, systematic monitoring of global glacier mass balance began only in the latter half of the 20th century, making these datasets shorter than many instrumental climate records. To address this limitation, since the 1970s, glacier mass balance has increasingly been simulated using hydrological models based on available climate inputs, offering a more complete picture of glacier-climate interactions and glacial responses to climate variability [1].

This work inevitably has some similarities with earlier studies on the evolution of glaciers in the Adamello region but introduces several key distinctions. By comparing it with [10], for example, it is evident that while earlier research primarily focused on small glaciers in Lombardy particularly sensitive to climate change, this work specifically analyses the Adamello Glacier, the largest and most significant glacier in the Adamello-Presanella group. Moreover, previous analyses relied on data and

imagery ranging from 1983 to 2003, whereas this thesis covers a more recent dataset, extending up to the most recent summer season, thereby providing a more relevant understanding of glacial dynamics in the context of accelerating climate change. Another notable difference lies in the image sources: orthophotos, stereoscopic aerial photography, and DGPS field surveys used to delineate glacier boundaries are replaced by satellite imagery from MODIS and Sentinel, processed through open-source GIS tools. By doing so, this study first updates the temporal framework of glacier surface analysis and shifts the focus to a larger representative spatial area using more recent types of data [10].

Furthermore, the innovative aspect of this thesis is its objective to investigate the correlation between the retreat of the Adamello Glacier and environmental changes in Valcamonica, a field which has not been addressed in detail before. Unlike previous studies that have focused primarily on the glacier itself, this research adopts a broader perspective and goes into further details. In fact, starting from the analysis of the glacier's surface evolution, it then concentrates on environmental parameters in the valley downstream. In doing so, the study seeks to assess the direct consequences of ice reduction on the surrounding territory, providing a new approach to understanding the interactions between a huge glacial ecosystem and its adjacent mountain environment.

## 3. Instruments and tools

#### 3.1 Satellite data overview

Satellite imagery is used across a wide range of applications and plays a vital role in monitoring environmental changes, as well as in agriculture, land and natural resources management. Nowadays, issues like land degradation, groundwater scarcity, and other climate-related risks are becoming increasingly severe, highlighting the need for more advanced predictive models. These models can be significantly improved using satellite data [15].

Remote sensing refers to the process of acquiring information about objects or phenomena by detecting electromagnetic radiation, naturally emitted or artificially generated, without making direct contact. These observed signals are then received at the ground stations and digitized as satellite images. Satellite data vary significantly not only in terms of sensing mode, but also in resolution and frequency of acquisition, depending on each satellite's revisit time. These differences are important and must be considered and understood when working with satellite data [15].

In *Figure 6* is illustrated the basic diagram of how satellite imagery works, from data acquisition in orbit to ground-based transmission and processing for analysis.

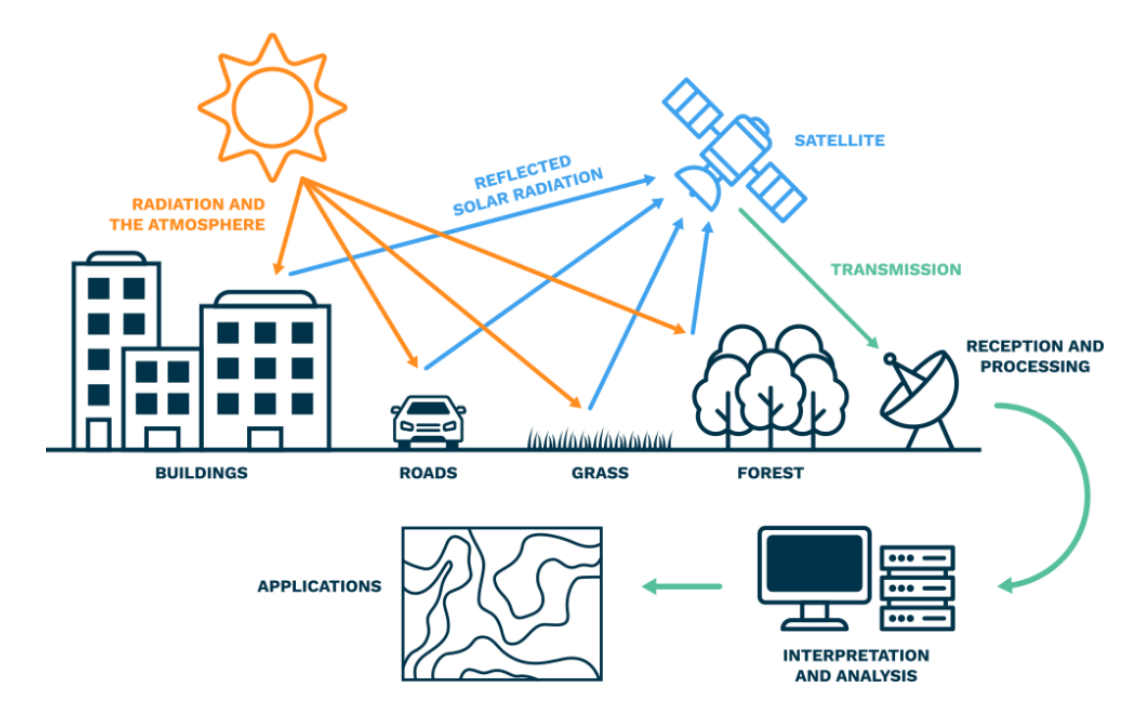


Figure 6: Satellite-based remote sensing diagram. [16]

Basically, satellites are launched into different orbits depending on their purpose, where polar orbits and geostationary orbits are most common for Earth observation, in which satellites respectively pass over the poles allowing for global coverage or remain stable over a specific location. As they travel over a given area, satellites collect data through onboard sensors that detect electromagnetic radiation. The type of data collected depends on the sensor: optical sensors capture visible and infrared light, while microwave sensors can collect information regardless of cloud cover and weather conditions. Once the data is acquired, it is transmitted back to Earth, through radio waves, where a network of ground stations positioned strategically around the world receives it and ensure consistent communication. After transmission, the raw data is processed to obtain useful imagery. This last step includes several procedures like calibration, atmospheric correction, and georeferencing, which assign geographic coordinates to the data so it can be properly visualized in platforms like QGIS [16].

Nowadays, the availability of satellite imagery has grown thanks to the launch of modern satellites with varying specifications, characteristics, and resolutions that are widely used to retrieve data for analysis across different fields. However, despite the numerous possibilities it offers, it also has some drawbacks to consider. In fact, the quality of satellite imagery largely depends on the type of sensors used, which can be affected by weather conditions and often results in lower image quality. Another key limitation in satellite image analysis is the availability of data itself. More advanced satellites can provide high-quality images using improved technologies, but free access to these resources is still limited. Moreover, due to security constraints, images of highly sensitive or strategically important areas are often not freely available to the public [15].

In the context of glacier monitoring, that is the scope of this work, satellite imagery is especially valuable since it offers a reliable and repeatable method for large-area analysis by detecting long-term trends such as ice retreat or seasonal variations. In the following paragraphs will focus on the two types of open-source satellite imagery used for the analysis of this project: MODIS and Sentinel-2.

#### 3.2 MODIS

The Moderate Resolution Imaging Spectroradiometer (MODIS) is a key instrument aboard NASA's Terra (originally known as EOS AM-1) and Aqua (originally known as EOS PM-1) satellites, launched in 1999 and 2002 respectively. Terra follows a sunsynchronous orbit with a 10:30 a.m. equatorial crossing time, while Aqua passes south to north over the equator in the afternoon at 1:30 p.m. This twin-satellite configuration was designed to maximize global coverage by viewing the entire Earth's surface every 1 to 2 days and thereby reducing cloud interference as well as optical effects such as shadows and glare [17].

Regarding the technical specifications, MODIS, with its wide swath of 2,330 km, acquires data in 36 spectral bands, ranging in wavelengths from 0.4 µm to 14.4 µm. These spectral responses have been specifically designed to meet the requirements of the user community, ensuring minimal out-of-band interference. The satellites acquire data at spatial resolutions of 250 m, 500 m, and 1 km, where two bands are imaged at a nominal resolution of 250 m at nadir, five bands at 500 m, and the remaining 29 bands at 1 km. In this way the measurements allow to monitor a broader range of Earth system indicators than any other sensor aboard Terra. These measurements allow a better understanding of global dynamics through a detailed monitoring of land, ocean, and atmospheric processes. MODIS also ensures continuity with earlier instruments like NOAA's Advanced Very High-Resolution Radiometer, contributing to long-term environmental data records. The resulting data products play a vital role for the development and validation of global Earth system models, whose purpose is to predict environmental change and help decision-making at policy level [18].

Between the MODIS instrument components (*Figure 7*), the core of the sensing system is its Scan Mirror Assembly that uses a continuously rotating, double-sided scan mirror capable of scanning  $\pm 55$  degrees. It is driven by a motor encoder designed for continuous operation over the instrument's intended six-year lifespan [18].

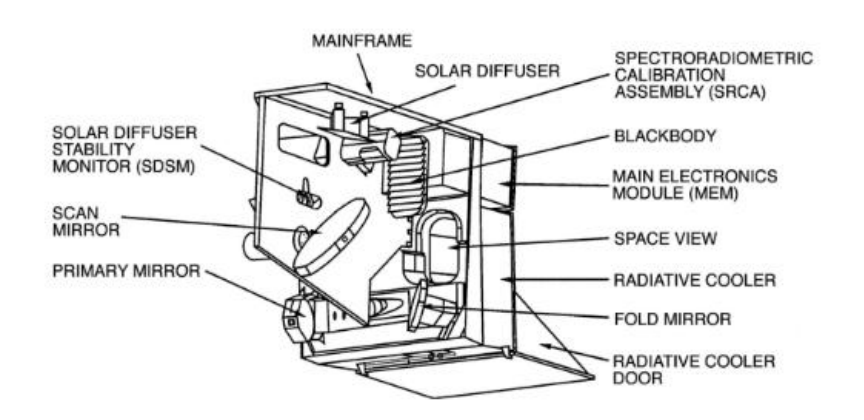


Figure 7: MODIS instrument components. [19]

MODIS continues the legacy of large-scale environmental monitoring by detecting changes in snow and ice cover, vegetation growth cycles, water vapor content, global carbon cycle and the spatial-temporal patterns of natural disasters such as wildfires, droughts, and volcanic eruptions. Its fire-sensitive bands are crucial to distinguish between active flaming and residual burning, giving the right assessment between aerosol and gas emission. MODIS is also used in ocean studies by tracking fluctuations in sea surface temperature and by giving important information for El Niño and La Niña events [20].

#### 3.3 Sentinel-2

Sentinel-2 arises as result of close collaboration between the European Space Agency (ESA), the European Commission, industry partners, service providers, and data users. The mission was designed and built by a consortium of approximately 60 companies, led by Airbus Defence and Space, with support from the French Space Agency (CNES) to optimize image quality and the German Aerospace Centre (DLR) to enhance data recovery through optical communication [21].

The Sentinels are a fleet of satellites specifically designed to provide the vast amounts of data and imagery that are essential to Copernicus, the Earth observation component of the European Union's Space Programme. In particular, the Copernicus Sentinel-2 mission consists of two identical satellites (Sentinel-2A and Sentinel-2B) in the same orbit but with a phase difference of 180° (*Figure 8*) that allows them to cover all Earth's land surfaces, islands and hinterlands [21].

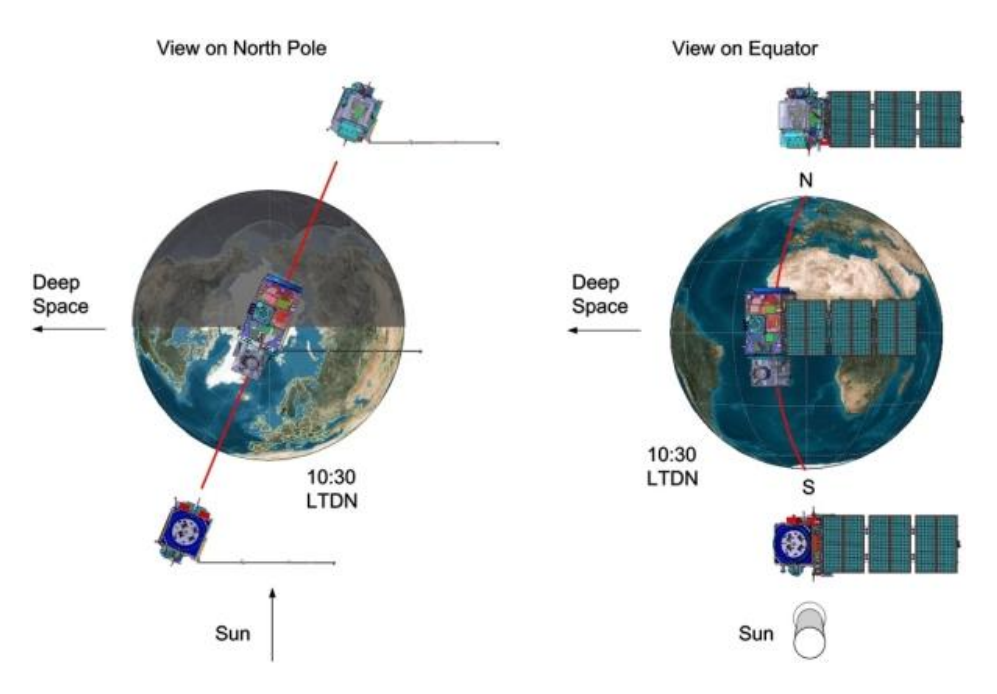


Figure 8: The Twin-Satellite Sentinel-2 Orbital Configuration. [22]

Sentinel-2A was launched on 23 June 2015, followed by Sentinel-2B on 7 March 2017. They were launched using the European VEGA launcher and each of these satellites weighs approximately 1.2 tonnes. On 5 September 2024, Sentinel-2C was launched into orbit to join its counterparts and replace Sentinel-2A, now close to the end of its operational life after a decade, with the goal to ensure the continuous provision of high-resolution data from the mission. After a period of parallel operations, Sentinel-2C officially replaced Sentinel-2A on January 21, 2025. Similarly, Sentinel-2D will eventually take over from Sentinel-2B. Looking ahead, the Sentinel-2 Next Generation mission is set to further enhance global monitoring capabilities and guarantee data continuity beyond 2035 [22].

Regarding the technical specifications, the satellites feature an innovative orbital swath width of 290 km, offering new perspectives on land and vegetation. They are equipped with a single payload: the optical Multi-Spectral Instrument (MSI) (Figure 9) operating at 10, 20, and 60 meters of spatial resolution, distributed across 13 spectral bands, respectively four bands at 10 m, six bands at 20 m, and three bands at 60 m. The mission is designed to achieve a revisit time of 5 days at the equator, ensuring frequent and consistent observations [22].

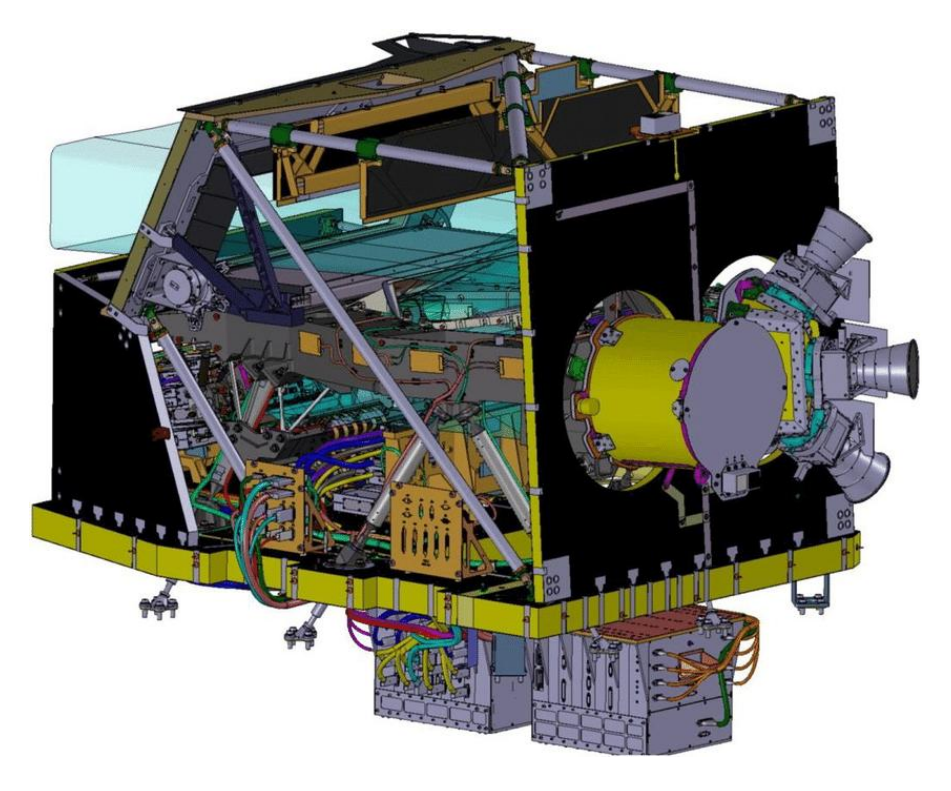


Figure 9: Multi-Spectral Instrument (MSI). [22]

The Sentinel-2 twin satellites deliver valuable image data that carry on the legacy of SPOT and LANDSAT and contribute to ongoing multispectral observations. They support a wide range of Copernicus services and applications, including [23]:

- Land monitoring
- Agriculture
- Emergency management
- Risk mapping
- Security
- Forestry
- Climate change
- Disaster response
- Marine monitoring
- Humanitarian relief operations

The primary goal of the mission is to monitor changes in land surface conditions in order to manage our environment, study and tackle climate change effects and protect daily life. Moreover, it enables the monitoring of plant indices like chlorophyll and water content, which are essential for yield prediction and vegetation analysis. Additionally, Sentinel-2 can be used to track land cover changes and assess pollution in lakes and coastal areas. Its imagery also gives a huge contribution to disaster mapping, including floods, volcanic eruptions, and landslides, aiding humanitarian relief efforts [21].

Sentinel data are open source, meaning that most of the data and information generated by the Copernicus programme are systematically made available free of charge to all users and citizens, as well as scientific and commercial entities globally. The Copernicus Data Space Ecosystem is the primary distribution platform for data from the Copernicus Sentinel missions. Sentinel-2 data, among others, are accessible through a range of APIs as well as via a newly developed, user-friendly interface known as the Copernicus Browser.

Sentinel-2 data are distributed at different processing levels, mainly Level-1C (L1C) and Level-2A (L2A), each corresponding to a specific stage of radiometric and geometric correction. Only Level-1C and Level-2A products are made openly available to users, while Level-1B products are reserved for expert users and accessible upon request. In the following sections, the characteristics and differences between L1C and L2A products are presented in detail.

#### 3.3.1 Level-2A Products

Level-2A products provide atmospherically corrected Surface Reflectance (SR) data, derived from Level-1C inputs. It's important to specify that the term Surface Reflectance replaces the older definition Bottom of Atmosphere (BOA) Reflectance. Each Level-2A product is organized into 110 km × 110 km tiles, following the UTM/WGS84 cartographic projection. Although the grid is based on a 100 km step, tiles are larger to ensure sufficient overlap with adjacent scenes.

The atmospheric correction applied to Sentinel-2 imagery accounts for several effects, including Rayleigh scattering by air molecules, absorption and scattering by

atmospheric gases, in particular ozone, oxygen, and water vapour, as well as absorption and scattering caused by aerosol particles.

In addition to surface reflectance data, Level-2A products include Aerosol Optical Thickness (AOT) maps, Water Vapour (WV) maps, and Scene Classification (SCL) maps. These image products are resampled at different spatial resolutions (10 m, 20 m, and 60 m) and organized in the following way:

- 10 m folder: bands 2, 3, 4, 8, TCI image, AOT and WV maps resampled from 20 m.
- 20 m folder: bands 1–7, 8A, 11, 12, TCI image, SCL map, AOT and WV maps (band 8 is omitted).
- 60 m folder: same as the 20 m folder, with the addition of band 9 (band 10 is omitted due to lack of surface information).

L2A products were initially released as pilot products (L2Ap) in March 2017, and they successively became operational in March 2018 for Europe and globally from December 2018.

Finally, users can generate Level-2A products from Level-1C data using tools such as the Sentinel Toolbox or Sen2Cor.

#### 3.3.2 Level-1C Products

Sentinel-2 Level-1C products are available globally from 2015 onwards. These products provide Top Of Atmosphere (TOA) reflectance images, which are derived from the associated Level-1B products. The Level-1C product is composed of 110 km × 110 km tiles, ortho-images in UTM/WGS84 projection. As for Level 2A, Earth is subdivided into a predefined set of tiles, defined using a 100 km step, although each tile has a surface of 110 km × 110 km to ensure large overlap with the neighbouring. This structure allows for easier temporal analysis and consistency in mapping.

Level-1C products result from the use of a Digital Elevation Model (DEM) to project the image in cartographic geometry. Per-pixel radiometric measurements are provided in TOA reflectance, along with parameters for transforming them into radiances. The formula for the conversion is (Equation 1):

$$radiance = reflectance * cos(Sun Zenith Angle) * Solar Irradiance *  $\frac{U}{\pi}$$$

Equation 1: formula for conversion of reflectance to radiance

#### Where:

- The Sun Zenith Angle value can be found in the metadata of the tile.
- The value of U (scaling factor linked to the Sun-Earth distance) and Solar Irradiance for the considered band can be found in the product metadata.

Level-1C products are resampled with a constant Ground Sampling Distance (GSD) of 10 m, 20 m, or 60 m, depending on the native resolution of different spectral bands. In Level-1C products, pixel coordinates refer to the upper left corner of each pixel.

#### **3.4** ARPA

ARPA Lombardia (Regional Agency for the Protection of the Environment of Lombardy) is the regional public body responsible for environmental monitoring and protection, established under Regional Law 16/1999. It operates with administrative and local institutions in numerous activities such as air and noise pollution control, protection of surface and groundwater, assessment of soil contamination, monitoring of electromagnetic fields and remediation processes [24].

With its consolidated technical and scientific expertise, ARPA collects and processes environmental data necessary to support decision-making by regional and local authorities such as the Lombardy Region, Provinces, Municipalities, Mountain Communities and other public institutions in the territory. Moreover, it also allows citizens and public users to know the state of the environment in which they live with accessible information on environmental quality and other climatic parameters, easy to find and free for everyone [24].

Trough an independent and multidisciplinary approach, ARPA addresses the complexity of environmental challenges by collaborating and interacting with institutions, stakeholders and the scientific community, both at national and international levels [24].

## 3.5 Data processing software

#### 3.5.1 QGIS

QGIS is an open-source Geographic Information System software tool, widely used world-wide since it allows the users to create and share maps, edit layers, process and analyse geospatial data. It can be downloaded for free from the official QGIS website and is compatible with different platforms like Windows, Mac OS, Linux, and even Android [25].

QGIS is developed by a global community of volunteers and organizations with the goal to be inclusive and accessible to everyone. This software is widely used across sectors like education, government, engineering, planning, military and research. Thanks to its international team, QGIS is a worldwide community available in many languages and continents [26].

The software is constantly updated with new versions thanks to an active and engaged developer community, and it's supported by various help channels, mailing lists, and through a global commercial support provider. For the current project was used the QGIS Desktop 3.40.4 version.

One of QGIS's strengths is its high level of customizability, allowing users to adapt the interface and workflows to their specific needs, ranging from custom data input forms to tailored visualizations. Additionally, QGIS is also characterized by extensibility thanks to its C++ core and Python integration, which gives the possibility to develop everything from simple scripts to full applications using the QGIS API [26].

The user can also enhance the functionality of QGIS application with thousands of free additional features and plugins developed by the community that basically grow the number of capabilities and services of the software. It supports a wide range of raster and vector files, database formats and functionalities.

QGIS plays a fundamental role in the management and visualization of satellite data, including both MODIS and Sentinel-2 imagery. These two different types of satellites, as previously mentioned, provide different kinds of data in terms of structure, spatial resolution, and format. Nevertheless, thanks to its flexibility, QGIS offers an environment to process and interpret satellite data from different sources, making it

suitable for both satellite models used for this project. In the case of MODIS, since the data are typically provided in hdf format, QGIS requires an initial step of reprojection from the original sinusoidal coordinate system to UTM in order to be correctly visualized. Sentinel-2 data, on the other hand, are easier to manage in QGIS because they are usually already available in TIF format and in UTM projection as well, being in this case ready to be used in the software immediately without any specific procedure. These initial operations are essential to visualize and prepare data correctly for further analysis. In the next section on Methodology, the workflow for downloading data from MODIS and Sentinel-2 and dealing with them, will be presented and discussed in detail.

#### 3.5.2 MATLAB

MATLAB is a numeric and programming computing platform, widely used in engineering environment and scientific research. It provides a dedicated programming language together with specialized libraries, interactive tools, and specific apps, that make it suitable for different tasks such as image processing, system modelling and data analysis. Furthermore, MATLAB serves as the foundation of the block diagram environment Simulink, designed to simulate complex multi-domain systems. Its applications are widespread across different scientific and industrial fields such as aerospace, energy, automotive, medical devices, earth and ocean sciences, communications and many others. MATLAB is chosen from more than five million users worldwide, particularly from engineers and scientists, startups, academic teachers and researchers, as well as students [27].

For this work, all data processing and statistical analyses were performed in MATLAB R2023b, using a student license provided by MathWorks. The software was employed to analyse and correlate glacier data, specifically area variations over different years, with climate variables such as temperature and precipitation data. By calculating statistical analysis, regression models and graphical representations, it was possible to provide a framework of the correlations and emerging trends between these climatic parameters and glacier surface changes.

# 4. Methodology

## 4.1 Data acquisition workflow for MODIS

Data collected by MODIS are openly available to the public and they can be freely accessed through NASA's Earthdata platform. To access and use MODIS data, users must first register and create a free account on NASA's Earthdata portal, which serves as the main gateway for downloading satellite imagery and related datasets.

The Level-1 and Atmosphere Archive and Distribution System (LAADS DAAC), located in Greenbelt, MD, is one of the twelve Distributed Active Archive Centers (DAACs) within NASA's Earth Observing System Data and Information System (EOSDIS). Primarily, it is specialized in the archiving and distribution of atmospheric products related to clouds, water vapor, and aerosols, as well as key instrument data for NASA, NOAA and European Space Agency (ESA). Secondarily, LAADS DAAC also serves as a backup source for MODIS and Visible Infrared Imaging Radiometer Suite (VIIRS) land products. It is crucial in providing users with access to Level-1 calibrated MODIS data, that are essential for atmospheric and surface monitoring [28].

For the analysis of Adamello glacier and in alignment with the objectives of this thesis, the MODIS Surface Reflectance product (MOD09GA) was selected. This choice was made because atmospherically corrected data were required to accurately represent the true surface conditions of the glacier. The MODIS Surface Reflectance products indeed estimate the spectral reflectance of the Earth's surface as it would appear without atmospheric effects such as scattering or absorption. By removing these atmospheric effects, surface reflectance data provides a more reliable and consistent comparison of multi-temporal observations, which is essential for monitoring long-term environmental changes.

Particularly, the MOD09GA product was selected for this study as it provides atmospherically corrected surface reflectance data on a daily basis, with a spatial resolution of 500 meters. MOD09GA is a daily Level-2G product that offers surface reflectance for Bands 1-7 at 500-meter resolution in a Sinusoidal projection, along with 1-kilometer observation and geolocation metadata. MOD09GA data are already

processed to remove atmospheric effects, ensuring greater accuracy and usability for surface analysis [29].

The decision to operate with 500 m resolution was taken because only Bands 1 and 2 are available at 250 m resolution, while the other Bands are available at 500 m. Since creating an RGB image requires Band 1 (red), Band 3 (blue) and Band 4 (green), it was decided to proceed using the native 500-meter resolution in order to avoid the need to rescale Bands 3 and 4, which are not available at 250 meters. This approach ensures consistency across all bands used in the RGB composition and preserves the radiometric integrity of the image by maintaining data fidelity without unnecessary resampling.

To download the MODIS images for each summer from the year 2000 to 2024, which corresponds to the period of data availability, the following steps were followed. First, an attempt was made to download from Earthdata the images of the Adamello glacier area with the least possible cloud coverage, starting with the month of July if available, and otherwise checking in the following order: August, September, and June. Then, the downloaded file with the .hdf (Hierarchical Data Format) extension was opened, and only bands 1, 3, and 4 were selected, which are the ones needed to create the true colour image.

After that, to build the color image, the following steps were taken: Raster > Miscellaneous > Build Virtual Raster, selecting the three bands as input layers in this order: band 1, band 4, and band 3. After ticking "Place each input file into a separate band", the process was run.

In this case, using an HDF file instead of a standard TIFF is not a problem because HDF files store all the relevant MODIS data, like reflectance bands, quality information, and metadata, in one structured container. Since only bands 1, 3, and 4 are needed to generate the RGB image, they can be extracted directly as raster layers in QGIS without losing information or quality. This procedure allows selecting only what's needed while keeping the original dataset intact.

Another aspect to consider when dealing with MODIS data in QGIS is the Coordinate Reference System, because they are originally provided in the Sinusoidal projection (ESRI:54008), which is not ideal for regional analysis or mapping. For this reason, it is necessary to set the correct CRS of the virtual layer. After loading the HDF file, the user has to right-click on the layer and go to Properties > CRS and then set the CRS to ESRI:54008 - World Sinusoidal, which is the original projection of MODIS data. After this step, the layer can be reprojected into EPSG:32632 WGS 84 UTM zone 32N using Raster > Projections > Warp (Reproject). This ensures the data are processed and shown in the right coordinate system.

EPSG:32632 refers to the WGS 84 UTM Zone 32N projection. WGS 84 (World Geodetic System 1984) is a global reference system for geographic coordinates, and UTM (Universal Transverse Mercator) is a projection that divides the world into 6-degree zones. Zone 32N includes parts of central Europe, particularly regions of northern Italy like Lombardy and Trentino-Alto Adige, as well as parts of southern Switzerland, western Austria, and surrounding areas. Therefore, it is a suitable zone for the study of the area of the Adamello glacier located there.

The choice to set "bilinear resampling method" was taken to keep smooth transitions between neighbouring pixel values and to optimize the visual quality of the satellite images without adding obvious artifacts. This method is particularly suitable for continuous data such as surface reflectance, which is typical in MODIS images. After running the process, the final image was exported and saved as a GeoTIFF file, ready for use.

## 4.2 Data acquisition workflow for Sentinel-2

The user logs into the Copernicus browser and, in the search section, selects *Sentinel-2, Level-2A*, and sets the cloud cover filter to 50%. The search for data begins in July; if no suitable images are found, the search continues in August, September, and June, in that order, selecting the image with the best definition and least cloud cover for the Adamello glacier area. In this case, the images were downloaded from the Copernicus Browser in TIFF format (32-bit float) with high resolution to ensure precision in the representation of reflectance values.

For this analysis, Level-2A products were chosen because they are already corrected for atmospheric effects as previously mentioned, making them suitable for surface analysis without the need for additional pre-processing and simplifying the workflow.

After downloading the .zip file, the user navigates into the unzipped folder, enters the *GRANULE* directory, then *IMG\_DATA*, and selects Band 2, Band 3, and Band 4 from the R10 folder. The 10-meter resolution bands were selected to ensure the highest possible spatial detail.

The next step is to create the true colour image. As previously done for MODIS, the procedure is identical: the user goes to *Raster*, *Miscellaneous*, and selects *Build Virtual Raster*. The bands are added in the order Band 4, Band 3, Band 2 to generate a correctly rendered RGB image. This selection is important because it ensures that the images closely resemble what would be seen by the human eye. After checking the option *Place each input file into a separate band*, the process is run.

At this point, the image appears as it would to the human eye, and the user can proceed to export and save it as a GeoTIFF file. This workflow is repeated for the consecutive years from 2015 to 2024, selecting the best available summer image for each period.

## 4.3 Comparison between MODIS and Sentinel-2

It is clear from the procedure carried out and from the available images that the quality and resolution of MODIS data are significantly lower compared to Sentinel. Contrary to what one might think, the availability of data from the year 2000 onwards is certainly a valuable resource, but for an analysis of this type, the insights that can be obtained are not particularly specific or reliable, mainly due to the relatively low spatial resolution of 500 m over an area like the Adamello Glacier. Therefore, having access to around 25 years of data does not necessarily mean a high-quality long-term surface change analysis, as these limitations must be considered when using MODIS for areas of this size.

On the other hand, the strong point of Sentinel is exactly its resolution: at 10 meters, it offers significantly better quality and allows for a much more accurate and reliable analysis compared to MODIS. In fact, even though some interpretation challenges such as distinguishing between ice and rock remain, the process of outlining the glacier's boundary is generally easier and more precise. The drawback of Sentinel, however, is its limited temporal availability, which only begins in 2015 as mentioned in the previous section. This limitation obviously prevents long-term surface change analysis, since it doesn't allow going as far back in time as MODIS does.

Another aspect previously mentioned in the data download workflow is that Sentinel-2 images are already provided in the UTM projection, so they don't require any correction, as they are already aligned with the correct reference system. On the other hand, MODIS data, available in .hdf extension, use a sinusoidal projection and therefore need to be reprojected to UTM to avoid spatial mismatches and ensure proper data processing. This additional step, of course, requires more time when preparing the data for analysis.

MODIS offers longer temporal coverage but a lower spatial resolution (250–1000 meters), making it more suitable for long-term trend analysis over large areas worldwide where specific details are not required. Sentinel-2, by contrast, provides higher spatial resolution (10-60 meters), making it better suited for detailed, localized studies, offering more accurate and reliable data for specific regions. Therefore, although it can be applied to different parts of the world, it was initially developed with a focus on Europe, and it is widely used across this mainland. Thus, Sentinel-2 excels in detailed, localized analysis, whereas MODIS is better for global, large-area assessments.

### 4.4 Delineation of contour

After the data search and download process, the actual analysis of the glacier area began, with the aim of observing and quantifying its changes over time. To achieve this, two different approaches were applied to three selected years: 2015, which is the first year with available imagery from both MODIS and Sentinel-2, 2020, and 2024, maintaining a consistent time interval to allow for meaningful comparisons.

A preliminary step involved reducing the size of the original satellite images to facilitate processing. This was done using QGIS by creating a polygon shapefile that delineated a small area of interest containing only Adamello glacier. This shapefile was then used to extract the relevant portion of the original image. The process involved opening both the image and the shapefile, navigating to *Raster* > *Extraction* > *Clip Raster by Mask Layer*, setting the original image as the input layer and the polygon as the mask layer, defining the appropriate CRS, and running the operation. The resulting clipped raster was saved as a new file. This procedure was carried out for both MODIS and Sentinel-2 images for all three selected years.

Once the images were prepared, the glacier perimeter for the year 2015 was delineated using two distinct approaches: manual visual interpretation and a semi-automated pixel classification based on spectral thresholds.

In the first method (visual method), the glacier outline was manually traced by setting the image scale to 1:100,000 and maintaining this fixed scale throughout the digitization process. A polygonal area was then created by visually identifying and including pixels considered part of the glacier, based on colour contrast and relying on human perception and empirical judgment to distinguish ice from the surrounding terrain.

The second method (automatic method) involved analysing the intensity values of the three RGB image bands to identify ice-covered areas. Threshold values for each band were manually defined to represent the limit of glacial ice by choosing as pixel as reference one. The *Raster Calculator* in QGIS was then used to apply these thresholds using the expression (*Equation 2*):

$$((band1 \ge value1) \ OR \ (band2 \ge value2) \ OR \ (band3 \ge value3))$$

Equation 2: Raster calculator expression for selecting only wanted pixels

Here, band1, band2, and band3 represent the red, green, and blue channels, with value1, value2, and value3 as the thresholds for identifying ice pixels. The formula enabled the software to classify all pixels meeting at least one of the specified conditions as part of the glacier, with the OR operator used intentionally instead of AND.

The following *Table 1* reports the threshold values of the selected spectral bands for each year, for both MODIS and Sentinel-2 imagery. Specifically, for the years 2020 and 2024, before determining new threshold values, the glacier area was first calculated using the band values established for 2015, which was taken as the reference year for comparison purposes.

Table 1: band values for 2015, 2020 and 2024 both for MODIS and Sentinel-2

Satellite:	MODIS		Sentinel-2			
Years:	2015	2020	2024	2015	2020	2024
band 1	0.5463	0.5472	0.5221	7424	7264	7068
band 2	0.5187	0.5179	0.4574	6888	7480	6636
band 3	0.4323	0.464	0.3492	6596	7564	5816

Subsequently, the same method was also applied to a winter month, specifically March 2020, to analyse the glacier's condition during the winter season and compare its maximum extent with that observed in the summer months. For this purpose, the spectral band threshold values previously determined for the year 2020 were used, both for MODIS and Sentinel-2.

After generating the area containing the selected pixels based on the defined threshold values using the Raster Calculator, the next step was to convert the raster file into a vector file by navigating to *Raster* > *Conversion* > *Polygonize* (*Raster to Vector*) and executing the operation.

To finalize the selection process and extract only the areas that meet the desired conditions from the binary raster, the polygonised shapefile needed to be filtered using the attribute field named "DN", which stands for Digital Number and represents the raw pixel value recorded by the satellite sensor. This field contains the raster values, where 1 indicates pixels that satisfy the logical condition, and 0 represents all other areas. By right-clicking on the resulting raster layer, selecting *Filter*, and entering in the provider-specific filter settings the expression DN = 1, only the relevant pixels satisfying the conditions were retained, excluding the background or outer frame generated during raster-to-vector conversion. The final output was then exported and saved as a shapefile format.

This entire process, including both manual and semi-automated methods, was repeated for the Sentinel-2 imagery of 2015, and subsequently for the years 2020 and 2024 across both satellite datasets.

After concluding the first analysis for the years 2015, 2020, and 2024 using both MODIS and Sentinel-2 data, a second analysis was carried out to obtain a more accurate and reliable evaluation of glacier variation over time. This time, only Sentinel-2 satellite images were considered, due to their higher resolution and better visualization capabilities in QGIS compared to MODIS. The key difference in this second phase was the addition of two intermediate years, specifically 2018 and 2022, to get a more detailed temporal assessment at two-year intervals. Also in this case, both methods (automatic and visual) were used to delineate the contours. Regarding the automatic method, the selected threshold values of the 3 spectral bands for 2018 and 2022 are reported in *Table 2*.

Table 2: band values for 2018 and 2022 for Sentinel-2

Satellite:	Sentinel-2	
Years:	2018	2022
band 1	6048	6492
band 2	6060	6316
band 3	5928	6192

This further procedure allowed to investigate glacier surface changes over shorter periods, which was crucial to observe surface changes more gradually and better understand the glacier's evolution and short-term variations, that may otherwise be overlooked in longer time spans.

#### 4.5 Glacier area calculation

To calculate the areas of the previously determined contours for both MODIS and Sentinel, the polygonal shapefiles were opened in QGIS. By accessing the attribute table of the vector layer, it was possible to view the area of each selected contour in square meters (m<sup>2</sup>), which was then converted into square kilometers (km<sup>2</sup>) for clearer and more meaningful representation.

This procedure was feasible in cases where the contours consisted of a single or a few coherent pixel clusters, as typically seen in the MODIS data and in visual methods, where a unique polygonal contour was manually created both for MODIS and Sentinel-2. In cases involving only a few clusters, the individual area values were simply summed to obtain the total area of the glacier contour.

On the other hand, the automatic method for Sentinel-2 contours presented a different situation, as the glacier outline appeared fragmented into numerous isolated pixel groups. In such cases, summing all the individual areas was not considered a convenient method. Instead, the *Field Calculator* tool in the attribute table of the vector layer selected was used to create a new field representing the area of each polygon. In this way, by entering the expression "\$area" and selecting decimal field type, a new column with all the area values of each individual cluster was added to the attribute table.

After that, by going to *Processing* > *Toolbox* and selecting *Basic Statistics for Fields* it was possible to calculate the statistics for the input layer and particularly by choosing "area mq" as the target field. The tool then provided different statistical measures, including the sum, which corresponds to the total area of all polygons combined.

These procedures were used for calculating the glacier area values for different years, allowing for temporal analyses to evaluate the changes along time and to make comparisons and different combinations that will be discussed in the "Results" section.

## 4.6 Data acquisition workflow for ARPA Lombardia

After the glacier surface analysis performed in QGIS, the next step of this work was to correlate the calculated glacier areas with climatic variables, in order to investigate possible relationships between surface changes and environmental parameters. For this purpose, climate data were retrieved from the ARPA Lombardia website, already introduced in Chapter 3.4. The procedure consisted of accessing the "Data and Indicators" section, selecting "Meteo and Climate", and then filling in the "Automatic

Data Request Form". Through this interface, it was possible to specify the province of Brescia, the Edolo Pantano d'Avio monitoring station, located just below Adamello Glacier, and the desired parameters of temperature and precipitation. Finally, by selecting the period of interest, the requested data were automatically delivered via email in CSV format within a few minutes.

# 4.7 Temperature and Precipitation correlations with Glacier area

To perform statistical analyses and investigate possible correlations between environmental data and glacier surface changes, temperature and precipitation data were retrieved from the monitoring station closest to Adamello Glacier. Specifically, the Edolo - Pantano d'Avio station was selected (dot yellow in *figure 10*), located in Upper Val Camonica just below Adamello Glacier, at an altitude of 2108 m a.s.l. The station, which lies in the Province of Brescia near Lake Avio, has been operating since 1 May 1993 [30].

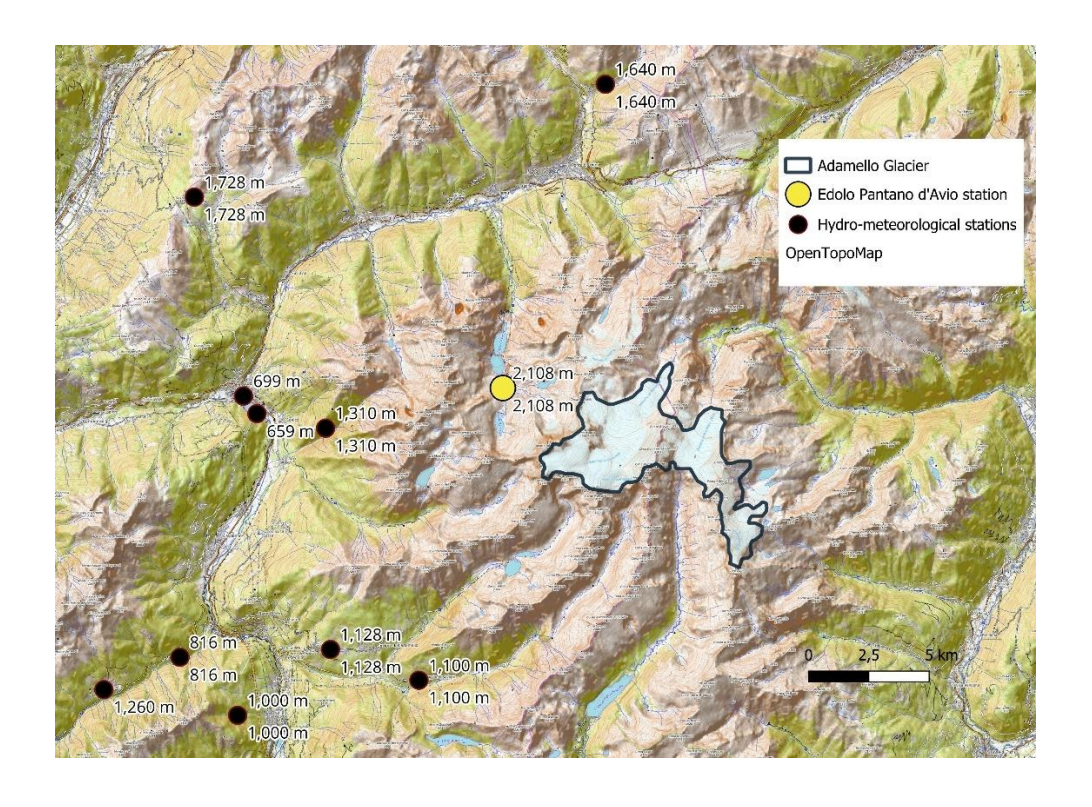


Figure 10: Edolo-Pantano d'Avio monitoring station chosen for retrieving data for the analyses

Before starting the correlation with glacier area, temperature and precipitation data, respectively in mean °C/day and mm/day, were analysed to better understand and observe the general trends of these two variables over the last ten years. Therefore, to obtain an overview in the selected area, both temperature and precipitation data were processed in MATLAB to calculate the time series of daily mean values for each year, obtaining a seasonal trend over the ten-year period for which Sentinel-2 images were available. Furthermore, to highlight the underlying seasonal trends, a 30-day moving average was computed by smoothing short-term fluctuations. In conclusion, a seasonal mean curve, obtained by averaging across all years, was plotted for each day of the month to represent the profile of typical temperatures and precipitation values. As regards the analysis of precipitation data, it is important to note that, unlike temperature, only the period from October to March was considered for calculations. This choice was made because it represents the most significant winter season in the Alpine region and corresponds to the months when the largest amounts of snowfall usually occur. For this reason, it is considered the most appropriate period which directly contributes to the glacier mass balance.

Subsequently, the aim was to correlate the precipitation and temperature records obtained from ARPA with the glacier surface changes calculated through QGIS in the previous chapter, to assess possible relationships and evaluate whether climate variations have an impact and influence glacier dynamics over the years. To carry out this analysis, MATLAB was used to examine the biennial periods previously defined for the calculation of glacier area variations, specifically 2015-2018, 2018-2020, 2020-2022, and 2022-2024. For this purpose, glacier surface changes derived from both the automatic and visual methods were considered, while mean summer temperature and cumulative precipitation values for each biennial period were calculated and used as references for the analyses. In particular, the choice to use the mean summer temperature (June - August) was taken because during the warm season, the largest part of glacier ablation usually occurs, and therefore it is a proxy for melt.

In the first step, Glacier delta area and biennial temperature and precipitation were plotted in the form of time series plots with dual y-axes. On the left axis, the biennial glacier area change, while on the right axis either the mean biennial temperature or the total accumulated biennial precipitation was displayed. The figures allow the visualization of how the different curves evolve across the biennial periods and whether phases of stronger glacier reduction coincide with warmer or drier conditions.

In addition, to explore these relationships more directly, scatter plots were also generated to visualize these correlations more directly. Therefore,  $\Delta$ Area (in km<sup>2</sup>) was plotted against biennial temperature (°C) and biennial precipitation (mm). Then, in both cases, to see the potential correlation between the two variables, a regression line was added in the plots. In these graphical representations, it is possible to identify whether a linear relationship exists and in which direction it goes, positive or negative.

In the third step, linear regression models were computed to evaluate the significance of the correlations and to analyse how well the data fit. Specifically, the two models  $\Delta$ Area-Temperature and  $\Delta$ Area-Precipitation were tested and used to assess the role of these variables in explaining glacier surface variations. The outputs included regression lines with their confidence bounds, providing a visual interpretation of the relationships. In addition, several statistical indicators were calculate to evaluate the reliability of the analysis: the Root Mean Squared Error (RMSE), which expresses the average deviation of observed data points from the regression line; the coefficient of determination ( $R^2$  and adjusted  $R^2$ ), which indicate how much the climate variables can explain the variance in glacier area change; and significance tests (F-statistic and p-value), which evaluate whether the observed relationships can be considered statistically reliable. These parameters served as a basis for assessing the potential correlations between glacier dynamics and climate variability, while the detailed interpretation of the trends is presented in the Results section (5.3).

The next step needed to achieve a more meaningful statistical analysis, was to consider the entire ten-year period from 2015 to 2024. This aim required calculating the glacier surface also for the years missing from previous tasks, using only the automatic method. The objective of this step was to repeat the same statistical analysis as before, through the scatter plots and the linear regression models, but this time with a larger dataset. The goals were, first, to verify whether increasing the number of data would lead to more statistically robust conclusions, and second, to determine which variable, between precipitation and temperature, had the strongest impact on glacier area.

# 5. Results and discussion

## 5.1 Initial analysis of Glacier area variation

The following paragraph presents the glacier area values calculated for the years 2015, 2020, and 2024, for the two different methods (automatic and visual) previously described in the 4.4 section. In addition, tables showing the percentage variations in glacier surface area between the considered years are provided. To support these data, graphical outputs are also provided, including the area overlays produced in QGIS. These visual representations help to better illustrate the concept and enhance the understanding of the results from a graphical perspective as well.

The most significant results that are noteworthy and stand out when observing *Table 3* and particularly *Table 4* concern the automatic method, which shows a substantial decrease in glacier area from 2015 to 2020: specifically, –41.84% for MODIS and –59.92% for Sentinel-2. In particular, the glacier area reduction detected using the automatic MODIS method (*Figure 11*) is equivalent to 11.71 km², which corresponds to approximately 1,640 football fields (7,140 m²) and is nearly equal to the surface of Monte Isola (12.61 km²) in Lake Iseo. Similarly, regarding Sentinel-2, the reduction in glacier area amounts to 22.34 km² (*Figure 12*), which in practical terms corresponds to approximately 3,130 football fields or about 17,870 Olympic swimming pools. This reduction is roughly 25% of the surface area of the city of Brescia (90.34 km²) and about 34% of the surface area of Lake Iseo (65.3 km²)

Table 3: Area (km²) for years 2015, 2020, 2024 using both methods (Automatic and Visual)

	Area (km²)		
Years	MODIS	Sentinel-2	Methods
2015	27.98	37.29	
2020	16.27	14.94	Automatic
2024	26.59	32.62	
2015	30.01	32.04	
2020	24.64	23.58	Visual
2024	22.42	25.71	

Table 4: Area variation (%) for years 2015, 2020, 2024 using both methods (Automatic and Visual)

	Area variation (%)		
Years	MODIS	Sentinel-2	Methods
2015 - 2020	-41.84	-59.92	
2020 - 2024	63.41	118.31	Automatic
2015 - 2024	-4.96	-12.51	
2015 - 2020	-17.88	-26.40	
2020 - 2024	-9.02	9.04	Visual
2015 - 2024	-25.29	-19.75	

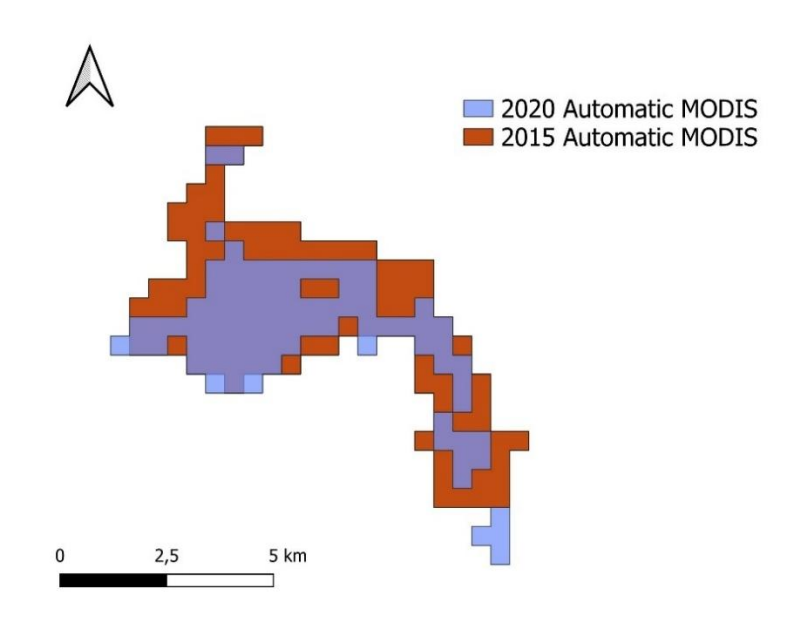


Figure 11: Area variation between 2015 and 2020 for MODIS (Automatic method)

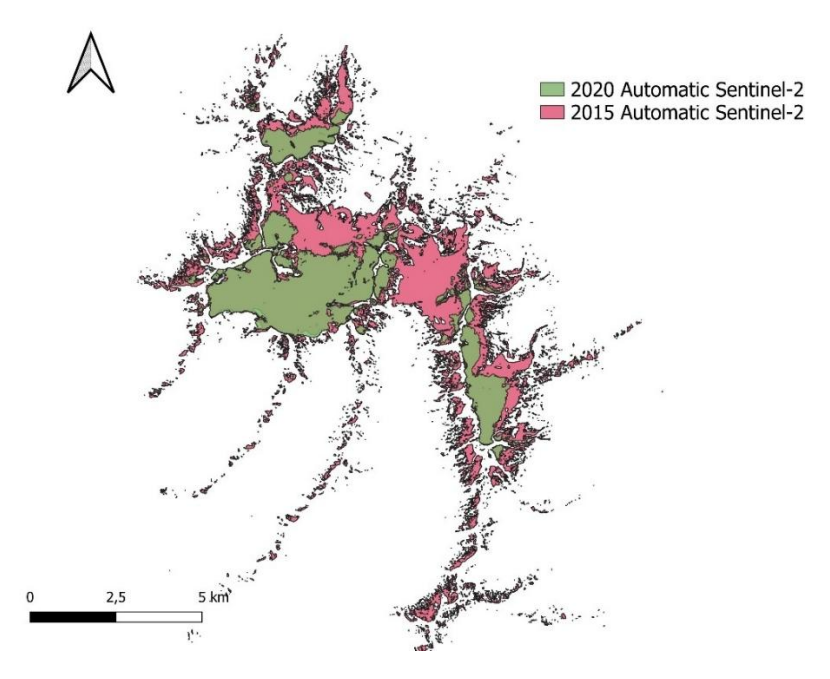


Figure 12: Area variation between 2015 and 2020 for Sentinel-2 (Automatic method)

This marked reduction, however, is followed by an opposite trend, where both methods indicate instead an increase in glacier surface area of +63.41% for MODIS (*Figure 13*) and even +118.31% for Sentinel-2 (*Figure 14*) in the period from 2020 to 2024.

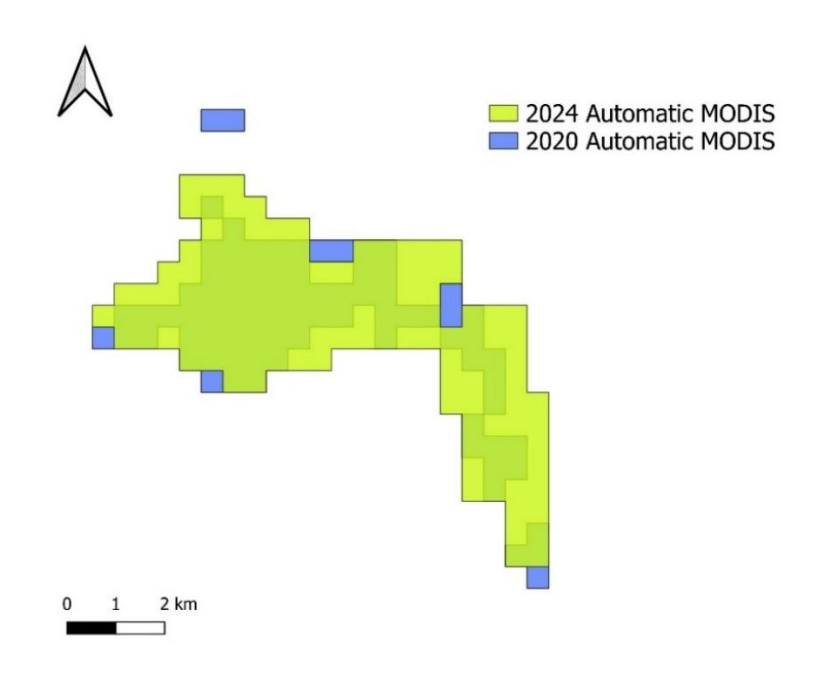


Figure 13: Area variation between 2020 and 2024 for MODIS (Automatic method)

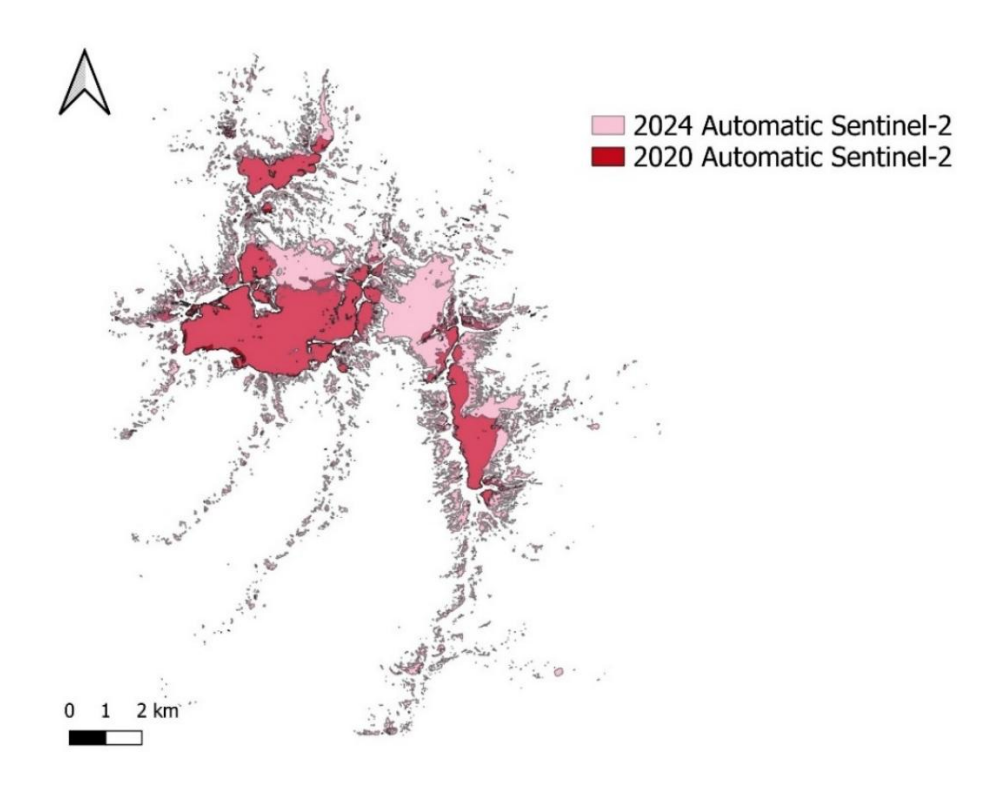


Figure 14: Area variation between 2020 and 2024 for Sentinel-2 (Automatic method)

This case highlights how the use of the automatic method is characterized by a high margin of error, since it is based on assigning pixel colour values above a certain threshold to the glacier class, while those below the threshold are classified as non-glacier. This approach can sometimes lead to misinterpretations, where a specific shade of grey may be considered as rock when instead it represents ice, or vice versa.

As concerns the visual method, for MODIS a clear decreasing trend is visible, which is more pronounced between 2015 and 2020 (–17.88%) compared to the period from 2020 to 2024 (–9.02%), as can be seen in *Figures 15* and *Figure 16*, respectively. The reduction in glacier area over the 9-year period considered (2015-2024) amounts to 7.59 km², which is approximately equivalent to 1,063 football fields or about 12% of the surface area of Lake Iseo.

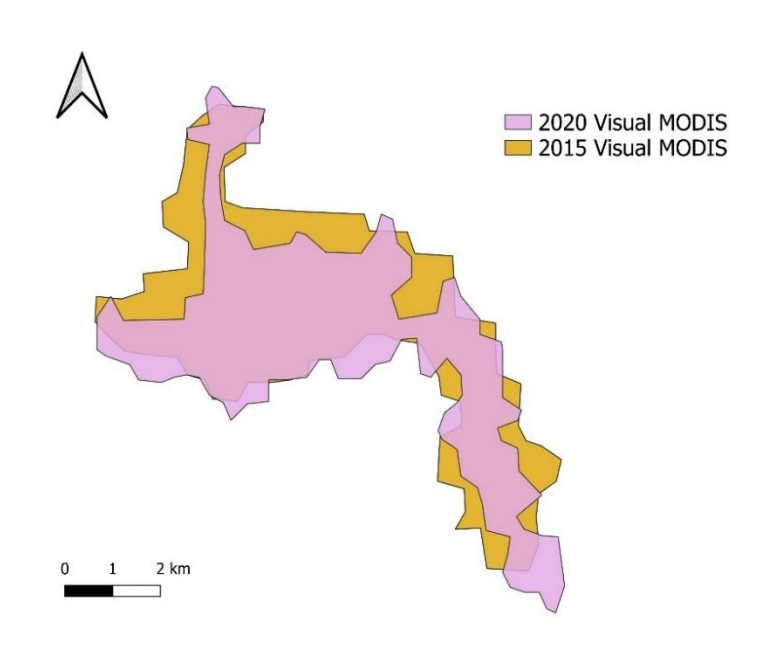


Figure 15: Area variation between 2015 and 2020 for MODIS (Visual method)

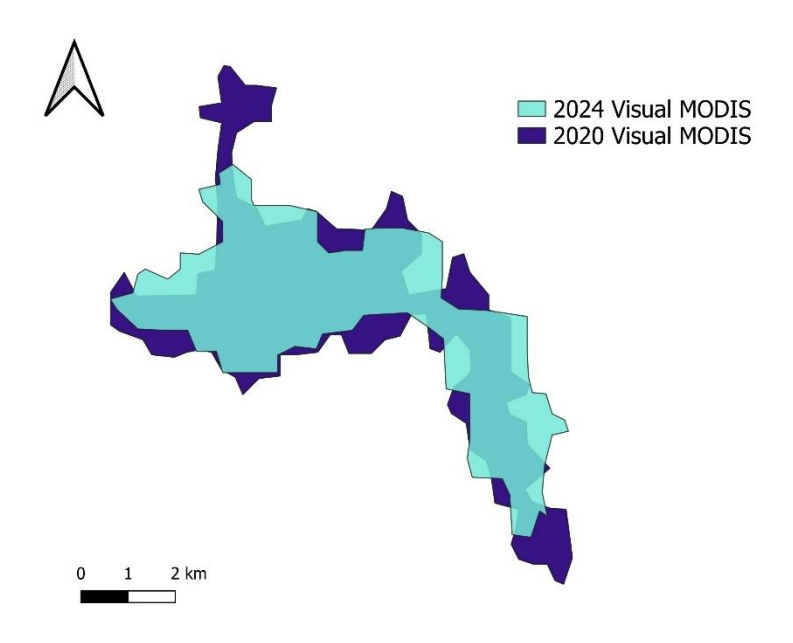


Figure 16: Area variation between 2020 and 2024 for MODIS (Visual method)

Regarding Sentinel-2, the overall trend from 2015 to 2024 also shows a decrease, presented in *Figure 17* and equivalent to –19.75%, but a slight increase (+9.04%), in glacier surface area is observed between 2020 and 2024 (*Figure 18*) which disagrees with the MODIS results. In this case, the overall decrease (2015-2024) is equal to 6.33 km², which corresponds to approximately 886 football fields or about 5,064 Olympic swimming pools.

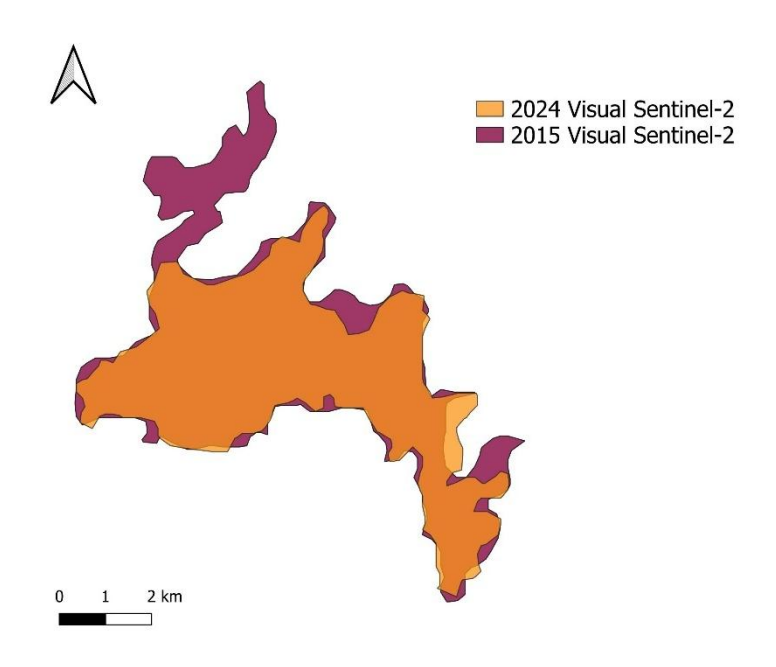


Figure 17: Area variation between 2015 and 2024 for Sentinel-2 (Visual method)

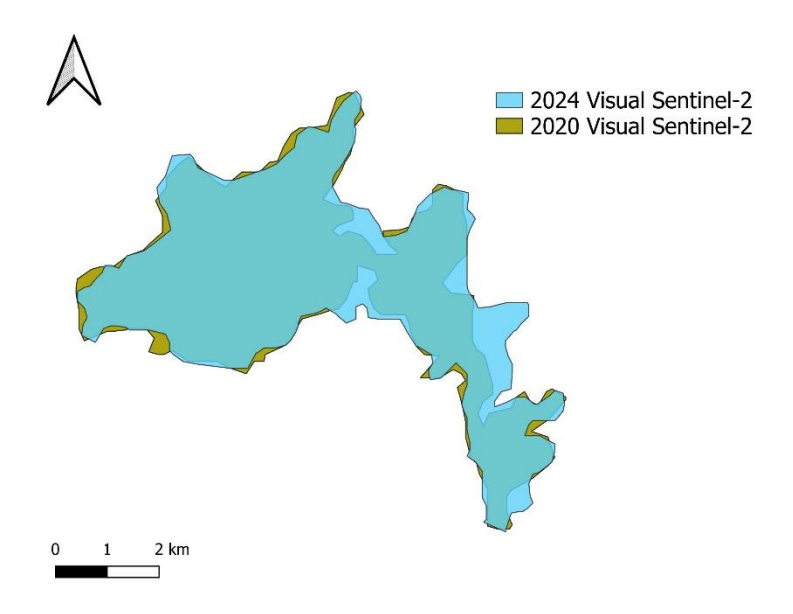


Figure 18: Area variation between 2020 and 2024 for Sentinel-2 (Visual method)

In any case, the area variation results obtained through the visual method appear more moderate and reliable than those obtained using the automatic method. This highlights how the operator's eye and sensitivity in distinguishing individual pixels and accurately outlining the glacier can, on the one hand, lead to personal and subjective interpretations, but on the other hand, allow for a better distinction between rock and glacier ice. Through this approach, it is possible to correctly identify portions of the glacier that may be more difficult to delineate and could be misclassified by the automatic method.

Considering now the variation in glacier area within the same year between the two satellite constellations (*Table 5*), the largest increase, equal to 9.30 km<sup>2</sup> (+33.25%), occurred in 2015 when moving from MODIS to Sentinel-2, using the automatic method (*Figure 19*). A similar increase (*Figure 20*) was observed in 2024 (+22.67%), while in 2020 there was a slight decrease (–8.17%), as reported in *Figure 21*. These results suggest that, in general, the automatic method applied to Sentinel-2 tends to include additional patches, such as isolated snow or disconnected glacier fragments, once the pixel range is set. This did not happen in 2020, possibly due to a suboptimal choice of the white shade threshold by the operator, an issue that can also occur with the automatic method itself.

Table 5: Area variation (%) between MODIS and Sentinel-2 for the same year (2015, 2020, 2024)

	Area variation (%)	
Years	<b>MODIS vs Sentinel-2</b>	Methods
2015	33.25	
2020	-8.17	Automatic
2024	22.67	
2015	6.77	
2020	-4.31	Visual
2024	14.69	

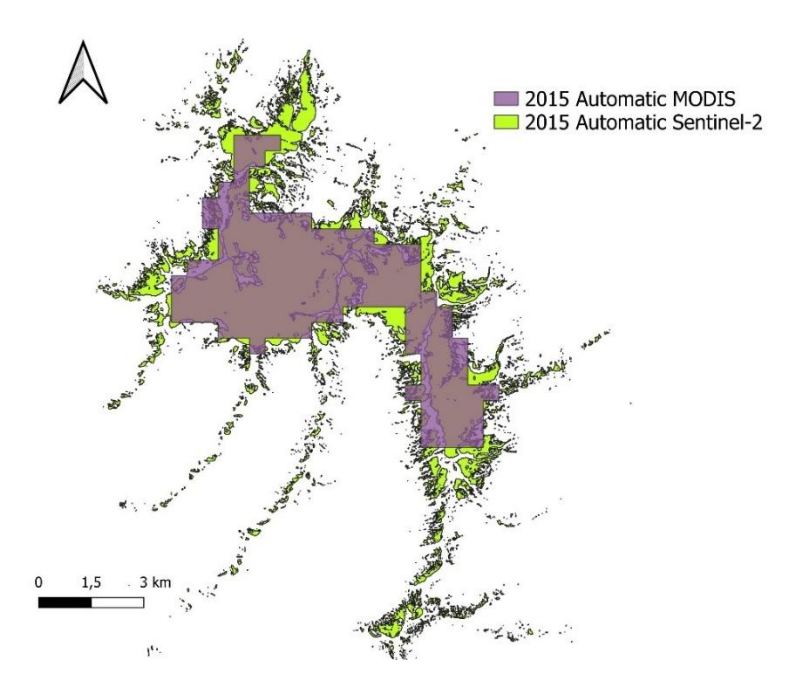


Figure 19: Area variation (%) between MODIS and Sentinel-2 in 2015 (Automatic method)

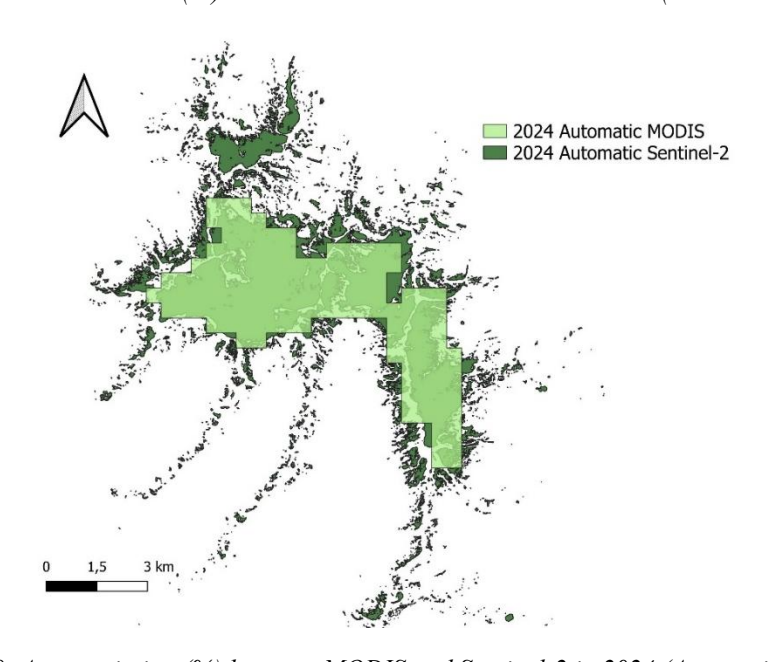


Figure 20: Area variation (%) between MODIS and Sentinel-2 in 2024 (Automatic method)

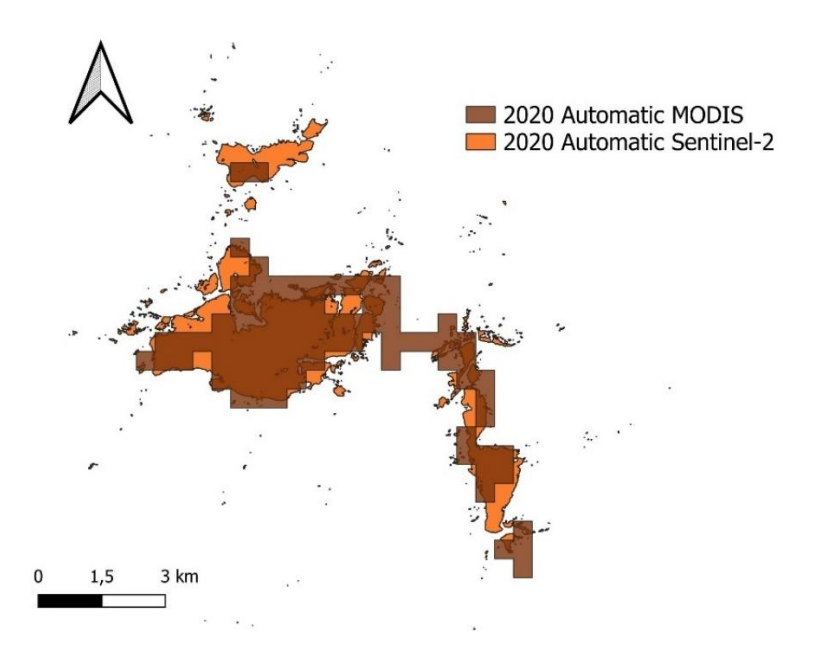


Figure 21: Area variation (%) between MODIS and Sentinel-2 in 2020 (Automatic method)

Regarding the visual method, similar results were obtained, though with more moderate values: +6.77% for 2015, -4.31% for 2020, and +14.69% for 2024, always considering the same year and the comparison between MODIS and Sentinel-2. The graphical outputs are shown in *Figures 22*, 23, and 24, respectively.

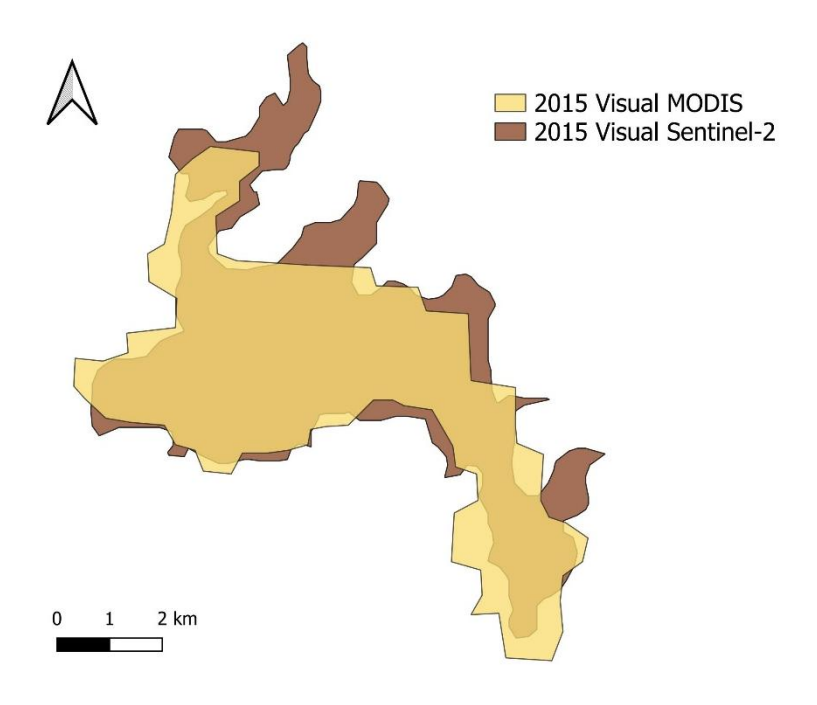


Figure 22: Area variation (%) between MODIS and Sentinel-2 in 2015 (Visual method)

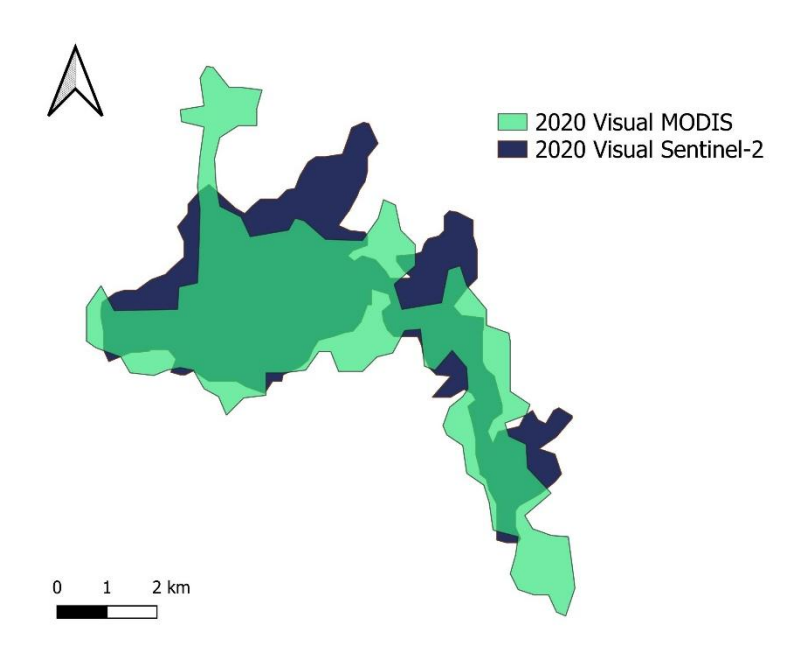


Figure 23: Area variation (%) between MODIS and Sentinel-2 in 2020 (Visual method)

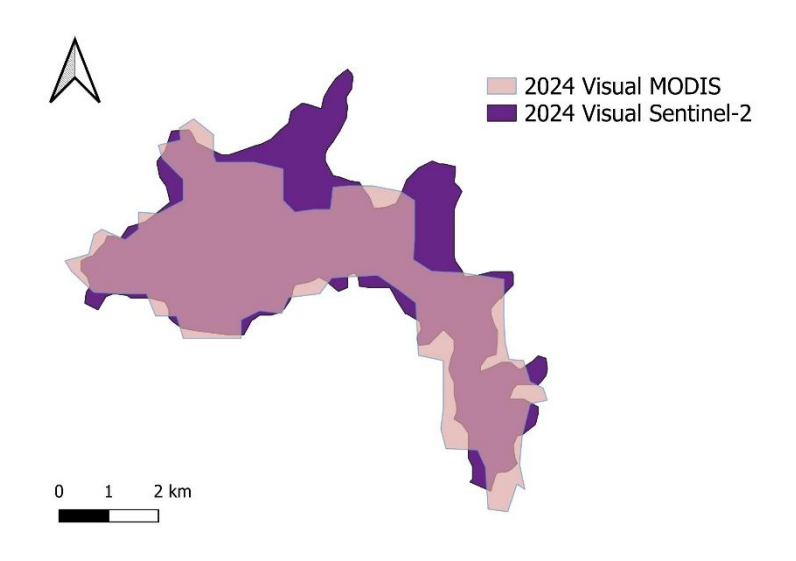


Figure 24: Area variation (%) between MODIS and Sentinel-2 in 2024 (Visual method)

To conclude the cross-analysis, a comparison was also carried out between the automatic and visual methods for the same year and the same satellite constellation. As shown in *Table 6*, the smallest variations were observed in 2015 (+7.22% for MODIS and –14.09% for Sentinel-2).

Table 6: Area variation (%) between Automatic and Visual method for the same year (2015, 2020, 2024)

	Area variation (%)		
Methods	Sentinel-2	MODIS	Years
	-14.09	7.22	2015
Automatic vs Visual	57.78	51.40	2020
	-21.20	-15.71	2024

This was not the case in 2020, when a significant increase in glacier area occurred when shifting from the automatic to the visual method, with a difference of +51.40% for MODIS (*Figure 25*) and +57.78% for Sentinel-2 (*Figure 26*).

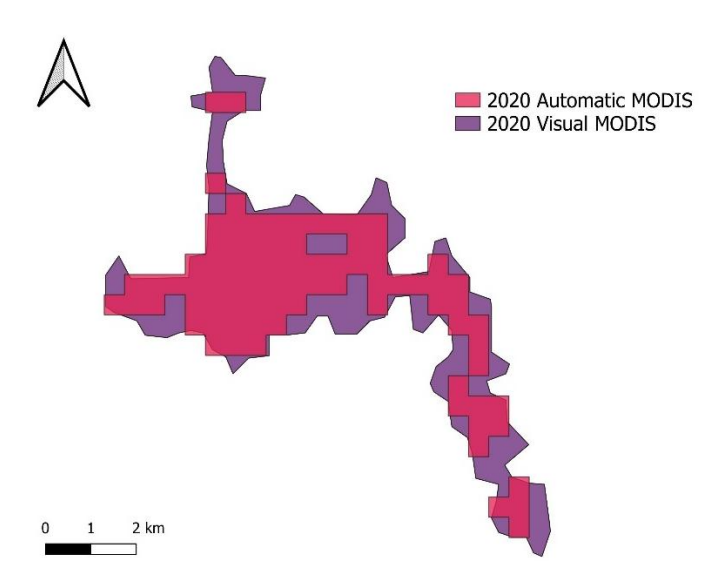


Figure 25: Area variation (%) between Automatic and Visual methods for MODIS in 2020

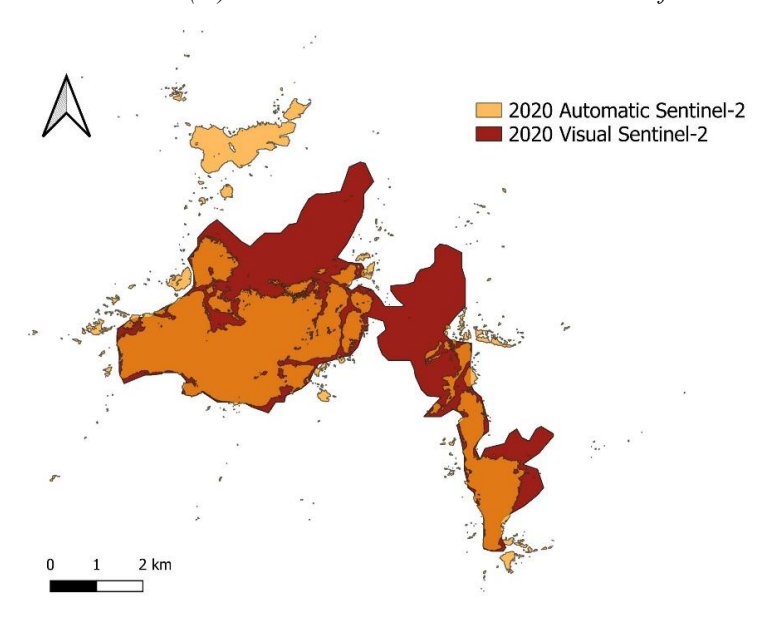


Figure 26: Area variation (%) between Automatic and Visual methods for Sentinel-2 in 2020

Finally, in 2024, both datasets showed a reduction in area: –15.71% for MODIS and – 21.20% for Sentinel-2. In particular, for Sentinel-2 in 2024, *Figure 27* clearly shows that the main difference between the two methods lies in whether or not Mandrone glacier tongue is included: it was classified as bare rock by the automatic method, while it was correctly identified as part of the glacier in the visual method thanks to the operator's knowledge and manual delineation of the contour.

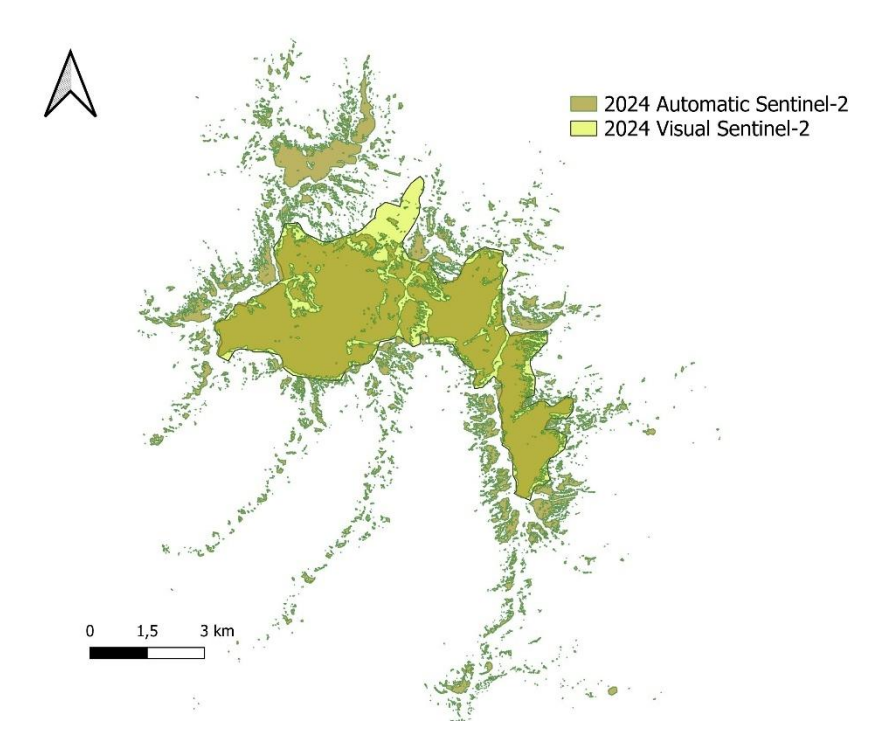


Figure 27: Area variation (%) between Automatic and Visual methods for Sentinel-2 in 2024

Then, as an additional analysis, the band range used for the year 2015 was taken as a reference, and the glacier area for 2020 and 2024 was calculated for both MODIS and Sentinel-2 using this reference range with the automatic method. The results for both the area values and the area variations are presented in *Tables 7* and 8, respectively.

Table 7: Area (km²) for years 2015, 2020, 2024 using the band range of 2015 with Automatic method

	Area		
Years	MODIS	Sentinel-2	Method
2015	27.98	37.29	
2020 (range 2015)	18.66	17.14	Automatic
2024 (range 2015)	22.03	29.25	

Table 8: Area variation (%) for years 2015, 2020, 2024 using the band range of 2015 with Automatic method

	Area va	riation (%)	
Years	MODIS	Sentinel-2	Method
2015 - 2020 (range 2015)	-33.33	-54.05	
2020 (range 2015) - 2024 (range 2015)	18.08	70.71	Automatic
2015 - 2024 (range 2015)	-21.28	-21.56	

As can be observed, there are significant discrepancies between the years, particularly for Sentinel-2, where from 2015 to 2020 (with the 2015 range) a decrease of –54.05% was recorded. Conversely, from 2020 (with the 2015 range) to 2024 (with the 2015 range), the trend shows a sharp increase of +70.71% in glacier surface area, which appears somewhat unusual and potentially illogical. In fact, both outcomes seem to show values that are likely overestimated. From 2015 to 2020, a reduction in glacier surface area of approximately 20 km² was measured (*Figure 28*), which is roughly equivalent to 2,800 football fields, or nearly one-third of the surface area of Lake Iseo. Similarly, but in the opposite direction, from 2020 to 2024, there was an increase of about 12 km² in glacier area (*Figure 29*), corresponding to around 1,680 football fields. This result, however, clearly does not reflect the real situation in recent years, where glaciers have continually retreated due to global warming. This divergence comes from the high margin of error in selecting the appropriate pixels by the operator through the automatic method, as previously discussed in other cases.

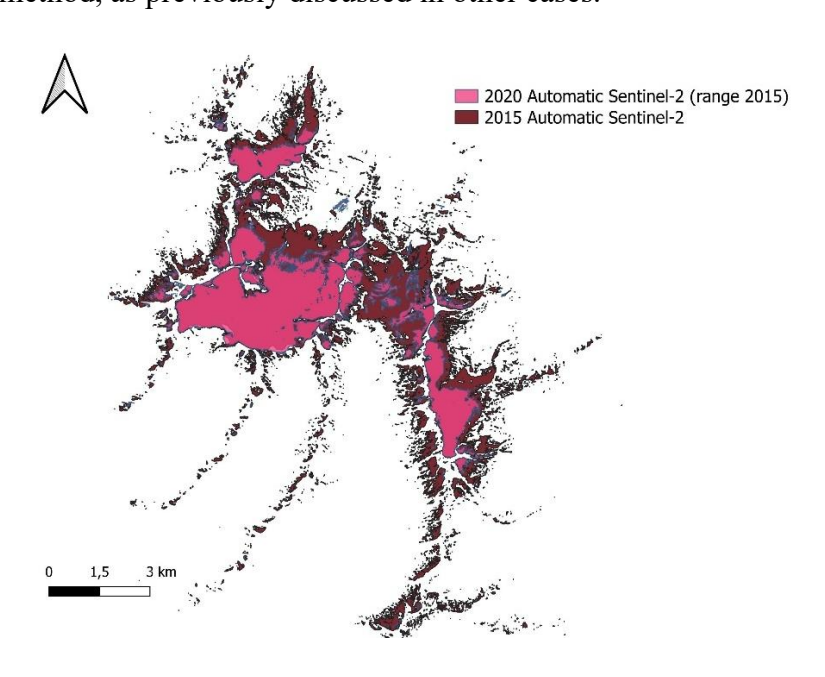


Figure 28: Area variation between 2015 and 2020 (with 2015 range) for Sentinel-2 (Automatic method)

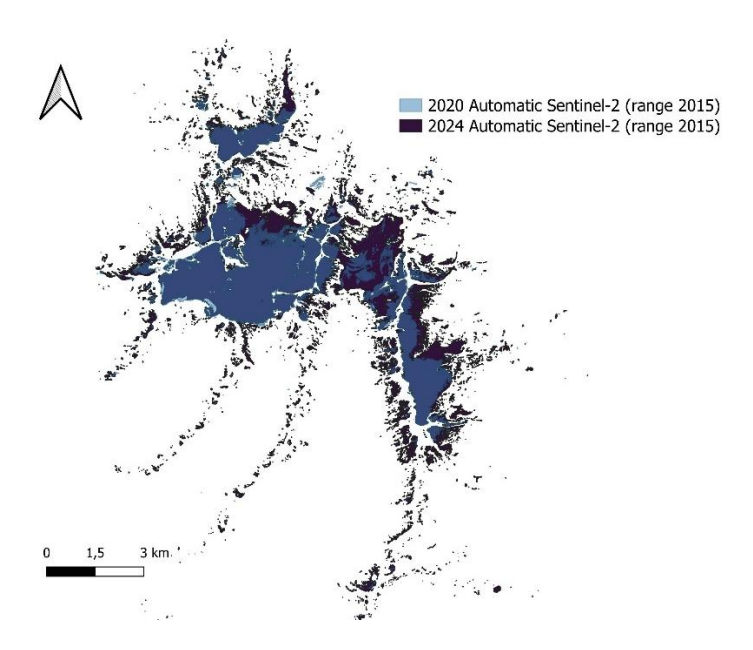


Figure 29: Area variation between 2020 and 2024 (with 2015 range) for Sentinel-2 (Automatic method)

Lastly, a further analysis was carried out with the aim of observing the maximum seasonal expansion and contraction of the glacier within the same year, essentially by capturing its widest breath between winter and summer. For this purpose, the year 2020 was selected, and satellite images with minimal cloud cover and with good visual clarity were chosen for both MODIS and Sentinel-2. This task was particularly tough for the winter period. In fact, for MODIS, an image from January 14, 2020, was used, while for Sentinel-2, the first available cloud-free image dated March 19, 2020, was selected. The results of glacier surface areas and variations between summer and winter are presented in *Tables 9* and *10*.

Table 9: Area (km²) of summer and winter 2020 with Automatic method

	Area (km²)		
Years	MODIS	Sentinel-2	Method
2020 summer	16274.56	14944.15	Automatic
2020 winter	219705.04	176656.82	Automatic

Table 10: Area variation (%) between summer and winter 2020 with automatic method

	Area variation (%)		
Years	MODIS	Sentinel-2	Method
2020 summer - 2020 winter	1249.99	1082.11	Automatic

As expected, a significant expansion of the glacier surface during the colder months occurred in both cases, with an increase exceeding 1000% and equivalent to 203 km<sup>2</sup> for MODIS and 162 km<sup>2</sup> for Sentinel-2. These values, which to give an idea correspond to half the size of Lake Garda, are graphically shown in *Figure 30* and *31*. However, it's important to interpret these results carefully because they are strongly influenced by winter snowfall, which can temporarily alter actual glacier mass. This analysis, which had the goal to illustrate how snow-covered area can change over just a few months, emphasizes the extent of snowmelt during summer period when the glacier shrinks and reaches its minimum extent.

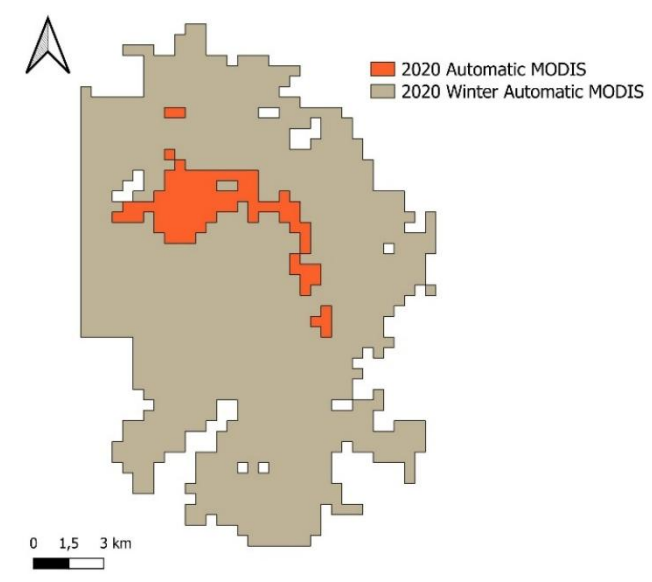


Figure 30: Area variation between summer and winter 2020 for MODIS (Automatic method)

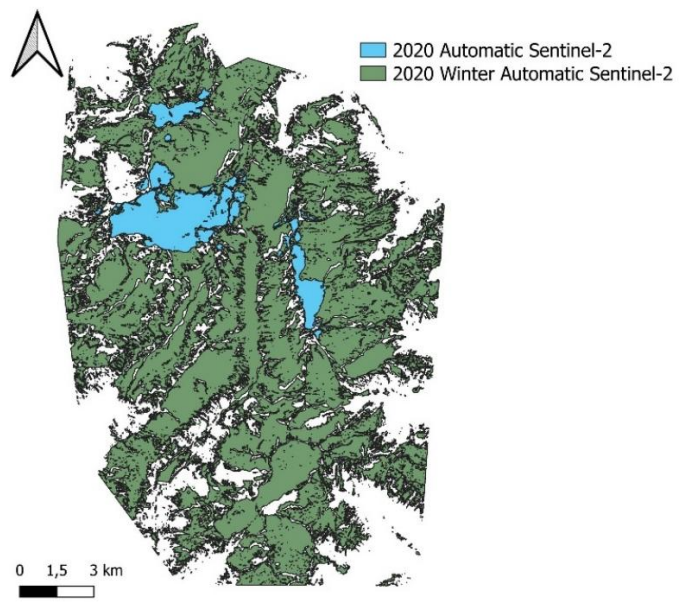


Figure 31: Area variation between summer and winter 2020 for Sentinel-2 (Automatic method)

#### 5.2 Enhanced biennial analysis of Glacier area variation

In this enhanced biennial analysis, as previously said, a more accurate temporal analysis has been conducted for Sentinel-2, now using a two-year time step as follows: 2015, 2018, 2020, 2022, 2024. In *Tables 11 and 12*, the area values and variations for the different years and for both automatic and visual methods are shown.

Table 11: Area for years 2015, 2018, 2020, 2022, 2024 using both methods (Automatic and Visual)

	Area (km²)	
Years	Sentinel-2	Methods
2015	37.29	
2018	24.15	
2020	14.94	Automatic
2022	17.72	
2024	32.62	
2015	32.04	
2018	24.11	
2020	23.58	Visual
2022	21.30	
2024	25.71	

Table 12: Area variation for years 2015, 2018, 2020, 2022 and 2024 using both methods (Automatic and Visual)

	Area variation (%)	
Years	Sentinel-2	Methods
2015 - 2018	-35.25	
2018 - 2020	-38.11	Automatic
2020 - 2022	18.61	Automatic
2022 - 2024	84.06	
2015 - 2018	-24.74	
2018 - 2020	-2.21	Visual
2020 - 2024	-9.66	visuai
2022 - 2024	20.70	

Analysing first the automatic method, it appears that from 2015 to 2018 there is a significant decrease equal to -13.14 km<sup>2</sup>, followed by a further decrease of -9.20 km<sup>2</sup> from 2018 to 2020 (*Figure 32*). So, this trend confirms the area reduction already noticed in the initial analysis. From 2020 onward, there is an inversion trend with a slight increase of +2.78 km<sup>2</sup> (+18.61%) from 2020 to 2022, followed by a more

relevant one of +14.90 km<sup>2</sup> leading up to 2024 (*Figure 33*). This last value seems unrealistic, especially since an increase of 84.06% between 2022 and 2024 is hard to justify based on what is really happening in recent years. While clearly unrealistic, this result effectively helps to highlight the method's critical limitations.

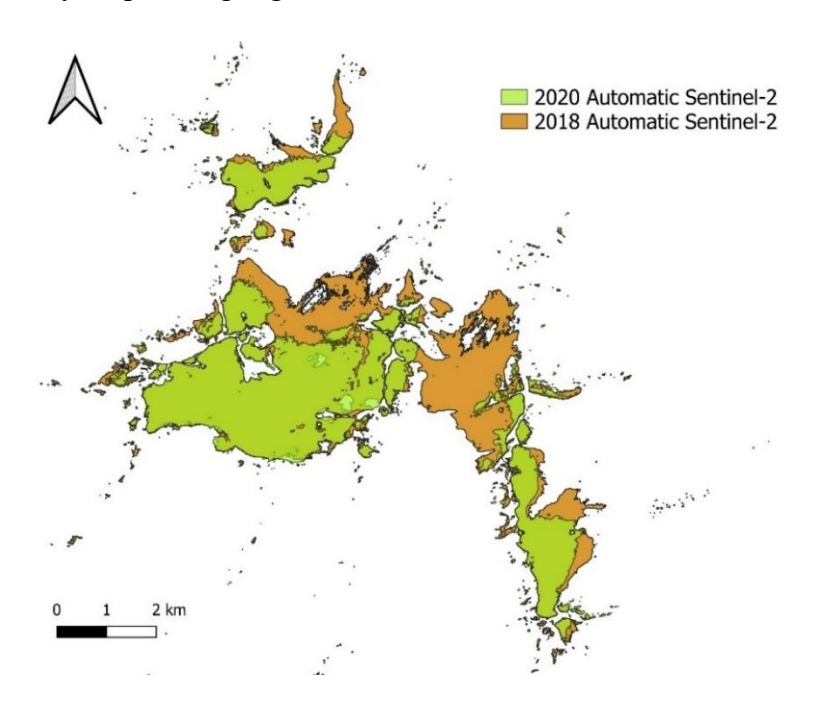


Figure 32: Area variation between 2018 and 2020 for Sentinel-2 (Automatic method)

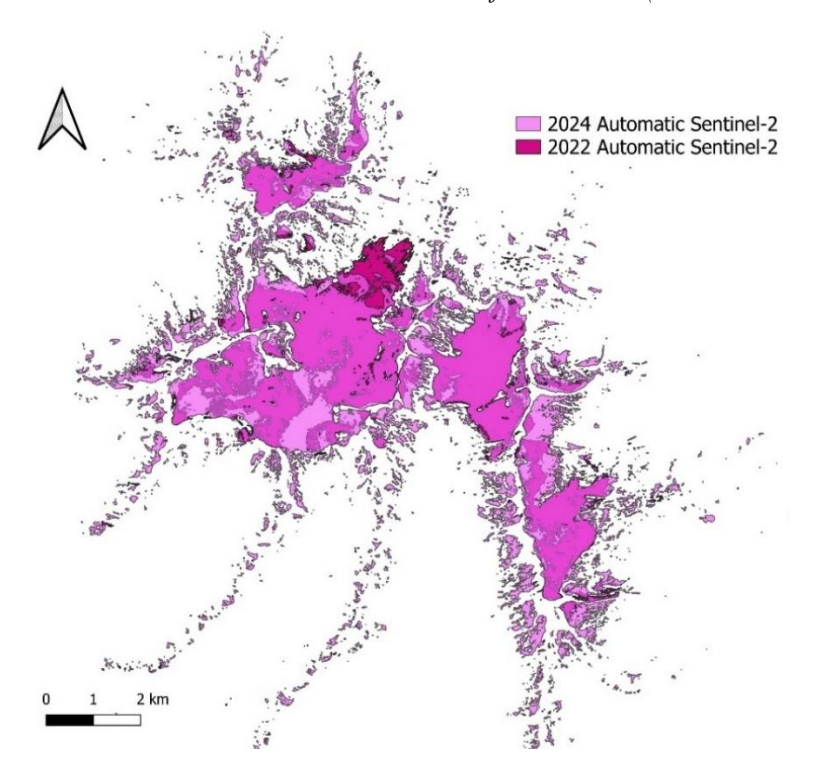


Figure 33: Area variation between 2022 and 2024 for Sentinel-2 (Automatic method)

These results can be interpreted in different ways. First of all, it is important to remember, as already highlighted for the initial analysis, that the reliability of the automatic method, contrary to what might be assumed, is highly dependent on the choice of threshold values for the three bands: These values inevitably influence which portions of ice are considered or not part of the main glacier body.

Secondly, it is evident that in 2024 the area value (32.62 km<sup>2</sup>) is very high if compared to the previous years and almost equal to that of 2015. This may suggest that the period in which the satellite image was captured in 2024 does not fully reflect the actual conditions of that year. Alternatively, more likely, the difficulty in selecting the correct band values for that year could have led to an inaccurate delineation of the glacier, resulting in an overestimation of the surface.

In the same way, for the visual method, the results show a more consistent and regular decreasing trend in glacier area from 2015 to 2022, with only a slight inversion from 2022 to 2024 (+20.70%), as shown in *Figure 34*. Remarkably, between 2018 and 2020, the area values are almost identical, with a decrease of only 0.53 km<sup>2</sup> (–2.21%), equivalent to about 74 football fields (*Figure 35*).

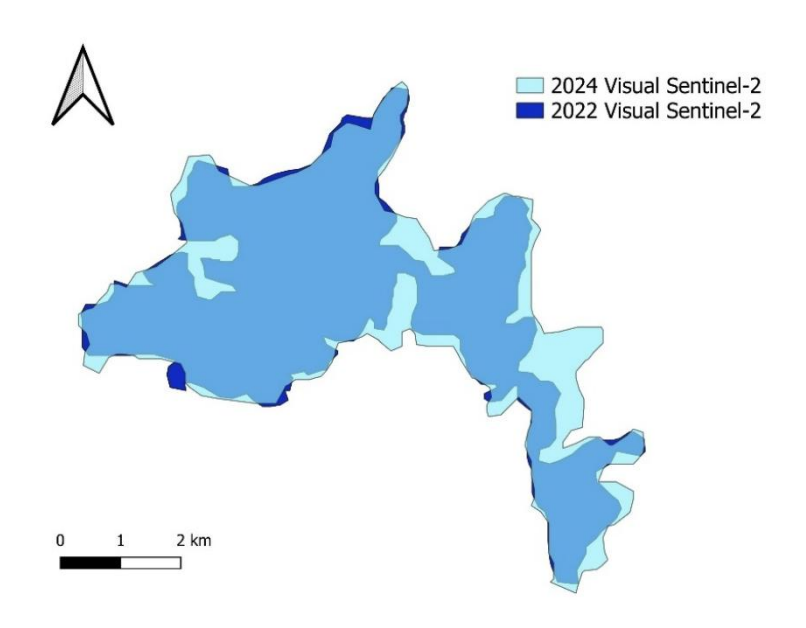


Figure 34: Area variation between 2022 and 2024 for Sentinel-2 (Visual method)

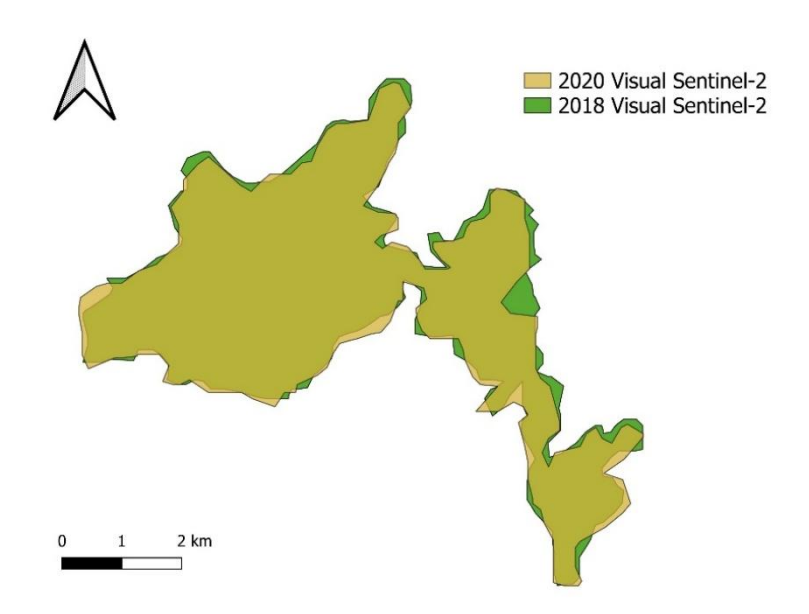


Figure 35: Area variation between 2018 and 2020 for Sentinel-2 (Visual method)

This trend, characterized by more realistic values and by much smaller two-year variations, highlights the greater reliability of the visual method compared to the automatic one, as it reflects reality more accurately thanks to the operator's ability to manually delineate the glacier boundaries in QGIS.

To conclude, as previously done in the initial analysis in Section 5.1, a comparison of area variation between automatic and visual methods, represented in *Table 13*, was carried out for the same years. Focusing on the two years not previously analysed, namely 2018 and 2022, it can be observed that in 2018 the variation between the automatic and visual methods, shown in *Figure 36*, is almost negligible (–0.15 km²), meaning that the area detected by both procedures is nearly identical. Conversely, in 2022, there is an increase of +20.18% when passing from the automatic to the visual method (*Figure 37*), corresponding to a difference of 3.58 km².

Table 13: Area variation (%) between Automatic and Visual method for the same year for Sentinel-2

	Area variation (%)		
Methods	Sentinel-2	Years	
	-14.09	2015	
	-0.15	2018	
Automatic vs Visual	57.78	2020	
	20.18	2022	
	-21.20	2024	

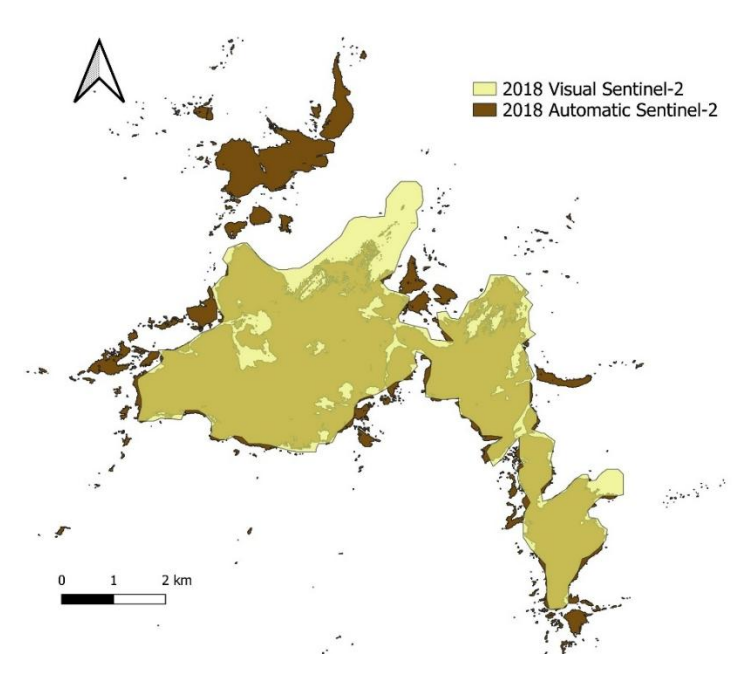


Figure 36: Area variation (%) between Automatic and Visual methods for Sentinel-2 in 2018

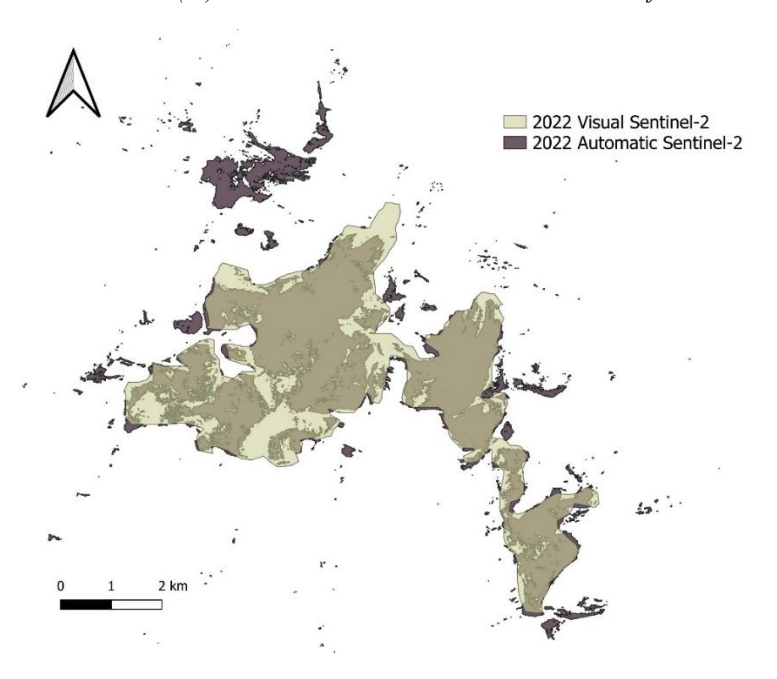


Figure 37: Area variation (%) between Automatic and Visual methods for Sentinel-2 in 2022

In both cases, the main difference lies in the fact that the automatic method tends to include small portions of ice or snow detached from the main glacier body, which increases the calculated glacier surface. Furthermore, it also includes the western Pisgana portion, located in the upper left area, which is relatively substantial. On the other hand, this portion is excluded by the visual method because it is separated from the main glacier body. However, in this case, the Mandrone tongue is included, whereas it tends to be excluded either completely or partially by automatic method.

# 5.3 Climate Effects on Glacier Area in the Adamello-Valcamonica Region

To estimate the climate effects on glacier area in the Adamello-Valcamonica region, data from the Pantano d'Avio monitoring station were used, as described in Chapter 4.7. It should be noted that this station, although it is the closest to the glacier, it is located at a lower elevation. For this reason, the recorded temperature and precipitation values may not exactly represent actual conditions on the glacier and could be slightly over- or underestimated depending on the season.

#### 5.3.1 Temperature trends

The following plot (*Figure 38*) presents the raw time series of daily mean temperatures recorded at the Edolo-Pantano d'Avio station (2108 m a.s.l.) for the 2015-2024 period. The series clearly shows the expected seasonal oscillations characterized by summer peaks and winter minima, which are typical of daily temperature variations. For most of the year, temperatures range between approximately –10 °C during the coldest periods and +15 °C in summer, with only a few extreme values dropping below –15 °C (in 2016 and 2018) or exceeding +20 °C (in 2015 and 2020).

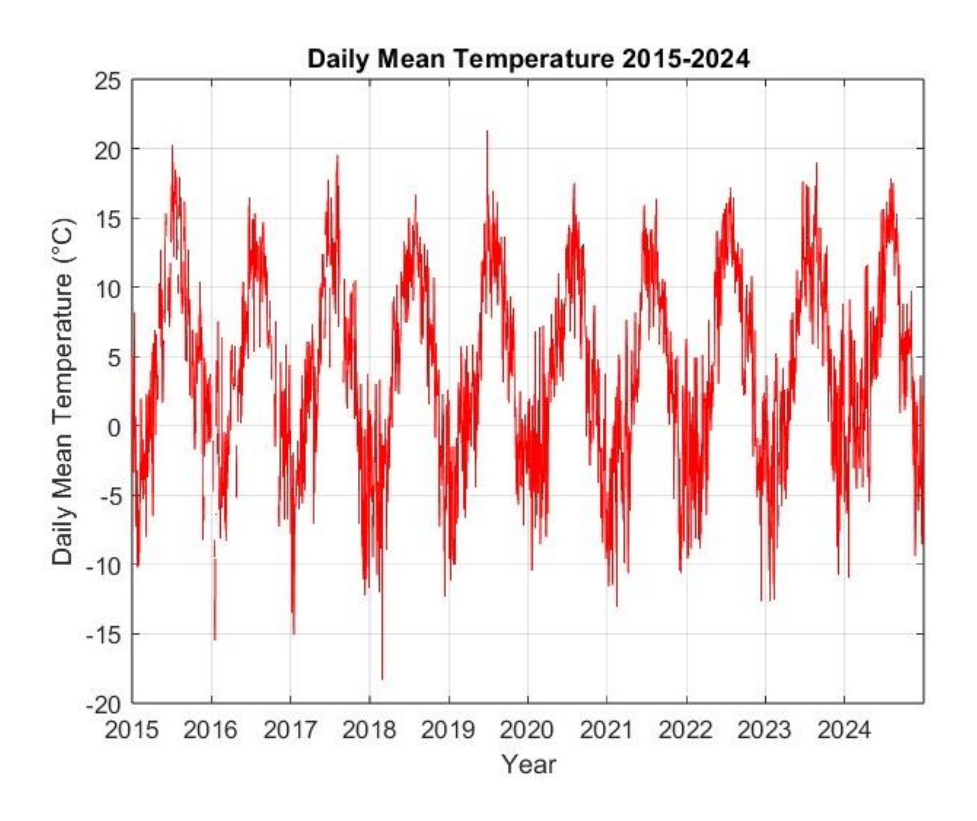


Figure 38: Daily mean temperature in the Adamello-Valcamonica region in the period 2015-2024

In addition, with the aim of better capturing the underlying trend, a 30-day moving average was applied to the previous graph (*Figure 39*). The black curve illustrates more clearly the general seasonal cycle by filtering out short-term fluctuations. By examining the figure, it can be note that from 2019 onwards, except for 2020, the smoothed trend line does not drop below –5 °C. This suggests a slight increase in mean temperatures compared to the earlier years, with 2024 showing the strongest anomaly because temperature values remain above 0 °C for most of the time. This pattern is a clear indicator of warmer winters in the recent period. In contrast, the maximum values appear more stable across the years, showing no clear evidence of significant changes over the considered period.

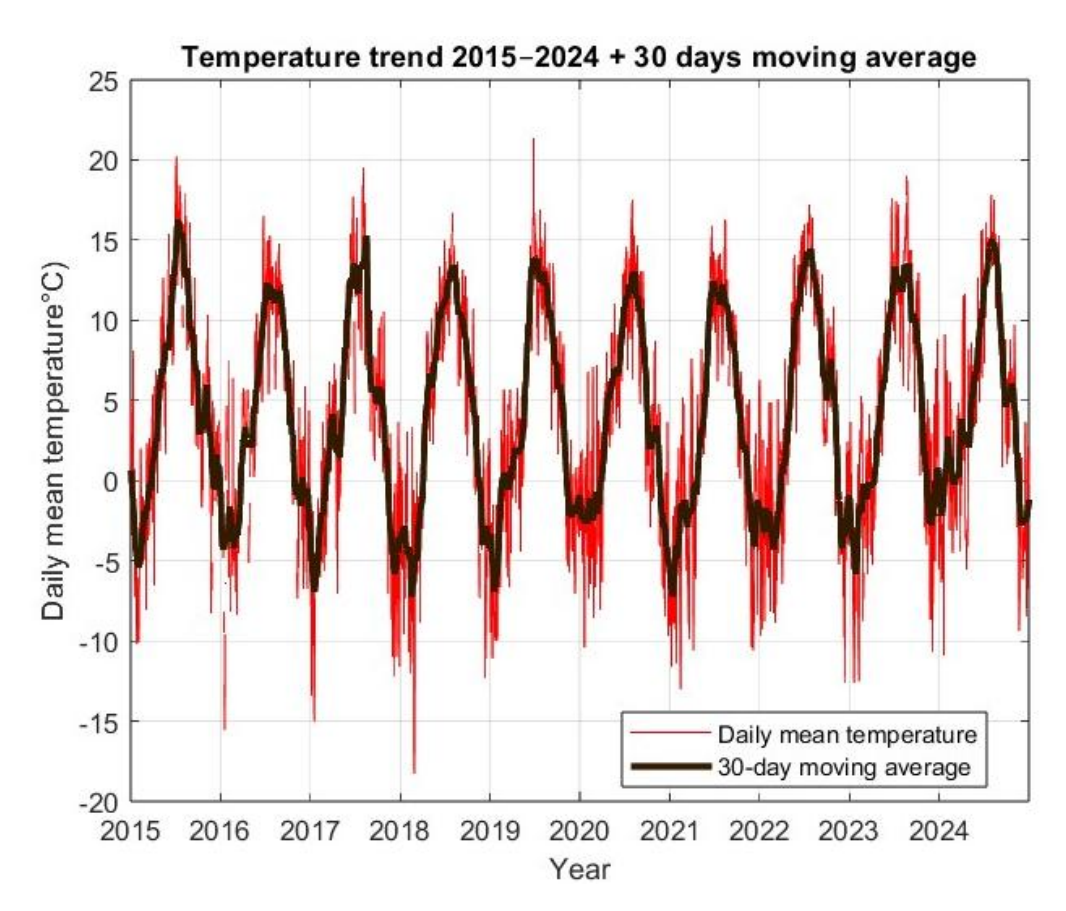


Figure 39: Temperature trend in the Adamello-Valcamonica region in the period 2015-2024 with a 30-days moving average

In the third figure (Figure 40) a seasonal mean temperature curve was obtained by averaging daily values across the entire ten-year period. The curve illustrates the typical annual cycle and provides an overview of the mean values across the months, with a steady rise from winter to summer and a decline from late summer to winter. The warmest month is July, when mean values remain just below 15 °C, followed by

June and the first half of August, after which temperatures quickly fall below 10 °C. As regards the coldest period of the year, which is characterized by temperatures consistently below 0°C, it extends from the second half of October to the first half of March, reaching minima values around mid-January. The smoothness of the curve facilitates a clearer interpretation of seasonal dynamics, which are independent of interannual variability.

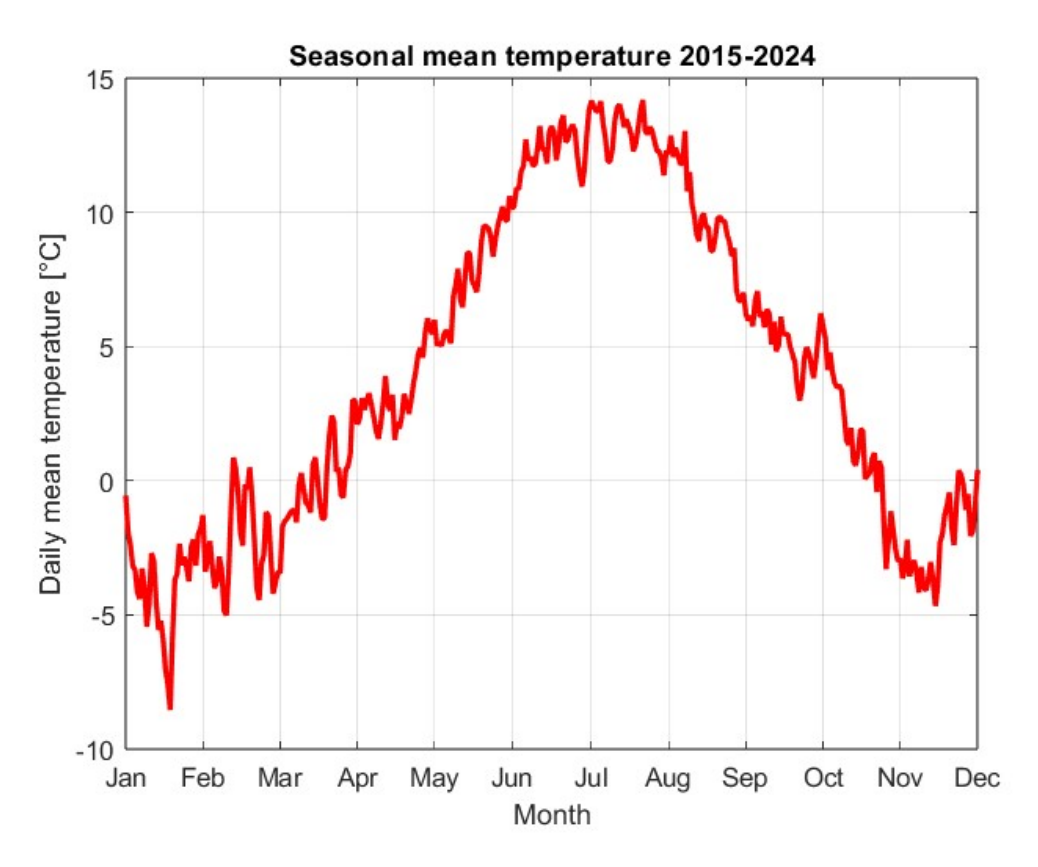


Figure 40: Seasonal mean temperature in the Adamello-Valcamonica region obtained by averaging daily values across the period 2015-2024

## 5.3.2 Precipitation trends

In the same way as for the temperature analyses, precipitation data were also examined and processed in MATLAB to obtain a general overview of precipitation trends over the last ten years in Adamello glacier area. The monitoring station used for retrieving data was the same, and the analytical procedure was also identical. The only difference, already mentioned in Chapter 4.7, is that for precipitation analyses only data from October to March were considered, since these months are the most relevant in terms of snow accumulation on the glacier and contribute vastly to the mass balance.

Figure 41 shows the cumulative daily precipitation for each winter in the period 2014-2024. As evident from the graph, there are clear outliers in the last winter (2023/2024), with daily precipitation reaching 160-180 mm on some days. Other significant records occurred in winter 2014/2015, with a daily maximum just above 80 mm, and in winter 2018/2019, when precipitation exceeded 100 mm in a day. Another interesting point is that only in winter 2017/2018 daily precipitation never exceed 20 mm, unlike in all other winters.

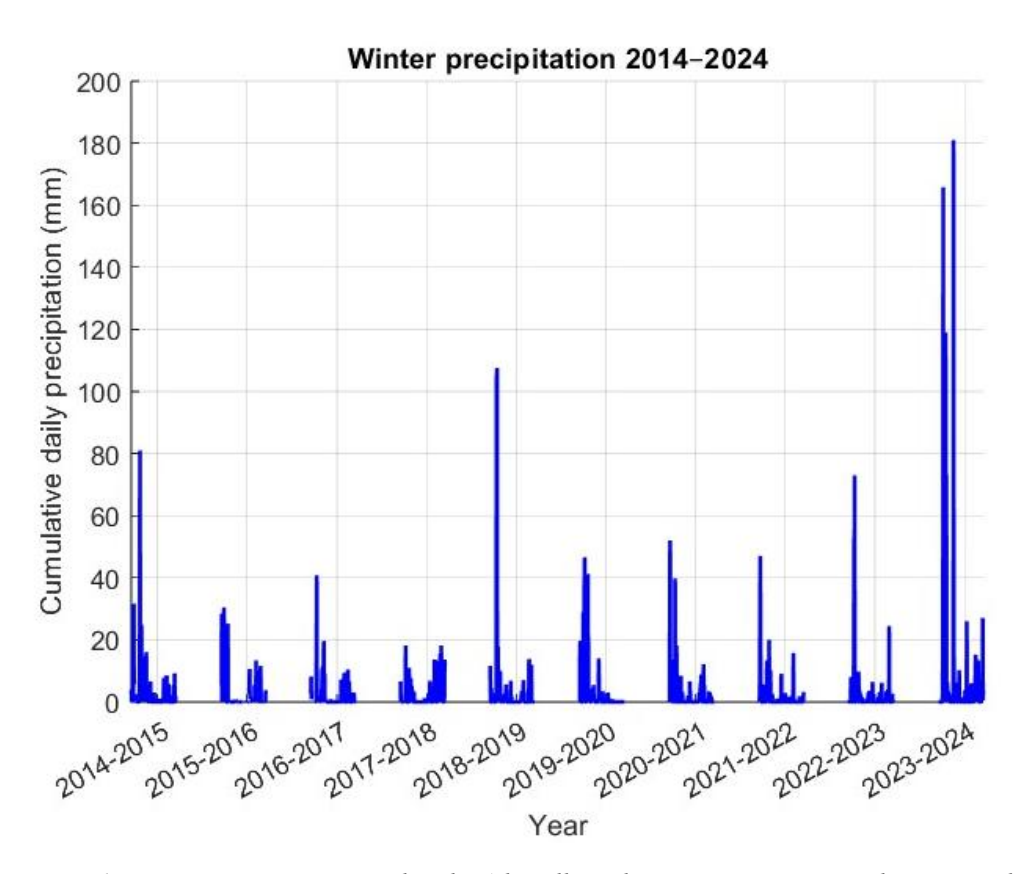


Figure 41: Winter precipitation trend in the Adamello-Valcamonica region considering cumulative daily precipitation (mm) from October to March in the period 2014-2024

Also in this case, a 30-day moving average was added to the previous graph to better visualize the winter precipitation trends over the different years (*Figure 42*). As already observed in the previous figure, winter 2023/2024 shows the highest values in terms of precipitation. In fact, it is the only winter in which the daily precipitation slightly exceeds 20 mm. Another noteworthy aspect is that, in all years except for winter 2017/2018, the largest amount of precipitation occurs in the first part of the winter season, mostly during October, November, and December.

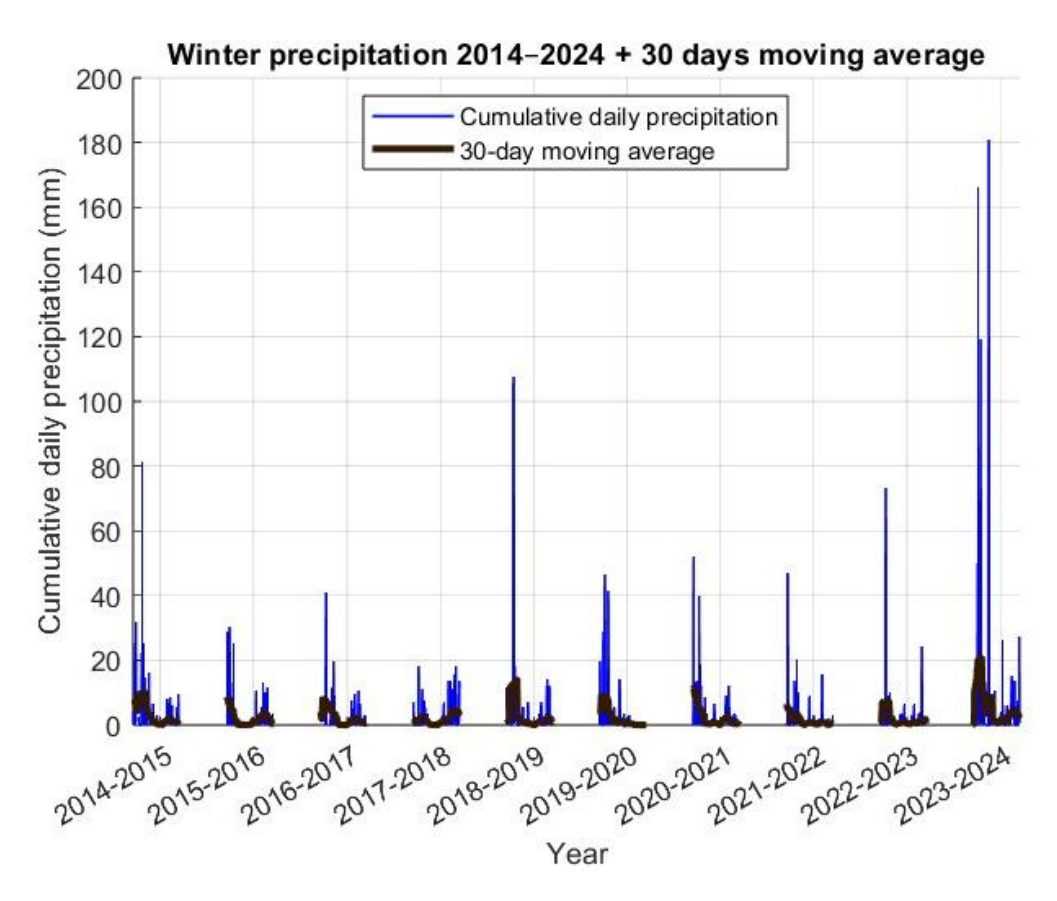


Figure 42: Winter precipitation trend in the Adamello-Valcamonica region considering cumulative daily precipitation from October to March in the period 2014-2024, with a 30-days moving average

Furthermore, *Figure 43* shows the winter mean precipitation curve, obtained by averaging daily values over the ten-year period. The curve highlights that the period around November is the most characterized by intense precipitation events, with an additional peak in December. This seasonal pattern confirms the findings of the previous figures. In the early months of the year, by contrast, precipitation never exceeds 5 mm per day and remains more stable, with fewer outliers or particularly intense days.

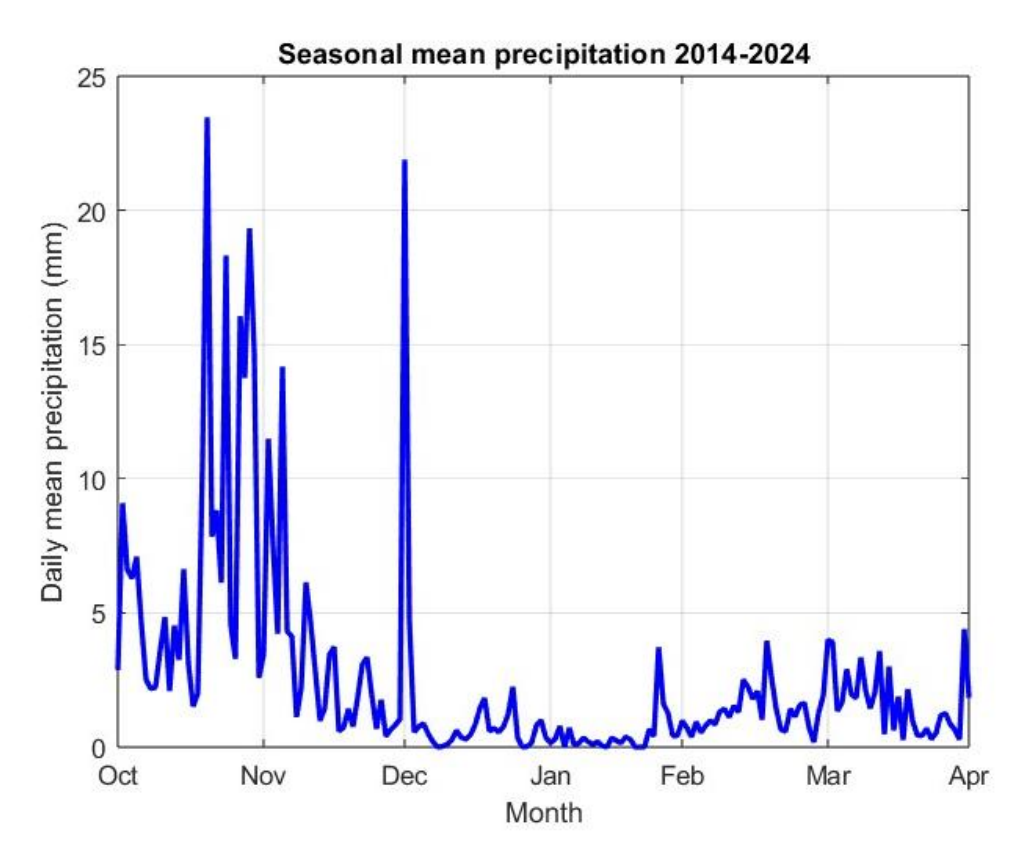


Figure 43: Winter mean precipitation in the Adamello-Valcamonica area obtained by averaging daily values across the period 2015-2024

It is important to note that the higher precipitation values observed in November and December, compared to the January-March period, reflect the typical climatic pattern of the Adamello–Valcamonica area. In fact, autumn in this region is usually characterized by more frequent and intense precipitation events. In contrast, lower values are generally recorded during the core winter months (January-March), although most of the precipitation in this period falls as snow. It must be remembered that these data are measured at the Pantano d'Avio station, located at a lower altitude than the glacier. As a consequence, winter precipitation values may be underestimated due to the difficulty of accurately measuring solid precipitation (snow) with standard pluviometers.

#### 5.3.3 Biennial Glacier-Climate relationships (Automatic method)

Considering the biennial Adamello Glacier surface changes already discussed in Chapter 5.2, the aim of the following section is to explore their correlation with temperature and precipitation biennial values obtained from the monitoring station and analysed in Chapters 5.3.1 and 5.3.2. *Table 14* reports the  $\Delta$ Area values calculated with the automatic method in QGIS, together with the corresponding mean biennial temperature and cumulative precipitation data.

Table 14: △Area obtained from the automatic method, mean summer biennial temperature and cumulative winter biennial precipitation for the biennia considered

Biennium	ΔArea (km²)	Temperature biennium (°C)	Precipitation biennium (mm)
2015 - 2018	-13.14	12.85	434.17
2018 - 2020	-9.20	11.35	321.28
2020 - 2022	2.78	11.93	304.58
2022 - 2024	14.90	12.72	808.50

Going into detail, Figures 44 and 45 illustrate the scatter plots of glacier  $\Delta$ Area against mean summer biennial temperature and cumulative winter biennial precipitation, respectively, using a double y-axis graph to represent the evolution of these parameters over time.

As shown in *Figure 44*, in the first biennium (2015-2018), the  $\Delta$ Area and mean biennial temperature appear discordant: despite the highest temperature of the four periods (almost 13 °C), the glacier experienced a significant reduction of  $-13.15 \text{ km}^2$ . In the subsequent biennia, however, an increase in temperature corresponds to a progressive rise in glacier surface change.

A slightly different behaviour emerges in the precipitation plot (*Figure 45*). Here, precipitation values decrease during the first three biennia, followed by an increase in the last period, which also coincides with the largest  $\Delta$ Area reduction.

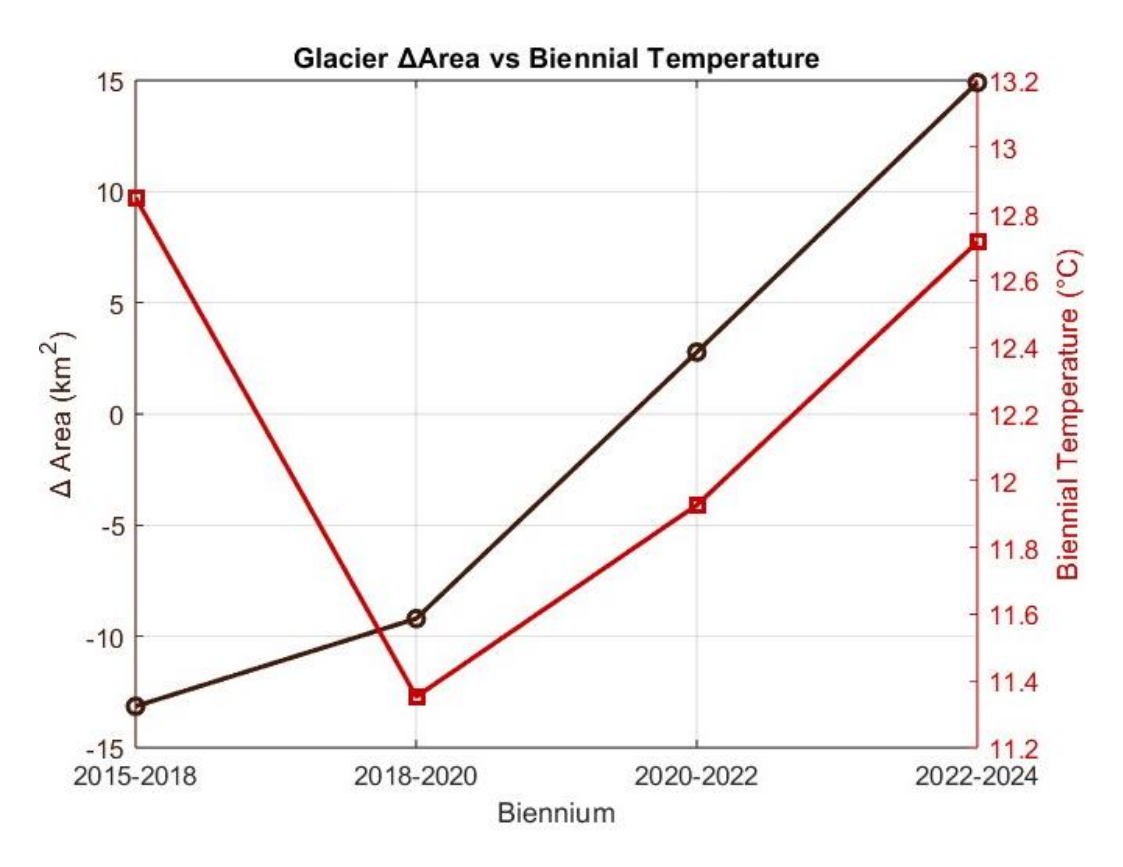


Figure 44: Comparison between glacier area change (left Y-axis) and mean biennial temperature (right Y-axis) over the biennium periods, calculated using the automatic method.

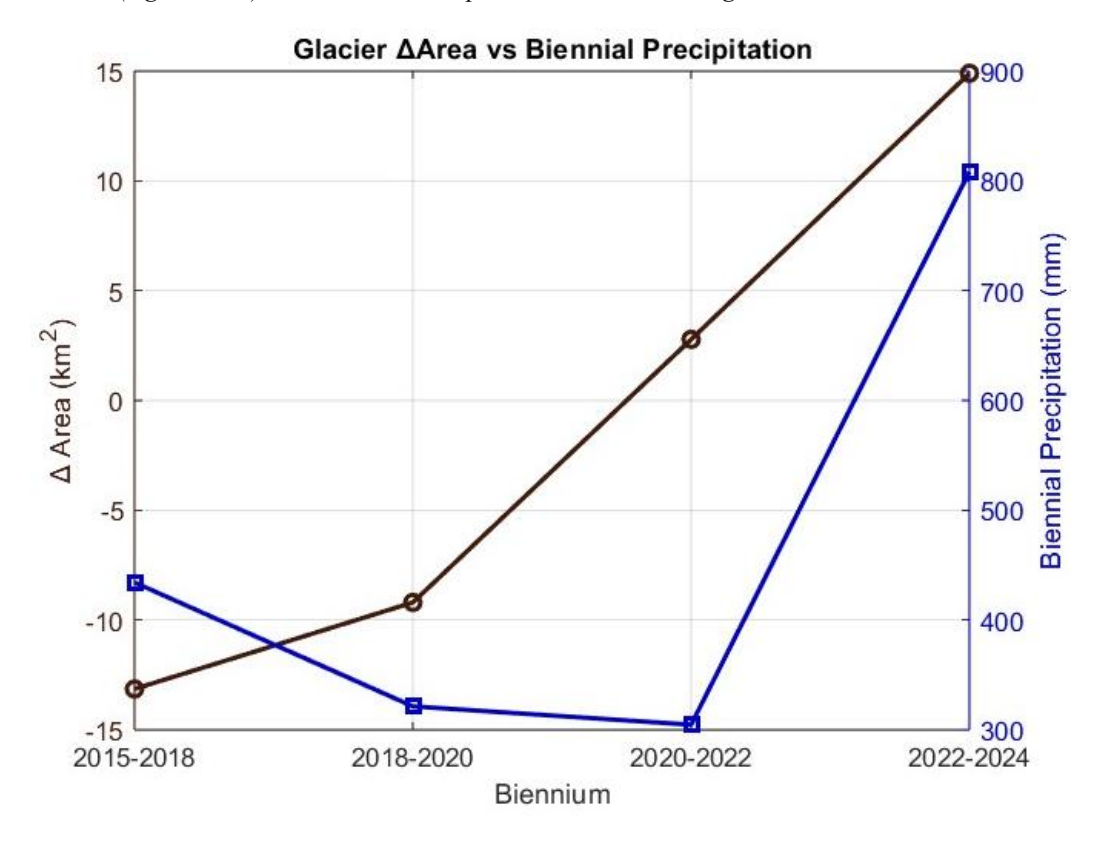


Figure 45: Comparison between glacier area change ( $\Delta A$ , left Y-axis) and cumulative biennial precipitation (right Y-axis) over the biennium periods, calculated using the automatic method.

The following two scatter plots (Figures 46 and 47), including least-squares fit lines, show the general trends between glacier area changes and climatic variables. In both plots, and especially in the temperature graph (Figure 47), the data points are widely scattered around the fit line, meaning that the relationship is weak due to the limited number of observations. Another observation is that the least-squares line in the precipitation graph is steeper than in the temperature plot. This aspect suggests that glacier surface variations are more sensitive to small changes in precipitation than to changes in temperature. Nevertheless, a larger dataset would be necessary to obtain statistically significant results and more reliable conclusions.

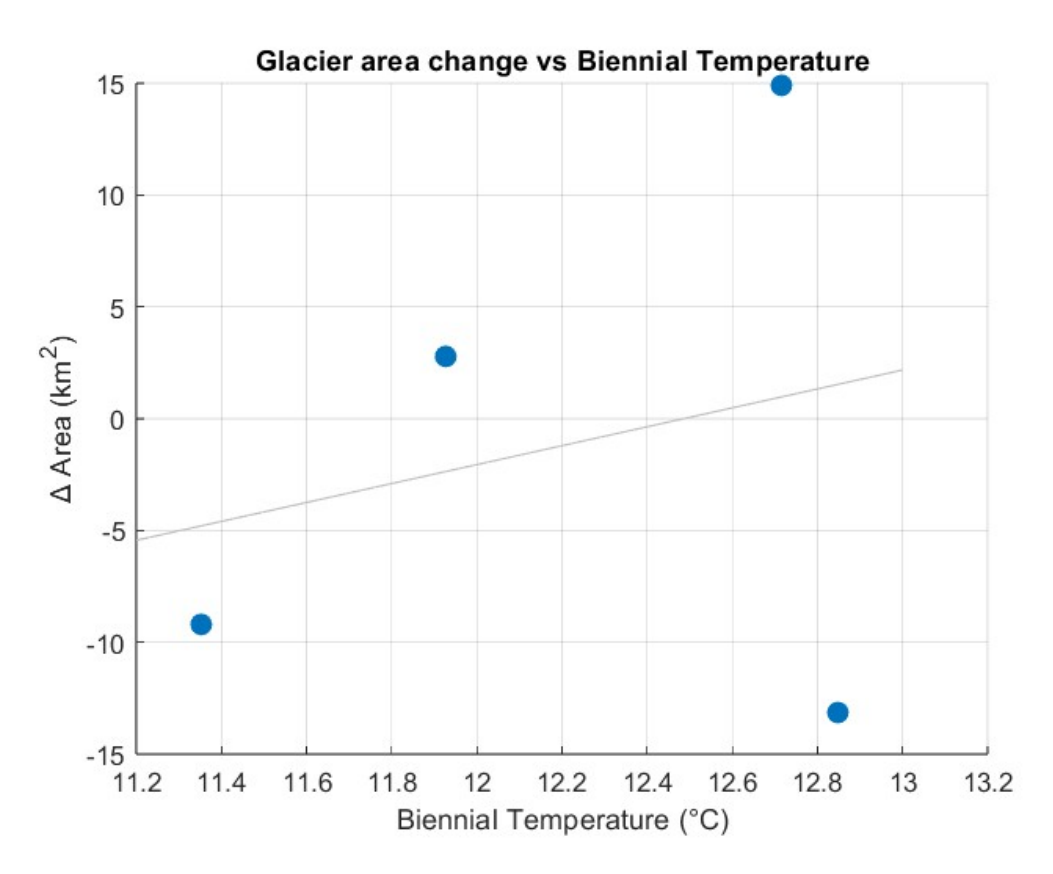


Figure 46: Scatter plot of glacier area changes in relation to biennial temperature with least-squares regression line using the automatic method

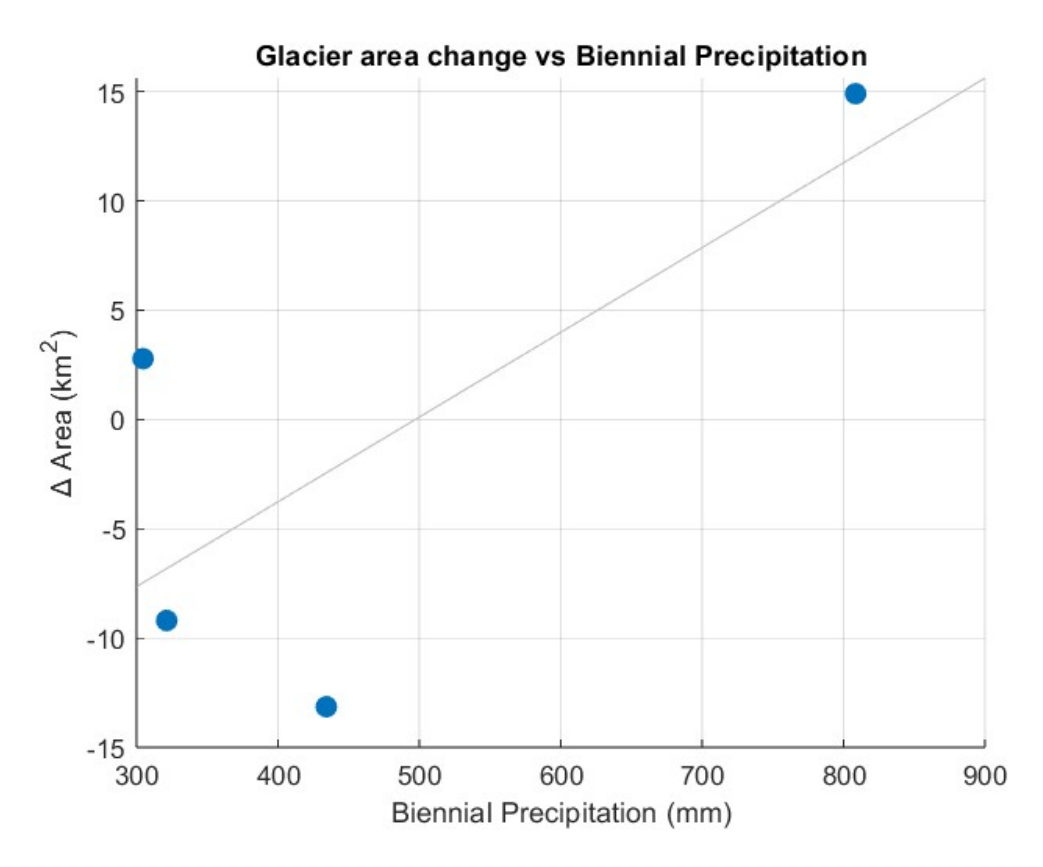


Figure 47: Scatter plot of glacier area changes in relation to biennial precipitation with least-squares regression line using the automatic method

Looking more closely at the statistical analysis, the linear regression models, generated using the "fitlm" function in MATLAB and shown in *Figures 48* and *49*, help to better understand the relationship between the response variable and the predictors. These plots not only represent the fitted regression line, but they also include confidence bounds, useful to understand and evaluate the relationship. Moreover, these calculations also provide statistical indicators that are used as reference to quantify the significance of the carried-out analyses.

When analysing the two regression models, even though precipitation data perform slightly better, both cases reveal weak statistical significance in explaining glacier area change. For the temperature regression, the Root Mean Squared Error (RMSE) of 15.1 km<sup>2</sup> means that predictions deviate on average by  $\pm 15$  km<sup>2</sup> from the observed  $\Delta$ Area. The coefficient of determination (R<sup>2</sup>) is only 0.055, while the adjusted R<sup>2</sup> is negative (-0.418). Furthermore, the F-statistic is very low (0.116) and the p-value very high (0.766). All these parameters explain the absence of any significant linear relationship. On the other hand, the precipitation regression model is characterized by a lower

RMSE of 10.8 km<sup>2</sup> and a higher R<sup>2</sup> of 0.516, with an adjusted R<sup>2</sup> of 0.274. Even though half of the variance in glacier change might be explained by precipitation, statistical robustness remains weak, as shown by the modest F-statistic (2.13) and the p-value (0.282). In summary, precipitation seems to be a stronger predictor than temperature; however, the only four biennia available are a limitation for statistically reliable analyses. These results should therefore be interpreted with caution, avoiding definitive conclusions.

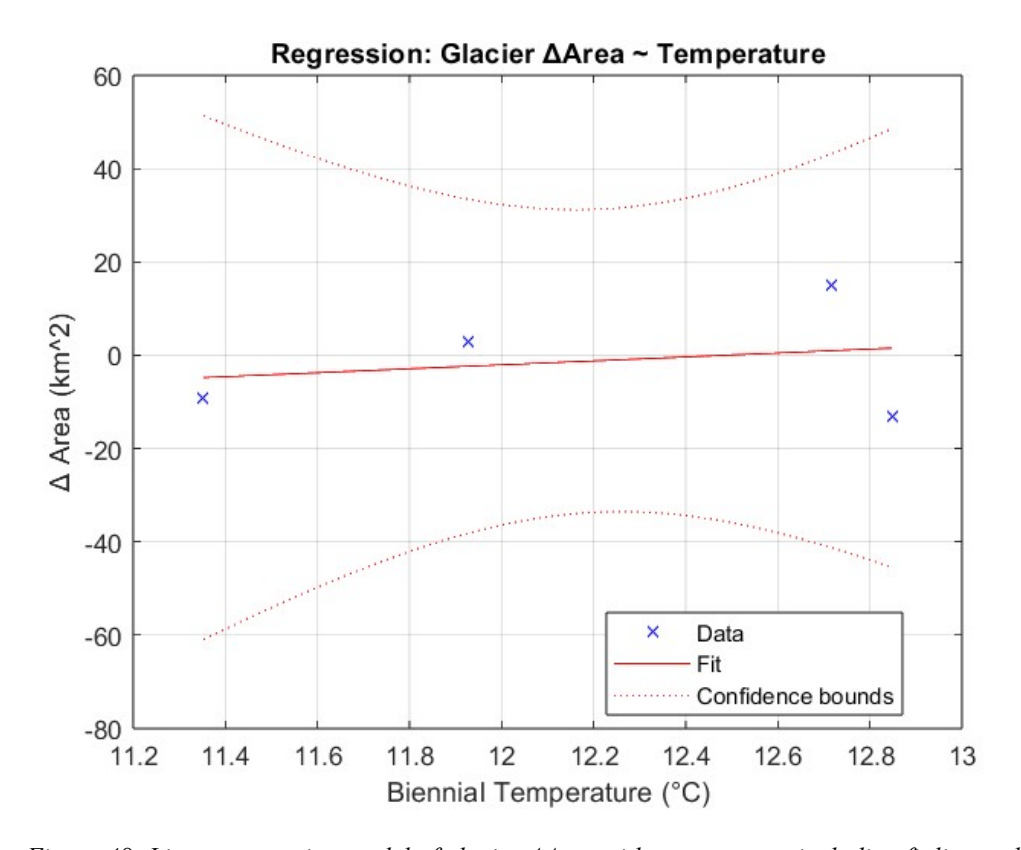


Figure 48: Linear regression model of glacier  $\Delta A$ rea with temperature, including fit line and confidence bounds using the automatic method

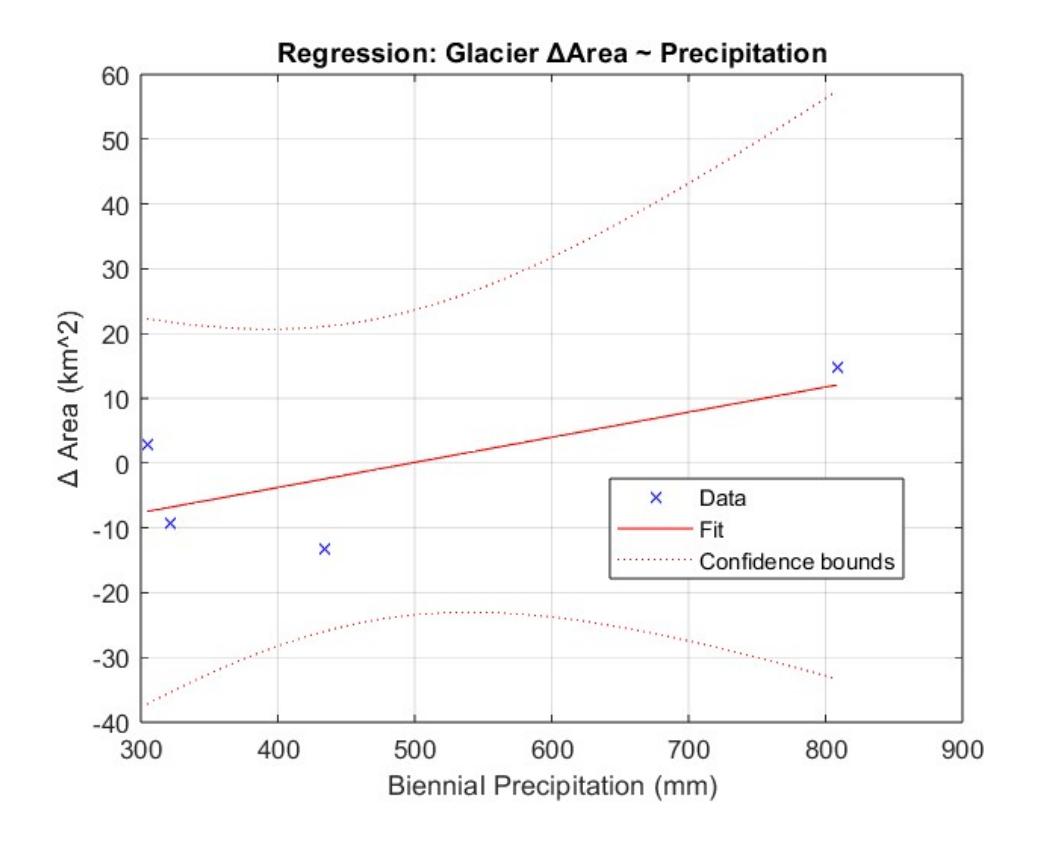


Figure 49: Linear regression model of glacier  $\Delta A$ rea with precipitation, including fit line and confidence bounds using the automatic method

## 5.3.4 Biennial Glacier-Climate relationships (Visual method)

As in Chapter 5.3.3, the objective of this section is to examine the correlation between glacier surface changes, now using the biennial values obtained with the visual method, and the temperature and precipitation values calculated in the previous analyses. *Table 15* reports the biennial periods along with the new  $\Delta$ Area values from the visual method and the corresponding mean biennial temperature and cumulative precipitation data.

Table 15: △Area obtained from the visual method, mean summer biennial temperature and cumulative winter biennial precipitation for the biennia considered

Biennium	ΔAreaVisual (km²)	Temperature biennium (°C)	Precipitation biennium (mm)
2015 - 2018	-7.93	12.85	434.17
2018 - 2020	-0.53	11.35	321.28
2020 - 2022	-2.28	11.93	304.58
2022 - 2024	4.41	12.72	808.50

Observing Figures 50 and 51, which present the scatter plots of glacier  $\Delta$ Area against biennial temperature and biennial precipitation using a double y-axis representation, it can be noted that in the first two biennia the glacier surface changes show a discordant pattern with respect to both temperature and precipitation, following an opposite trend. By contrast, in the biennium 2022-2024, an increase in both temperature (+0.79 °C) and precipitation (+503.92 mm) corresponds to an increase in glacier  $\Delta$ Area (+4.41 km²), indicating a positive correlation between the variables.

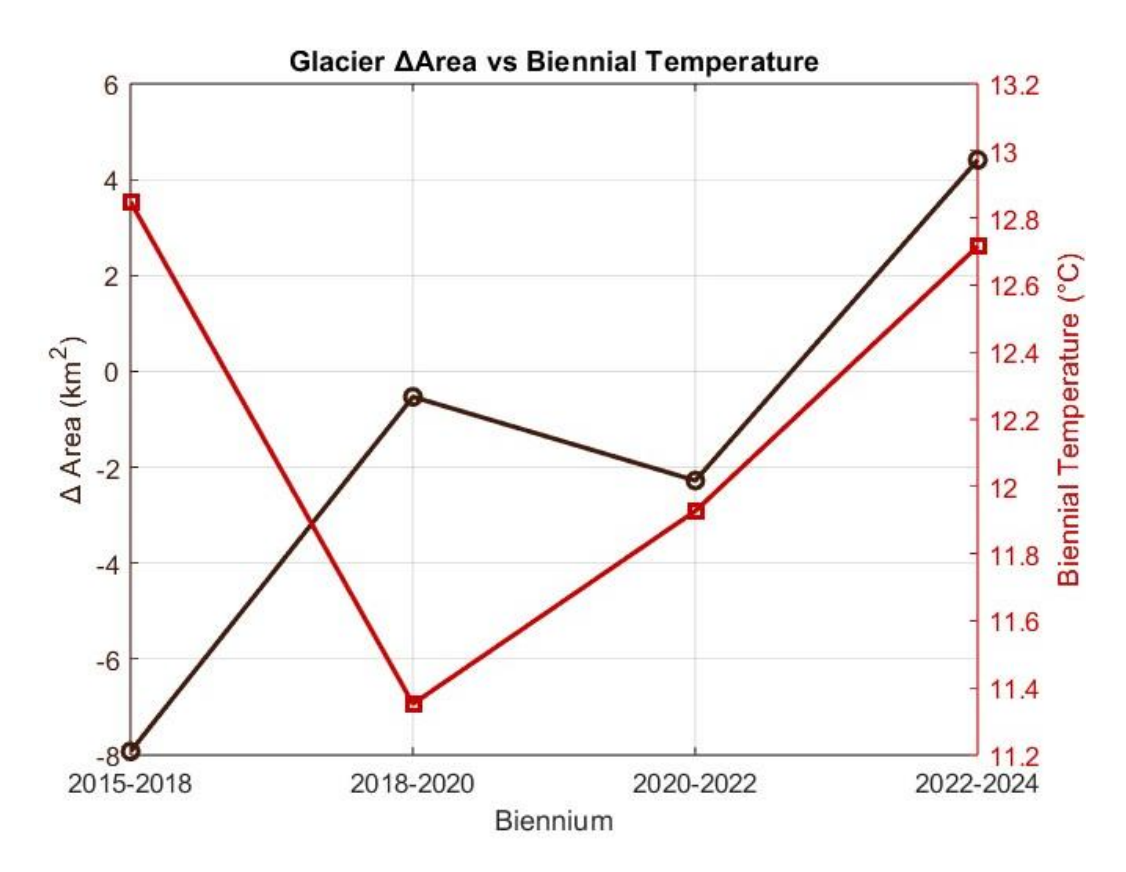


Figure 50: Comparison between glacier area change (left Y-axis) and mean biennial temperature (right Y-axis) over the biennium periods, calculated using the visual method.

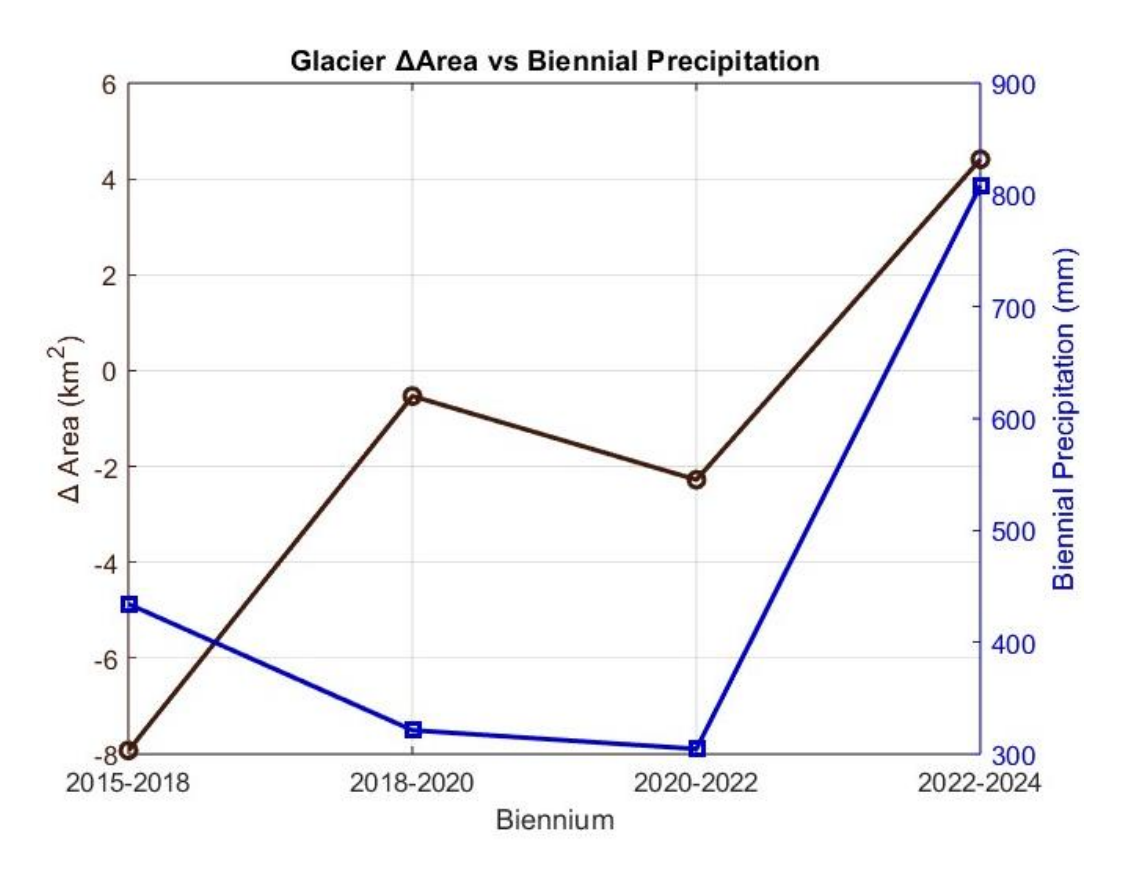


Figure 51: Comparison between glacier area change (left Y-axis) and cumulative biennial precipitation (right Y-axis) over the biennium periods, calculated using the visual method.

The following two scatter plots (*Figures 52* and *53*), which illustrate the general trends between glacier area changes and climatic variables, also include least-squares fit lines compared to the previous graphs. In both cases, the data points are scattered and particularly distant from the least-square line, underlying the weak relationship due to the limited number of observations. The main difference between the two models regards the slope of the regression lines, where the biennial temperature graph is characterized by a least-squares line with a downward trend, meaning that higher temperatures are generally associated with greater glacier area loss. Conversely, a positive correspondence between higher precipitation values and an increase in glacier surface is highlighted by the precipitation least-square line that slopes upward. These outcomes are in accordance with the expected physical mechanisms because increasing temperatures generally enhance glacier melting; conversely, higher precipitation in the form of winter snowfall, contributes positively to the glacier mass balance. However, given the very limited dataset, these results must be interpreted with caution and regarded only as indicative trends rather than definitive evidence.

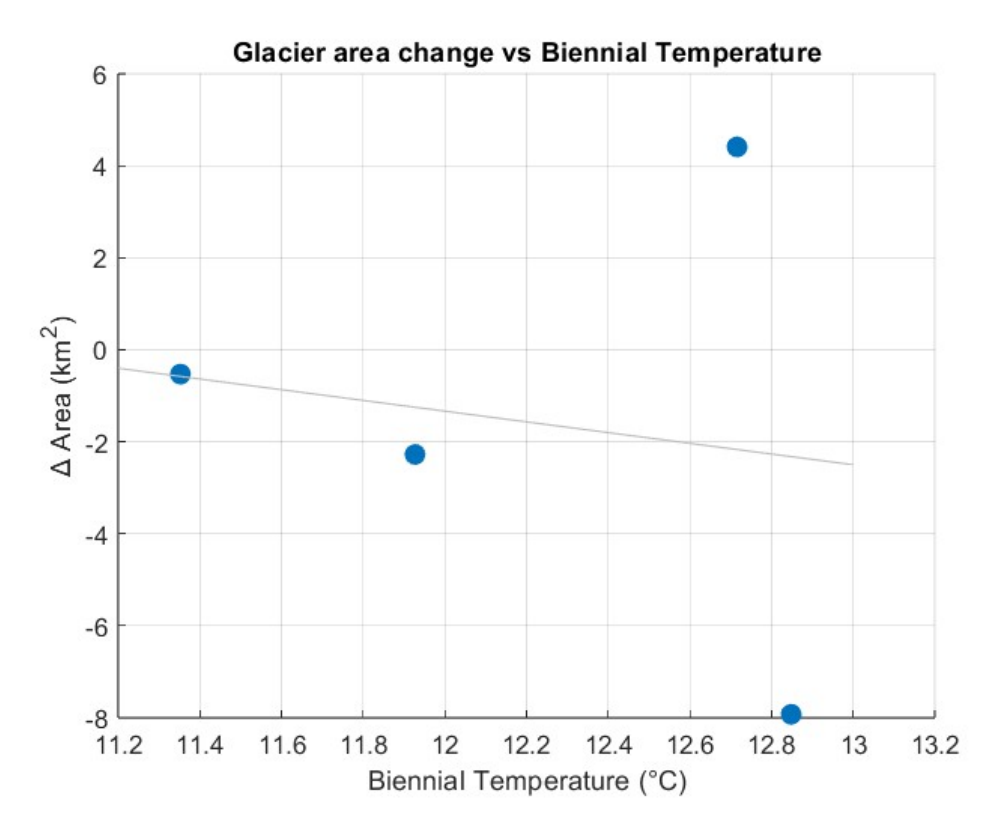


Figure 52: Scatter plot of glacier area changes in relation to biennial temperature with least-squares regression line using the visual method

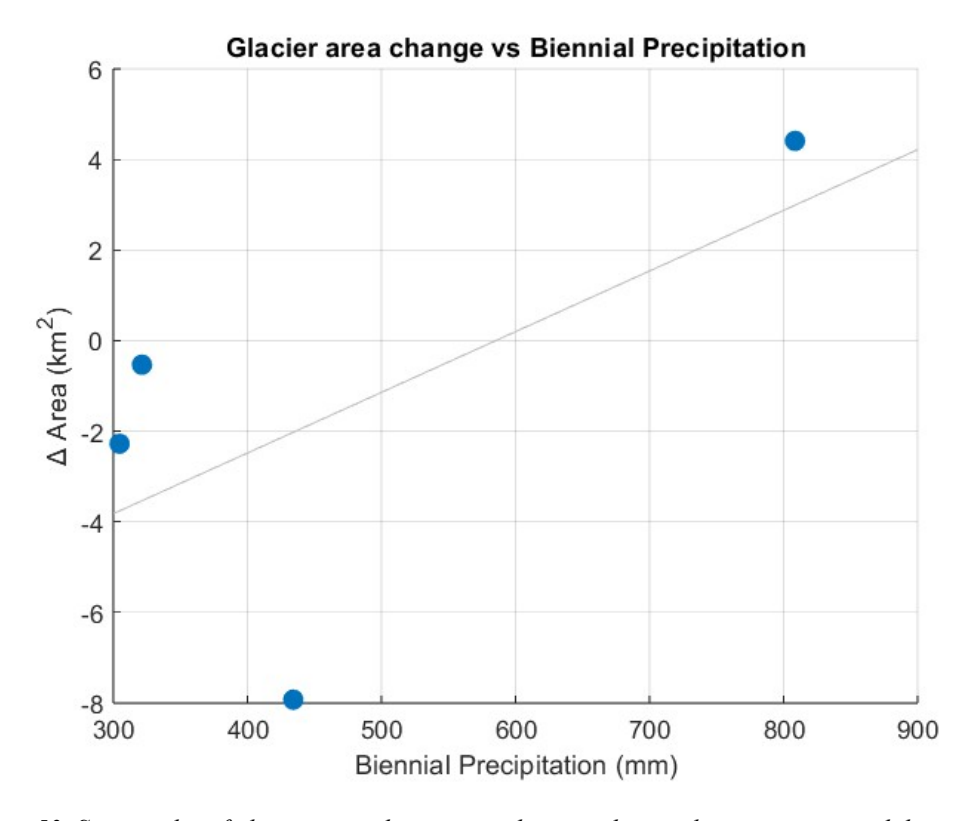


Figure 53: Scatter plot of glacier area changes in relation to biennial precipitation with least-squares regression line using the visual method

Also in this case, when comparing the two regression models represented in *Figure 54* and *55*, both temperature and precipitation show only weak relationships with glacier area change. The Root Mean Squared Error (RMSE) of the temperature model is 6.15 km², meaning that predictions deviate by about ±6 km² from observed values on average. The coefficient of determination (R²) is just 0.026, and the adjusted R² is even negative (-0.461), indicating that temperature explains virtually none of the variance in glacier change. The very low F-statistic (0.053) and the high p-value (0.839) confirm the absence of statistical significance. Regarding the precipitation model, the values are slightly better: the RMSE is 4.9 km², with an R² of 0.381 and an adjusted R² of 0.072. However, the F-statistic is equal to 1.23 and the p-value is equal to 0.382, which again highlight that the relationship is not statistically significant. Overall, as already note for the automatic method, the limited number of observations strongly affects the reliability of both models. For this reason, in the next chapter, the same analysis will be performed with a larger dataset in order to verify whether more reliable statistical evidence can be obtained with more data points.

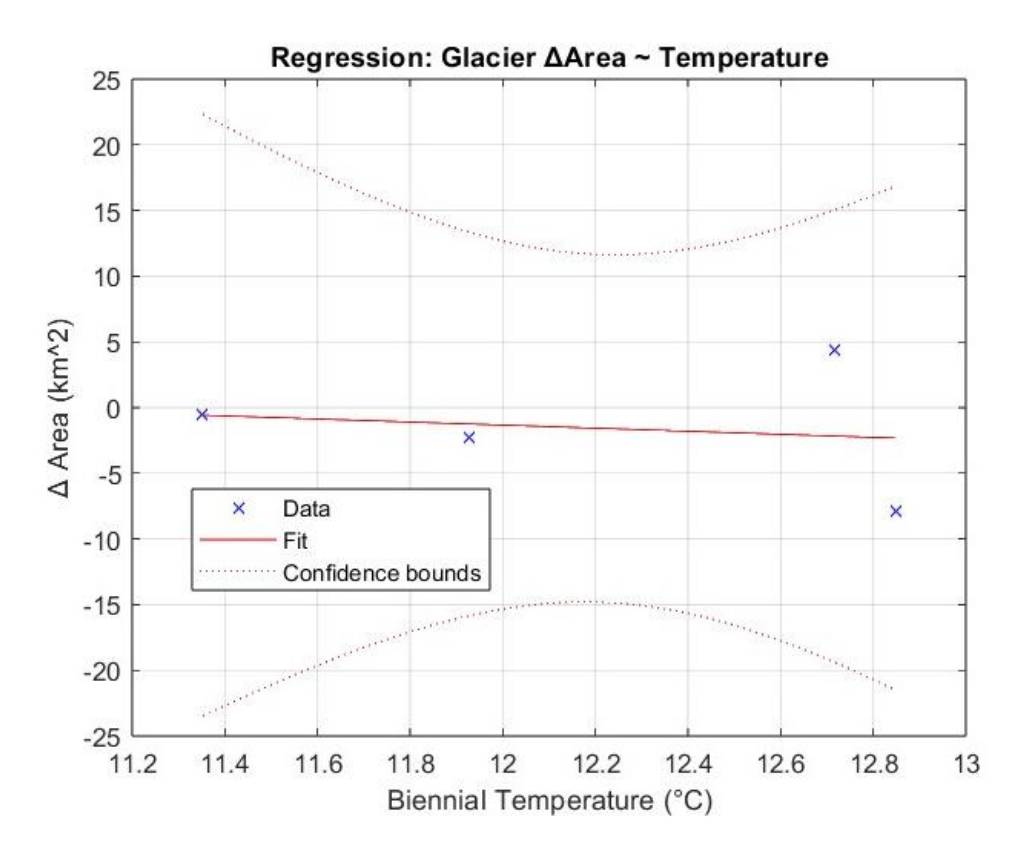


Figure 54: Linear regression model of glacier  $\Delta A$ rea with temperature, including fit line and confidence bounds using the visual method

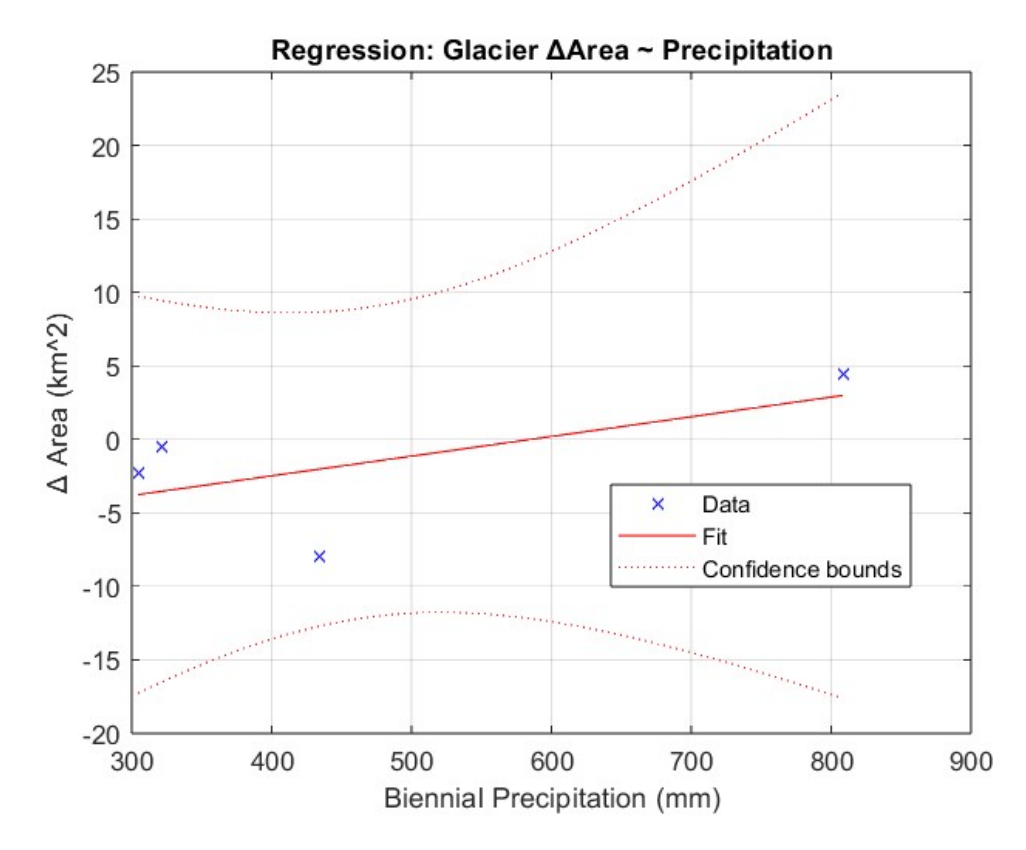


Figure 55: Linear regression model of glacier △Area with precipitation, including fit line and confidence bounds using the visual method

## 5.3.5 Annual Glacier-Climate relationships

In this chapter, the annual analysis of glacier-climate relationships is presented in order to better understand the correlation between surface changes and the climatic variables of precipitation and temperature. A larger dataset was obtained by calculating glacier area from Sentinel-2 images also for each year, starting from 2015 and using the automatic method, combined with the mean summer temperature and the cumulative winter (October-March) precipitation for the same years. The following table (*Table 16*) reports all the parameters that were used for the MATLAB analysis of linear regression and cross-correlation, which will be presented below. The overall dataset consists of 9 datapoints, from 2016 to 2024, in order to match the number of  $\Delta$ Area values with the corresponding temperature and precipitation parameters.

Table 16:  $\Delta A$ rea, mean summer annual temperature and cumulative winter annual precipitation for the nine years considered

Year	ΔArea (km²)	Temperature (°C)	Precipitation (mm)
$2016 \rightarrow 2015$	8.00	10.79	325.40
$2017 \rightarrow 2016$	-14.57	12.83	268.00
$2018 \rightarrow 2017$	19.71	11.69	293.60
$2019 \rightarrow 2018$	-6.06	12.66	529.00
$2020 \rightarrow 2019$	15.26	10.81	366.00
$2021 \rightarrow 2020$	-13.73	11.27	408.20
$2022 \rightarrow 2021$	10.95	12.87	252.80
$2023 \rightarrow 2022$	-17.30	11.99	324.00
$2024 \rightarrow 2023$	2.40	12.63	1110.40

As already observed in the previous graphs related to the biennial analyses, the double y-axis plots in *Figures 56* and 57 also show the relationship between  $\Delta$ Area and temperature and precipitation, respectively, over the years. Regarding the temperature representation, it can be noted that during the first years (2016-2020),  $\Delta$ Area and temperature values are discordant because when temperature increases,  $\Delta$ Area decreases and vice versa. However, from 2021 to 2024 there in an inversion of this trend, where temperature and glacier area follow a more direct relationship. In the precipitation graph, the most evident aspect is that  $\Delta$ Area fluctuates considerably from one year to the next for the already discussed reasons. However, overall area values show a decreasing trend, especially from 2018 to 2024. A similar decreasing trend can be observed in cumulative winter precipitation from 2019 onwards, except for 2024, when a peak of 1100 mm was recorded.

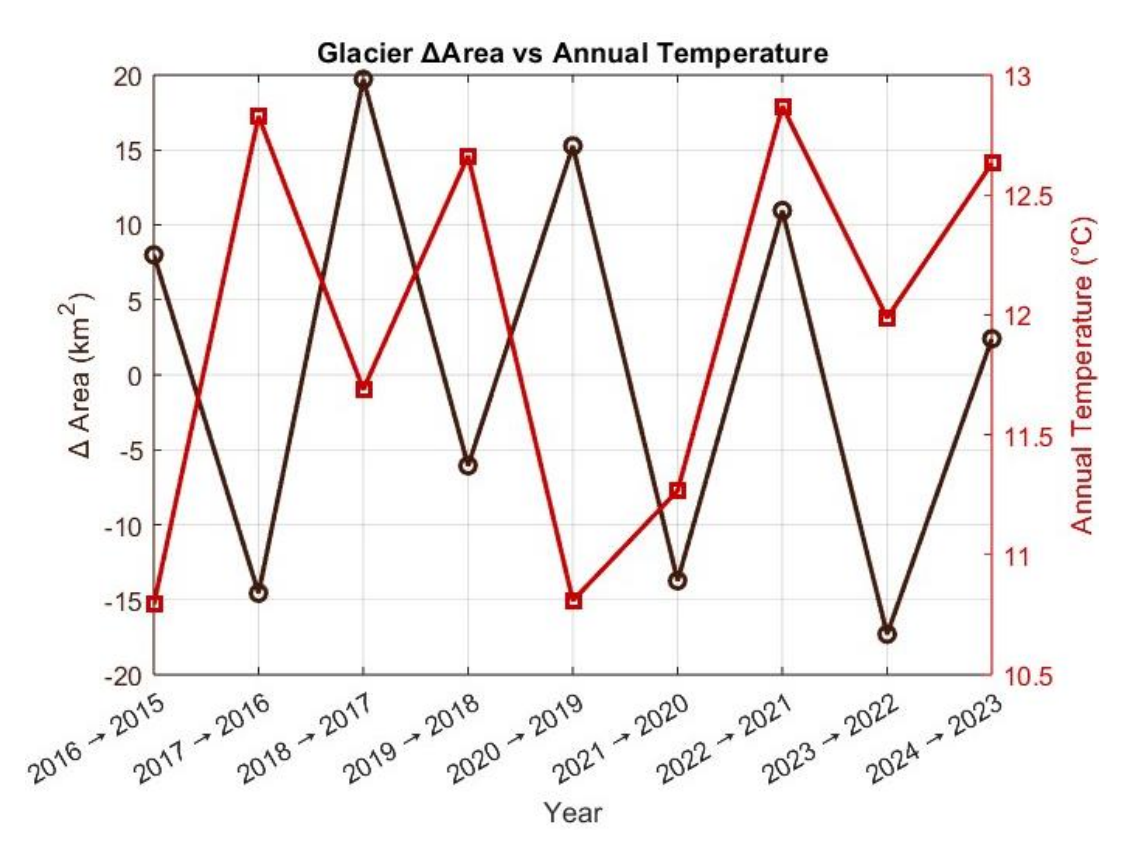


Figure 56: Comparison between glacier area change (left Y-axis) and mean annual temperature (right Y-axis) over the nine years

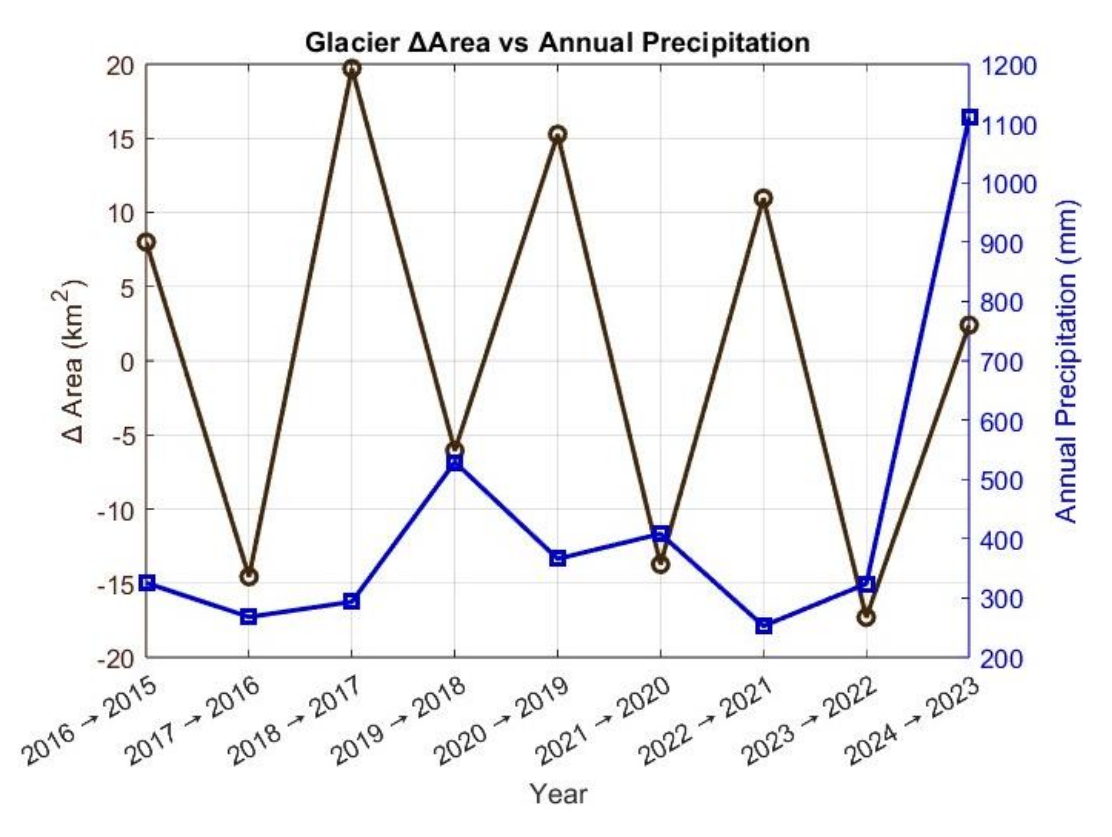


Figure 57: Comparison between glacier area change (left Y-axis) and cumulative annual precipitation (right Y-axis) over the nine years

The following two scatter plots (Figures 58 and 59), which include least-squares fit lines, emphasize once again the weakness of the relationship between  $\Delta$ Area and climate variables, mainly due to the limited number of observations, as shown by the scattered data points that do not follow a clear trend. The main difference between the two models is the slope of the regression lines because for annual temperature the line goes downward, while for precipitation it remains almost horizontal. This indicates that higher summer temperatures cause greater glacier area loss, suggesting that temperature, more than precipitation, is the dominant driver of glacier area variations. However, given the limited dataset, these outcomes and interpretations should be treated with caution and consequently not considered as a reliable statistic.

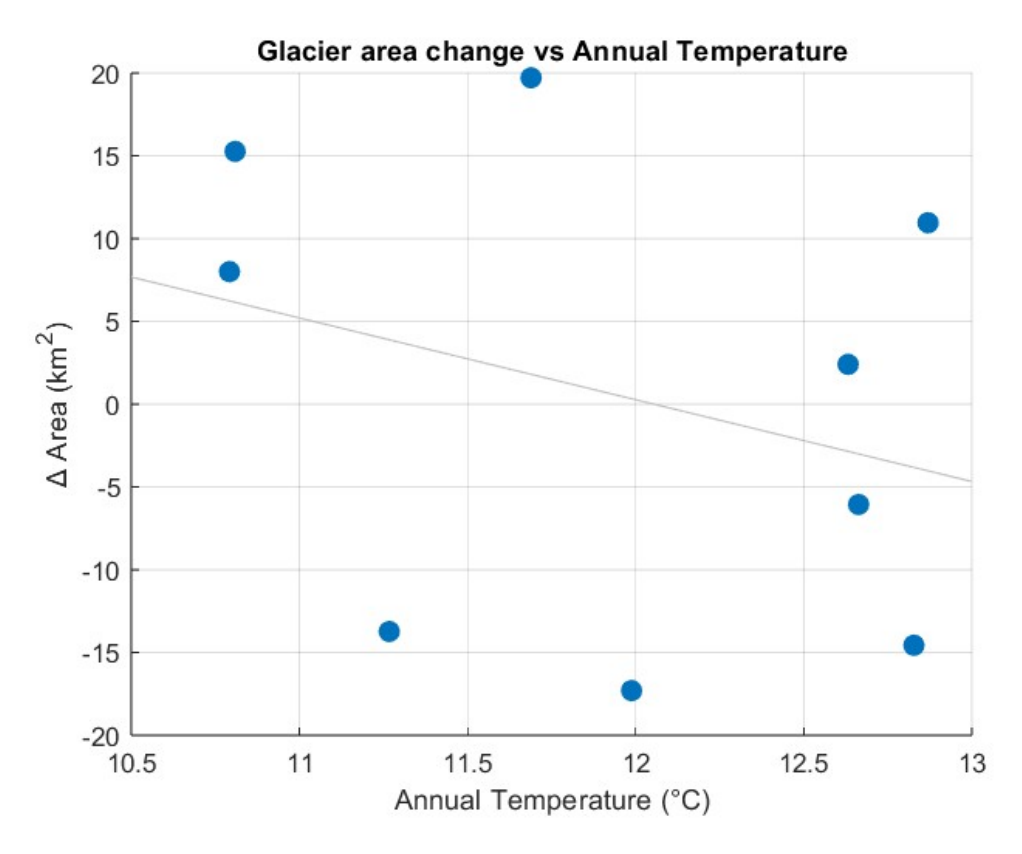


Figure 58: Scatter plot of glacier area changes in relation to mean summer annual temperature with least-squares regression line

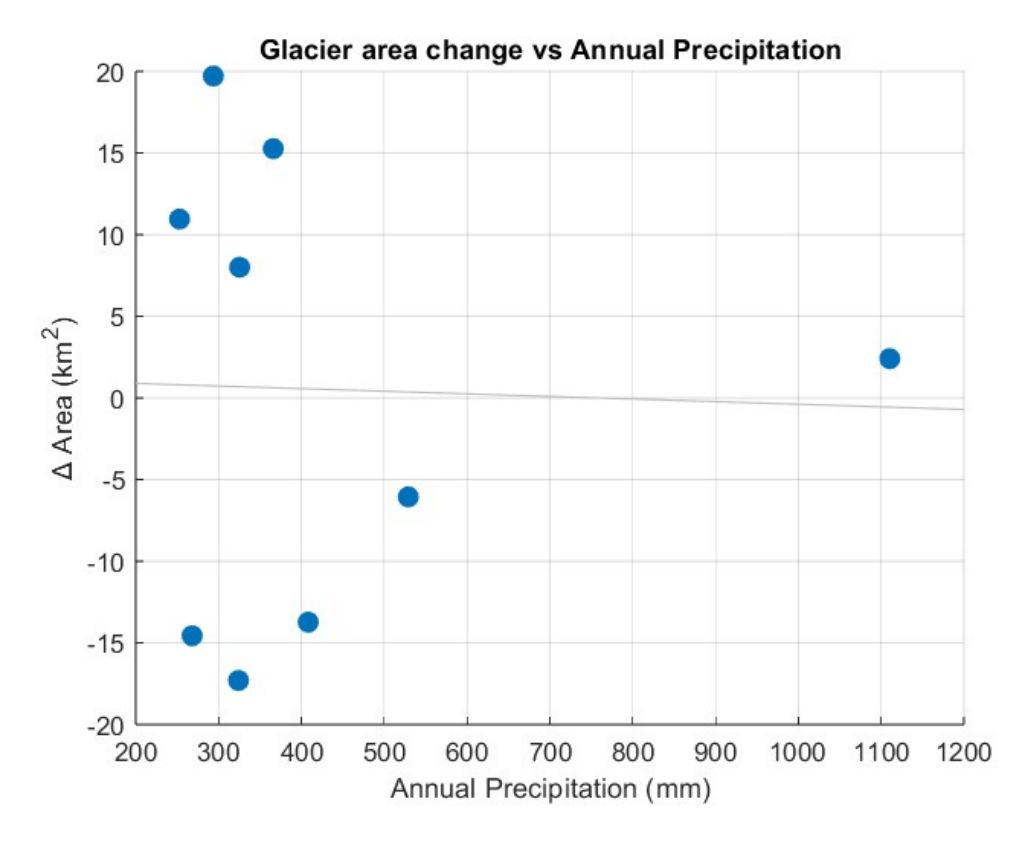


Figure 59: Scatter plot of glacier area changes in relation to cumulative winter annual precipitation with least-squares regression line

Also in this case, when comparing the two regression models (Figures 60 and 61), both temperature and precipitation show only weak and statistically insignificant relationships with glacier area change. The Root Mean Squared Error (RMSE) of the temperature model is  $14.2 \text{ km}^2$ , meaning that predictions deviate by about  $\pm 14 \text{ km}^2$  from observed values on average. The coefficient of determination (R<sup>2</sup>) is 0.091, while the adjusted R<sup>2</sup> is slightly negative (-0.039), with consequently no explanation of the variance in glacier change. The low F-statistic (0.701) and the high p-value (0.43) further confirm the lack of statistical significance.

Regarding the precipitation model, the results are even weaker: the RMSE is  $14.9 \text{ km}^2$ , with an  $R^2$  of 0.001 and a negative adjusted  $R^2$  (-0.142). The extremely low F-statistic (0.0066) and the very high p-value (0.937) show that there is no correlation in this dataset between precipitation and glacier surface variations.

Overall, both models confirm that even with nine observations, the statistical evidence is too weak to draw robust results. Consistently with the biennial analysis, the limited dataset reduces the reliability of the regressions, and a larger sample would be needed.

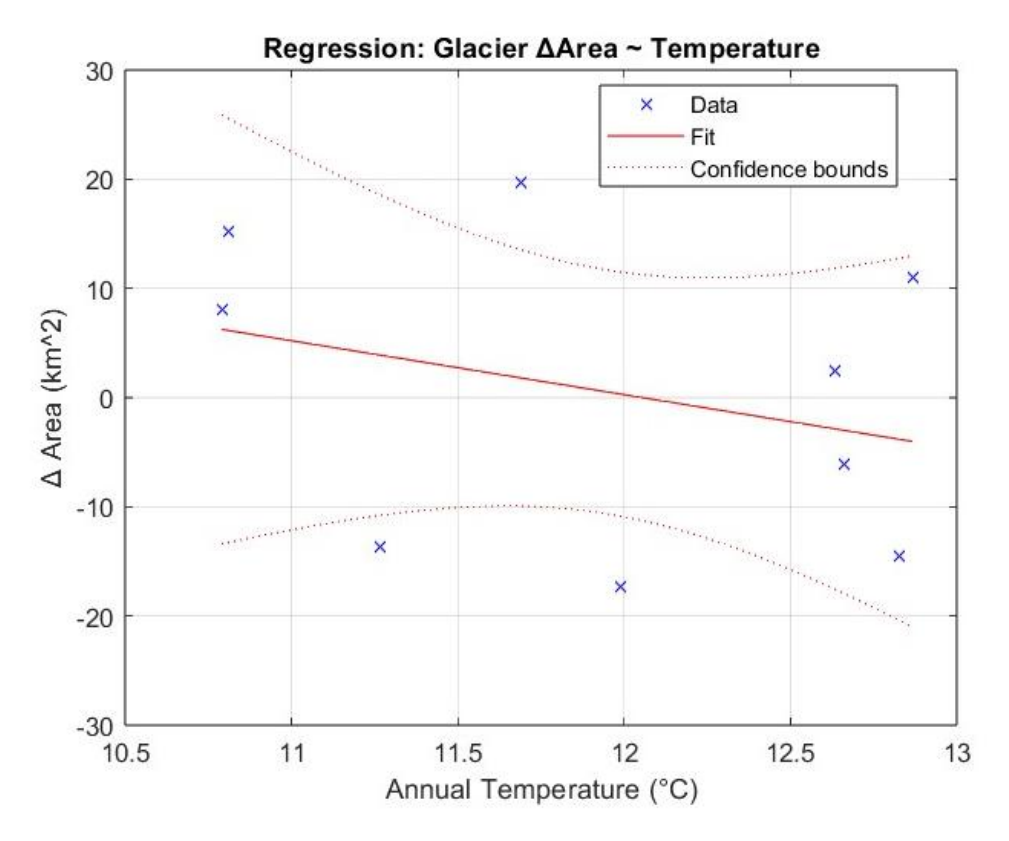


Figure 60: Linear regression model of glacier  $\Delta A$ rea with mean summer annual temperature, including fit line and confidence bounds

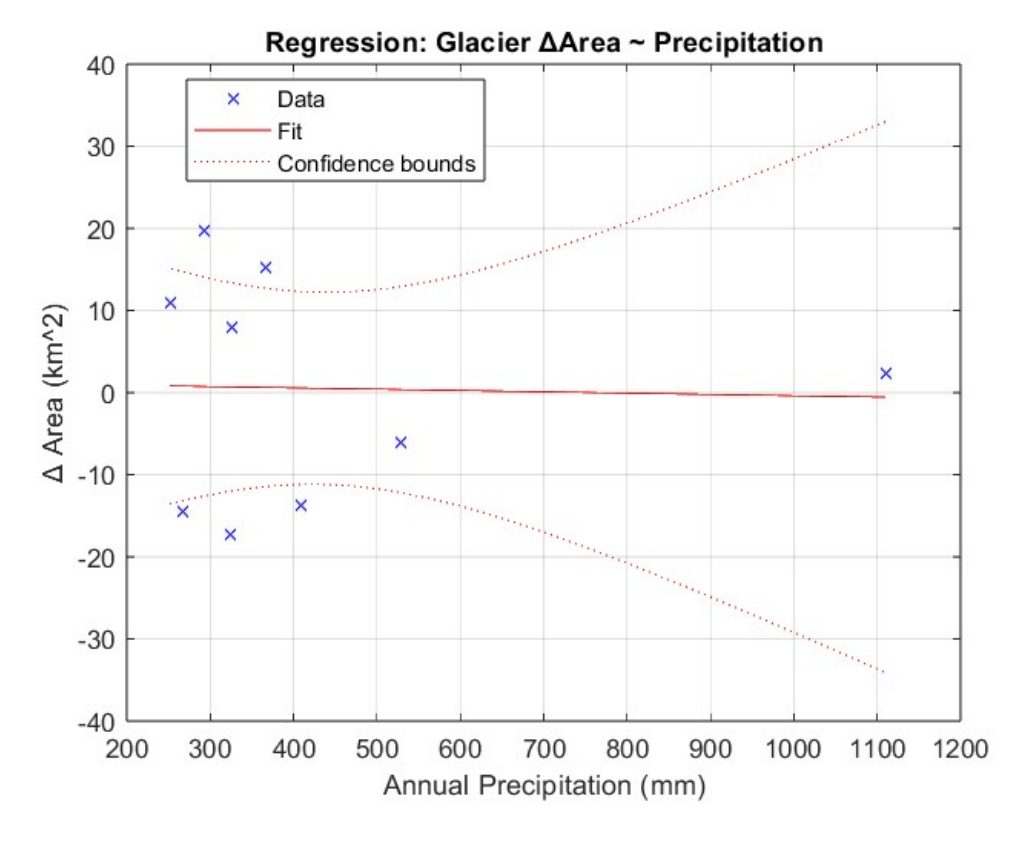


Figure 61: Linear regression model of glacier  $\Delta A$  rea with cumulative winter annual precipitation, including fit line and confidence bounds

In the next two figures, *Figure 62* and *63*, the "crosscorr" function in MATLAB computed the cross-correlation function (XCF) between glacier area changes and the annual temperature or precipitation time series, returning correlation values at different lags together with approximate upper and lower confidence bounds. Although it provided useful insights, the reduced dataset of only nine annual points strongly limited the statistical robustness of the results.

For the temperature case (Figure 62), the coefficients around negative lags remain close to zero, while at positive lags they tend to increase or decrease, moving further away from the x-axis and approaching the confidence bounds (around 0.6). The cross-correlation between glacier  $\Delta$ Area and temperature reaches its peak at lag 3, which is the highest between the two graphs, suggesting that temperature variations precede glacier surface changes by about three years. This pattern reflects the delayed glacier response to thermal forcing, where changes in temperature require time to produce significant effects on melting and glacier mass balance.

On the other hand, precipitation (Figure 63) behaves in the opposite way: coefficients are closer to the confidence bounds at negative lags, indicating a slightly stronger correlation in this range, but they decrease at positive lags. This would suggest that glacier area variations tend to occur before precipitation events, which seems to be inconsistent with physical expectations. Furthermore, although precipitation shows more positive coefficients overall, they remain close to zero, indicating a weak relationship. Conversely, temperature shows fewer positive coefficients but with higher and more significant peaks, as they get closer to the confidence bounds.

The difference between the two variables highlights that temperature appears to play a stronger and more direct role than precipitation in driving glacier surface changes. However, the fact that in both cases all the points remain within the confidence bounds, with no values exceeding them, means that no solid statistical evidence can be drawn from these results. This outcome is mainly due to the limited dataset used for the analysis, since nine observations are not enough for getting a robust cross-correlation study and, meanwhile, the high interannual variability further reduces reliability. Therefore, these findings can only be considered preliminary, and a larger dataset would be necessary to provide robust confirmation.

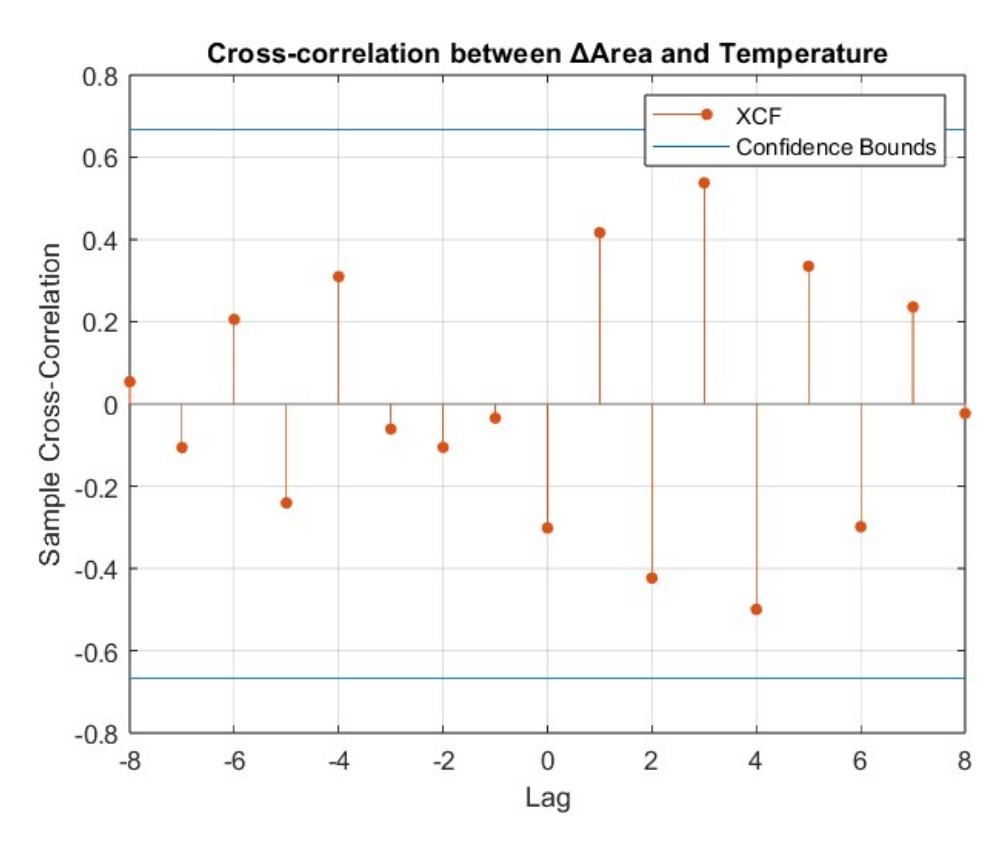


Figure 62: Sample cross-correlation function (XCF) between glacier  $\Delta A$ rea and temperature, with the blue line representing the approximate 95% confidence bounds

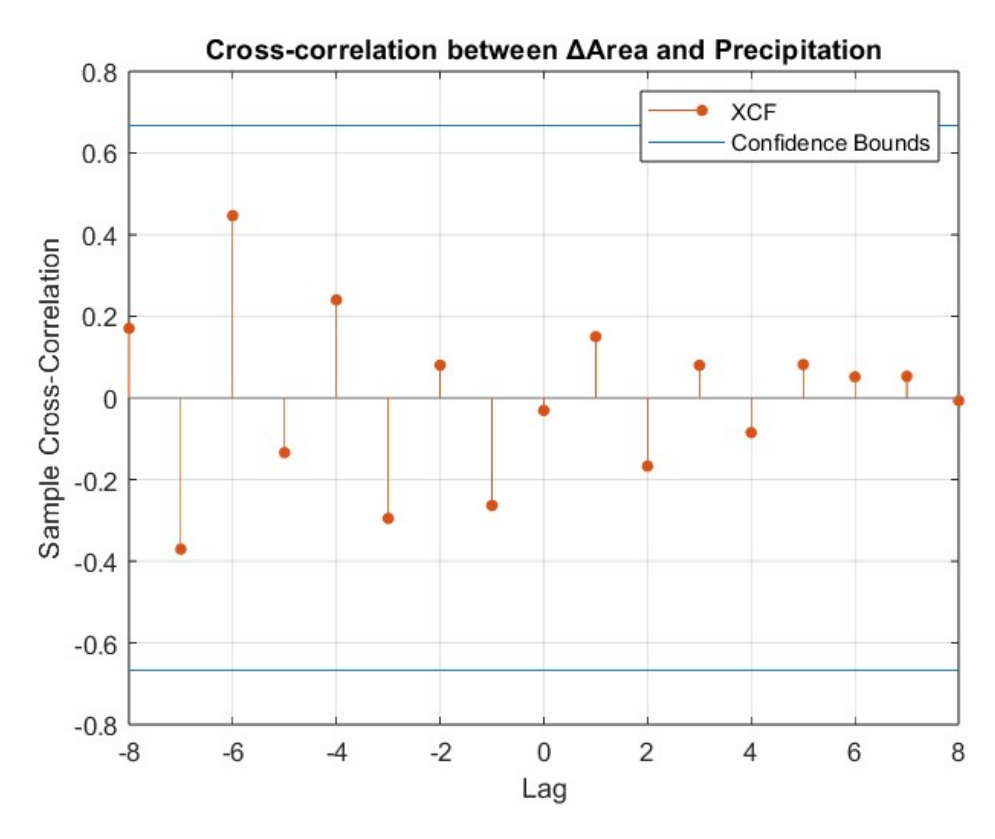


Figure 63: Sample cross-correlation function (XCF) between glacier  $\Delta$ Area and precipitation, with the blue line representing the approximate 95% confidence bounds

## 6. Conclusions and future trends

Climate change impacts on the environment are well known and evident. This work aimed to provide a perspective on glacier dynamics in alpine regions and to study the trend of their surface changes over the last years. By calculating the area of the Adamello glacier in QGIS using MODIS and Sentinel-2 satellite images, it was possible to compare the two platforms and the variations year by year. The two methods used for area calculation, namely automatic and visual, also highlighted the differences between approaches, showing both their advantages and drawbacks. As already noted, the visual method also allowed to include those glacier parts that in the QGIS images appeared greyish or not clearly ice, as the Mandrone tongue. On the other hand, its limitation was the high dependence on operator judgment in delineating the contour and deciding which pixels to include. In contrast, the automatic method performed well in identifying detached parts of the glacier around the main body and in providing a standardized approach once the spectral bands were selected. However, this method also had important limitations because it often failed to capture darker glacier areas, and it still relied on the operator's choice of reference pixels, who maintains a critical role. These issues were evident in the fluctuating area values, which alternated between increases and decreases, making it difficult to identify the clear retreating trend expected from recent studies and reports.

Another factor that affected the analysis was the limited availability of cloud-free summer images, essential for accurate glacier delineation. Contrary to what might be expected, such images were relatively scarce, forcing the operator to rely on different summer months, sometimes in July and sometimes even late September. This had consequences, since late-summer images were occasionally affected by early snowfalls, temporarily enlarging the glacier surface and misleading the calculations.

Furthermore, a difference was also found between the two satellite constellations, MODIS and Sentinel-2. As already mentioned, MODIS provided lower-resolution images but had the advantage of a longer time series, extending back to the early 2000s. Sentinel-2, in contrast, has been available only since 2015, when it was launched, but it offers much higher resolution. For this reason, Sentinel-2 was chosen for the biennial analysis of surface changes and for the subsequent correlation with climate variables.

In the second part of the work, the relationship with temperature and precipitation values recorded from the closest station to the glacier, located in upper Valcamonica just below the glacier itself, was investigated. In this way, it was possible to estimate the influence of these two climatic variables on glacier area changes in the last ten years, to assess the consequences of climate change in the region. The main results obtained from the correlation analyses and linear regression models showed that temperature has a stronger influence than precipitation, and that glacier response to temperature variations is delayed by about three years. This is an important finding, as it indicates that the time available to intervene and implement mitigation strategies is approximately three years, an aspect to consider for future scenarios.

However, it was difficult to find reliable statistical evidence of the relationship between glacier  $\Delta$ Area and temperature and precipitation due to the limited dataset of only ten years, as well as the high variability in the area calculations. Overall, the statistical analyses carried out in this thesis represent a good starting point for studying this type of correlation but should be further developed in the future with more data.

Possible applications of this work could include expanding the dataset with measurements from additional monitoring stations around the glacier to obtain a broader coverage, or by extending the observation period. Although going back in time before 2015 with high-resolution images is difficult, in the coming years, as the dataset grows, similar analyses could be carried out over 20 years or more. Another way to enlarge the dataset could be to consider multiple images per summer, although finding high-quality images with minimal cloud cover remains challenging.

Future applications could also involve expanding the set of climate variables considered in the analysis, such as including Oglio River discharge, snow gauge data, wind velocity, solar radiation and others. Moreover, while this thesis was developed entirely with free-access tools, software, and web resources, the use of private or paid services could provide additional data, more advanced tools, and more detailed analyses. All these possibilities could improve the present work and expand it further, depending on the research interests. As stated in the Introduction (Chapter 1.3), this study was also conceived from a local perspective, to be useful for local municipalities, mountain communities, civil protection and researchers in the field.

Nowadays, numerous articles and images on the internet document glacier retreat, often comparing past and present conditions to highlight the dramatic ice loss and potential future scenarios if current trends persist. For this reason, the present study fits into a highly relevant context, which has been gaining increasing public attention due to the worsening conditions of glaciers in recent years. In the future, it would be interesting to analyse the effects of mitigation strategies and assess whether such measures could reduce glacier mass balance loss or at least slow down this process.

Among the most widely known measures at a global scale to protect glaciers from global warming and climate change are geotextile sheets, made of polyester or polypropylene fibres. This geoengineering technique is used to cover glacier surfaces, increasing albedo and reducing melt rates by reflecting solar radiation. For instance, geotextiles have been applied in the Swiss Alps since 2009 and are clearly visible on the Presena Glacier (*Figure 64*), located next to the Adamello Glacier. While they can locally reduce glacier melt by up to 59% on small and economically relevant areas, their large-scale application is unsustainable and presents numerous drawbacks [31].



Figure 64: Geotextile sheets covering the Presena Glacier, located next to the Adamello Glacier on the border between Lombardy and Trentino-Alto Adige, at an altitude of almost 3000 m [32]

From an environmental and climate change perspective, the practice of covering glaciers with geotextiles raises environmental, ecological, and economic problems. Although these covers can locally slow down melting, the use of large amounts of fuel and plastic materials as well as the possible release of microplastics into meltwater, can cause potentially harmful effects and indirectly contribute to CO<sub>2</sub> emissions, the very driver of glacier retreat. Covered glaciers also become artificial and isolated bodies of ice, disrupting natural ecological processes and eliminating microbial communities that play a vital role in carbon cycles. As a result, such measures risk altering landscapes, natural eco-systems and water resources, with possible consequences on flora, fauna and the population.

This approach is unfeasible on a large scale due to prohibitive costs, limited accessibility and logistical challenges. In fact, protecting even a small glacier sector requires investments of hundreds of thousands of euros per year. Consequently, these projects often have as a primary motivation the preservation of ski slopes and local tourism revenues, rather than real climate mitigation. As confirmed by several studies, glaciers cannot be saved with plastic sheets but only through global reductions in greenhouse gas emissions. If emissions are limited in line with the Paris Agreement, approximately 40% of Alpine ice could still be preserved. For this reason, financing glacier covers has little to do with long-term glacier protection or climate action and instead risks becoming a form of greenwashing that prioritizes short-term local economic interests while presenting itself as an environmental solution [33].

The other numerous possible consequences of glacier retreat and melting in Valcamonica emphasize the necessity to consider mitigation strategies in order to prevent severe damage. Moving forward in time, glacier retreat may increase hydrogeological risks, such as floods of Oglio River caused by excessive meltwater, landslides, or sudden collapses of glacial fronts, causing further strains to small villages and local populations. Other secondary impacts could concern agriculture, water supply, biodiversity and tourism, with changes in the local microclimate and reduced water availability potentially compromising hydroelectric production systems in the area.

Glacier retreat is undoubtedly one of the most visible signs of climate change worldwide. Although this study focused on a local region in northern Italy, it highlights the urgency of raising public awareness and the need for global interventions to address this challenge. All these aspects reiterate the importance of continuous study and monitoring of these changing ecosystems. Moreover, comparing results across different research can help to identify the most effective strategies to reduce greenhouse gas emissions and safeguard what remains of these glaciers. The data and tools are available, the changes are evident, and the need to pursue collective efforts to preserve a significant share of these vulnerable ecosystems is crucial.

## References

- [1] G. Grossi, P. Caronna, and R. Ranzi, 'Hydrologic vulnerability to climate change of the Mandrone glacier (Adamello-Presanella group, Italian Alps)', *Adv. Water Resour.*, vol. 55, pp. 190–203, May 2013, doi: 10.1016/j.advwatres.2012.11.014.
- [2] 'Parco regionale dell'Adamello Il Ghiacciaio dell'Adamello'. Accessed: Apr. 14, 2025. [Online]. Available: https://www.parcoadamello.it/conoscere-il-parco/il-ghiacciaio-delladamello
- [3] V. Maggi *et al.*, 'Late Holocene Evolution of the Adamello Glacier (Rhaetian Alps): New Insights for Alpine Temperate Glaciers', *Geogr. Fis. E Din. Quat.*, vol. 46, no. 1–2, pp. 193–210, Dec. 2023, doi: 10.4454/1312gf6j.
- [4] 'COMUNICATO STAMPA CFC 5'.
- [5] 'Il Ghiacciaio dell'Adamello Comitato Glaciologico Italiano'. Accessed: Sep. 01, 2025. [Online]. Available: https://glaciologia.it/ghiacciai/chardonney/
- [6] 'Adamello Glacier', Glacier Change. Accessed: May 25, 2025. [Online]. Available: https://glacierchange.com/en/adamello-glacier/
- [7] 'Parco regionale dell'Adamello Il territorio'. Accessed: May 25, 2025. [Online]. Available: https://www.parcoadamello.it/conoscere-il-parco/il-territorio
- [8] 'Il Parco Naturale', Parco Naturale Adamello Brenta Geopark. Accessed: May 25, 2025. [Online]. Available: https://www.pnab.it/il-parco/il-parco-naturale/
- [9] C. Baroni, S. Martino, M. C. Salvatore, G. Scarascia Mugnozza, and L. Schilirò, 'Thermomechanical stress-strain numerical modelling of deglaciation since the Last Glacial Maximum in the Adamello Group (Rhaetian Alps, Italy)', Geomorphology, vol. 226, pp. 278–299, Dec. 2014, doi: 10.1016/j.geomorph.2014.08.013.
- [10] D. Maragno et al., 'NEW EVIDENCE FROM ITALY (ADAMELLO GROUP, LOMBARDY) FOR ANALYSING THE ONGOING DECLINE OF ALPINE GLACIERS', 2009.
- [11] FLA Fondazione Lombardia per l'Ambiente, *Ada270 documentario*, (2021). Accessed: May 26, 2025. [Online Video]. Available: https://www.youtube.com/watch?v=6xnEPVLkf3M

- [12] 'Tre secoli di clima dai ghiacci dell'Adamello', Focus.it. Accessed: May 26, 2025. [Online]. Available: https://www.focus.it/scienza/scienze/studio-clima-ghiacciaio-adamello
- [13] Clim-Admin-Key, 'CLIMADA', ClimADA L'evoluzione climatica e il Ghiacciaio dell'Adamello. Accessed: May 26, 2025. [Online]. Available: https://www.climada.eu/
- [14] Neunau, 'UN SUONO IN ESTINZIONE', UN SUONO IN ESTINZIONE.

  Accessed: May 20, 2025. [Online]. Available: https://www.unsuonoinestinzione.eu/
- [15] Jenice Aroma R and K. Raimond, 'A review on availability of remote sensing data', in 2015 IEEE Technological Innovation in ICT for Agriculture and Rural Development (TIAR), Chennai, India: IEEE, Jul. 2015, pp. 150–155. doi: 10.1109/TIAR.2015.7358548.
- [16] 'What is Satellite Imagery? | Geoimage'. Accessed: May 08, 2025. [Online]. Available: https://www.geoimage.com.au/blog/what-satellite-imagery
- [17] 'Moderate Resolution Imaging Spectroradiometer (MODIS) LAADS DAAC'.

  Accessed: Apr. 29, 2025. [Online]. Available: https://ladsweb.modaps.eosdis.nasa.gov/missions-and-measurements/modis/
- [18] 'MODIS Web'. Accessed: Apr. 29, 2025. [Online]. Available: https://modis.gsfc.nasa.gov/about/
- [19] 'MODIS Web Components'. Accessed: May 01, 2025. [Online]. Available: https://modis.gsfc.nasa.gov/about/components.php
- [20] K. Thome, 'MODIS | Terra'. Accessed: Apr. 29, 2025. [Online]. Available: https://terra.nasa.gov/about/terra-instruments/modis
- [21] 'Introducing Sentinel-2'. Accessed: Apr. 27, 2025. [Online]. Available: https://www.esa.int/Applications/Observing\_the\_Earth/Copernicus/Sentinel-2/Introducing Sentinel-2
- [22] 'Sentinel-2'. Accessed: Apr. 27, 2025. [Online]. Available: https://sentiwiki.copernicus.eu/web/sentinel-2
- [23] 'Sentinel-2 | Copernicus Data Space Ecosystem'. Accessed: Apr. 27, 2025.
  [Online]. Available: https://dataspace.copernicus.eu/explore-data/data-collections/sentinel-data/sentinel-2

- [24] 'ARPA Lombardia | Chi siamo'. Accessed: Aug. 27, 2025. [Online]. Available: https://www.arpalombardia.it/chi-siamo/
- [25] 'QGIS overview · QGIS Web Site'. Accessed: May 06, 2025. [Online]. Available: https://qgis.org/project/overview/
- [26] 'QGIS Desktop', OSGeo. Accessed: May 06, 2025. [Online]. Available: https://www.osgeo.org/projects/qgis/
- [27] 'What Is MATLAB?' Accessed: Aug. 27, 2025. [Online]. Available: https://it.mathworks.com/discovery/what-is-matlab.html
- [28] 'About the LAADS DAAC LAADS DAAC'. Accessed: May 01, 2025. [Online]. Available: https://ladsweb.modaps.eosdis.nasa.gov/about/
- [29] E. Vermote and R. Wolfe, 'MOD09GA MODIS/Terra Surface Reflectance Daily L2G Global 1kmand 500m SIN Grid V006'. NASA Land Processes Distributed Active Archive Center, 2015. doi: 10.5067/MODIS/MOD09GA.006.
- [30] 'SIDRO | Sistema Informativo Idrologico'. Accessed: Aug. 29, 2025. [Online]. Available: https://idro.arpalombardia.it/it/map/sidro/
- [31] 'Coprire i ghiacciai per salvarli? Professor Marco Grasso', Grivel. Accessed: Sep. 11, 2025. [Online]. Available: https://grivel.com/it/blogs/news/wrapping-glaciers-to-save-them-by-marco-grasso
- [32] P. Farina, 'Ghiacciaio Presena, rimossa la "coperta" di protezione', Radio Lombardia. Accessed: Sep. 12, 2025. [Online]. Available: https://www.radiolombardia.it/2021/09/27/ghiacciaio-presenza-rimossa-la-coperta-di-protezione/
- [33] 'Salviamo i Ghiacciai SGL'. Accessed: Sep. 12, 2025. [Online]. Available: https://www.servizioglaciologicolombardo.it/salviamo-i-ghiacciai-2/